

**CHARACTERIZATION OF MECHANICAL
AND THERMOMECHANICAL BEHAVIOR OF SUSTAINABLE
COMPOSITE MATERIALS BASED ON JUTE**

Abdul Jabbar, M.Sc.

SUMMARY OF THE THESIS

Title of the thesis: Characterization of mechanical and thermomechanical behavior of sustainable composite materials based on jute

Author: Abdul Jabbar, M.Sc.

Field of study: Textile Technics and Materials Engineering

Mode of study: Full time

Department: Material Engineering

Supervisor: prof. Ing. Jiří Militký, CSc.

Committee for the defense of the dissertation:

Chairman:

prof. RNDr. Oldřich Jirsák, CSc.

FT TUL, Department of Nonwovens and Nanofibrous Materials

Vice-chairman:

doc. Ing. Maroš Tunák, Ph.D.

FT TUL, Department of Textile Evaluation

prof. Dr. Ing. Miroslav Černík, CSc.

The Institute for Nanomaterials, Advanced Technology and Innovation TUL

prof. Ing. Michal Šejnoha, Ph.D., DSc. (opponent) Czech Technical University in Prague, Fac. of Civil Engineering, Dpt. of Mechanics

prof. Ing. Jakub Wiener, Ph.D.

FT TUL, Department of Material Engineering

doc. Ing. Antonín Potěšil, CSc. (opponent)

TUL, Institute of New Technologies and Applied Informatics

Ing. Blanka Tomková, Ph.D.

FT TUL, Department of Material Engineering

This dissertation is available at the Dean's office FT TUL.

Liberec 2017

Abstract

Natural fiber reinforced polymer composites (NFPC) have gained considerable attention in the recent years due to their environment and economic benefits and low energy demand in production. The use of cellulosic stiff reinforcing fillers in polymer composites have also attracted significant interests of material scientists. Waste of natural fibers, produced in the textile industry during mechanical processing, offers a cheaper source of availability for the preparation of these stiff cellulose fibrils/fillers. The poor adhesion between the fiber and polymer matrix is also considered a major drawback in the use of natural fiber composites. Therefore, surface modification of natural fibers is necessary before using them as a reinforcement in composites.

This thesis is dealing with the effect of addition of stiff cellulose micro fibrils and nanocellulose extracted from jute waste and its coating over woven jute reinforcements and some novel environment friendly fiber treatment methods on the bulk properties, including mechanical and dynamic mechanical properties of jute/green epoxy composites. Waste jute fibers were used both to produce jute cellulose fibrils through pulverization and as a precursor to purify and extract nanocellulose. Woven jute fabric was treated with novel techniques such as CO₂ pulsed infrared laser, ozone, enzyme and plasma. Three different categories of composite laminates were prepared by hand layup method and compression molding technique using same green epoxy matrix. The first composite type was comprised 1, 5 and 10 wt % of pulverized micro jute fibers (PJF), used as fillers along with alkali treated jute fabric. The second type was enclosed with nanocellulose coated jute fabric with different nanocellulose concentrations (3, 5 and 10 wt %) and third type was consisted of surface treated jute fabric. The surface topologies of treated jute fibers, jute cellulose nanofibrils (CNF), pulverized jute fibrils (PJF), nanocellulose coated jute fabrics and fractured surfaces of composites were characterized by scanning electron microscopy (SEM). The crystallinity of jute fibers after different chemical treatments was measured by X-ray diffraction (XRD). The novel surface treated jute fabrics, alkali treated jute fabric and chemically pretreated waste jute fibers were characterized by Fourier transform infrared spectroscopy (FTIR).

The mechanical properties of composites were determined according to recommended international standards. The creep and dynamic mechanical tests were performed in three-point bending mode by dynamic mechanical analyzer (DMA). Three creep models i.e. Burger's model, Findley's power law model and a simple two-parameter power law model were used to model the creep behavior in this study. The time temperature superposition principle (TTSP) was applied to predict the long-term creep performance. The results revealed the improvement in tensile modulus, flexural properties, fatigue life and fracture toughness except the decrease in tensile strength of only nanocellulose coated woven jute/green epoxy composites as compared to uncoated jute composite. The incorporation of PJF and novel surface treatments were found to significantly improve the creep resistance of composites. The Burger's model fitted well the short term creep data. The Findley's power law model was found to be satisfactory in predicting the long-term creep behavior. Dynamic mechanical analysis revealed the increase in storage modulus and reduction in tangent delta peak height of all three composite categories.

Keywords: Jute fiber, Natural fiber composites, Mechanical properties, Creep, Dynamic mechanical analysis

Anotace

V posledních letech je zájem soustřeďován na kompozity z přírodních polymerních vláken díky jejich ekonomickým benefitům, vlivu na životní prostředí a nízké spotřebě energie při jejich výrobě. Materiáloví inženýři se soustředí na využití výplní z celulózových vláken pro polymerní kompozity. Během mechanického zpracování textilních vláken vzniká odpad, který slouží jako levný zdroj suroviny pro přípravu těchto celulózových vláken/ kompozitních výplní. Hlavní nevýhodou přírodních vláken jako výztuže do kompozitu je nízká adheze mezi vláknem a polymerní maticí. Proto je nutné modifikovat jejich povrch.

Tato práce se zabývá vlivem přídavku tuhých mikroskopických fibril celulózy a nanocelulózy extrahovaných z odpadu juty a jejich depozicí na jutovou tkaninu. Dále se zabývá metodami její aplikace a testováním mechanických vlastností i z hlediska dynamických zkoušek kompozitních struktur na bázi juta a ekologicky šetrné epoxidové pryskyřice. Odpad z vláken juty byl použitý v obou případech jak pro výrobu jutových celulózových fibril včetně jejich fragmentování, tak i jako prekurzor pro čištění a extrahování nanocelulózy. Jutová tkanina byla zpracována novými technikami jako je CO₂ pulzní infračervený laser, ozón, enzymy a plazma. Tři různé kategorie vrstvených kompozitních materiálů byly připraveny metodou ručního vrstvení a kompresní technikou s použitím stejné ekologické epoxidové matrice. První kompozit obsahoval 1, 5 a 10 hmotnostních % mikro fragmentů jutových vláken (PJF) použitých jako plnivo spolu s alkalicky ošetřenou jutovou tkaninou. Druhý typ byl tvořen jutovou tkaninou povrstvenou nanocelulózou v koncentracích 3, 5 a 10 hmotnostních %. Třetí typ byl vytvořen z povrchově upravené jutové tkaniny. Povrchová topologie upravených jutových vláken, jutových a celulózových nanofibril (CNF), drcených jutových fibril (PJF), nanocelulózou potažené jutové tkaniny a zlomy v povrchu kompozitu byly charakterizovány pomocí rastrovací elektronové mikroskopie (SEM). Krystalinita jutových vláken po různém chemickém ošetření byla měřena pomocí rentgenové difrakce (XRD). Nově povrchově upravené jutové tkaniny, alkalicky ošetřené jutové tkaniny a chemicky předupravená odpadní jutová vlákna byla charakterizována pomocí spektroskopie FTIR.

Mechanické vlastnosti kompozitů byly stanoveny podle doporučených mezinárodních norem. Tečení a dynamické mechanické zkoušky byly prováděny v režimu tříbodového ohybu pomocí dynamického mechanického analyzátoru (DMA). Tři modely tečení materiálu, tj. Burgerův model, model Findleyho zákona a jednoduchý dvouparametrový mocninový model byly použity k modelování tečení materiálu (creep) v této studii. Princip časově teplotní superpozice (TTSP) byl použit k predikci dlouhodobého tečení. Výsledky ukázaly zlepšení modulu v tahu, ohybových vlastností, doby do únavy materiálu a odolnosti v lomu, s výjimkou poklesu pevnosti v tahu u nanocelulózou potažené jutové tkaniny/ekologického epoxidového kompozitu ve srovnání s kompozitem s nepotaženou jutou. Inkorporace PJF a nových povrchových úprav výrazně zvyšuje odolnost proti tečení kompozitů. Burgerův model byl dobře použitelný k modelování tečení v krátkodobém horizontu, zatímco Findleyho model byl uspokojivý při předvídání chování dlouhodobého tečení. DMA ukázala, že u všech tří kategorií kompozitů došlo ke zvýšení paměťového modulu a ke snížení výšky tangentských píků.

Klíčová slova: Vlákna juty, kompozity z přírodních vláken, mechanické vlastnosti, tečení, analýza dynamických mechanických vlastností

Table of Contents

1	<i>Introduction</i>	1
2	<i>Purpose and aim of the thesis</i>	2
3	<i>Overview of the current state of problem</i>	2
4	<i>Methods used, studied materials</i>	3
4.1	Materials	3
4.2	Methods	3
4.2.1	Chemical pre-treatment of jute fabric and waste jute fibers	3
4.2.2	Pulverization of waste jute fibers	3
4.2.3	Purification and extraction of nanocellulose from waste jute fibers and nanocellulose coating	4
4.2.4	Treatment methods	5
4.2.5	Preparation of composites	6
4.2.6	Characterization and testing	6
5	<i>Summary of results achieved</i>	10
5.1	Effect of pulverized micro jute fillers loading on the mechanical, creep and dynamic mechanical properties of jute/green epoxy composites	10
5.1.1	Characterization of jute fibers	10
5.1.2	Tensile properties	11
5.1.3	Flexural properties	12
5.1.4	Short term creep	13
5.1.5	Time-temperature superposition (TTS)	14
5.1.6	Dynamic mechanical properties	18
5.2	Extraction of nanocellulose from waste jute fibers and characterization of mechanical and dynamic mechanical behavior of nanocellulose coated jute/green epoxy composites	19
5.2.1	SEM study of chemically treated jute fibers and jute cellulose nanofibrils	19
5.2.2	Surface topology of nanocellulose coated jute fabric	21
5.2.3	XRD analysis of jute fibers	22
5.2.4	Tensile properties	23
5.2.5	Flexural properties	24
5.2.6	Fatigue life	24
5.2.7	Fracture toughness	26
5.2.8	Dynamic mechanical analysis	28
5.3	Flexural, creep and dynamic mechanical evaluation of novel surface treated woven jute/green epoxy composites	31
5.3.1	SEM observation of jute fibers after surface treatments	31
5.3.2	FTIR analysis	32

5.3.3	Flexural properties	33
5.3.4	Creep behavior	34
5.3.5	Dynamic mechanical analysis	36
6	<i>Evaluation of results and new findings</i>	38
6.1	Proposed applications and limitations	39
7	<i>References</i>	39
8	<i>List of papers published by the author</i>	44
8.1	Publications in journals	44
8.2	Contribution in conference proceedings	45
8.3	Citations	45
	<i>Curriculum Vitae</i>	47
	<i>Brief description of the current expertise, research and scientific activities</i>	50

1 Introduction

The impact of global climatic change is quite visible in the recent years due to increase in greenhouse gas emissions. Synthetic fibers whose main feedstock is petroleum, are being widely used in polymer composites because of their high strength and stiffness. However, these fibres have serious drawbacks in terms of their non-biodegradability, toxicity, initial processing costs, recyclability, energy consumption, machine abrasion, health hazards, etc. [1]. Therefore, the increasing environmental awareness and international legislations to reduce greenhouse gas emissions have forced the material scientists and researchers to shift their attention from synthetic fibers to natural/renewable fibers. Natural fibers are now increasingly used as reinforcement in biocomposites because of many advantages such as cost effectiveness, easy to process, renewable, recyclable, available in huge quantities, low fossil-fuel energy requirements and the most importantly their high specific strength to weight ratio [2]. This is of distinctive importance especially in interior transportation applications as it leads to reduction of vehicle weight for higher fuel efficiency, reduction in cost and energy saving. Thus natural fibers are considered promising candidates for replacing conventional synthetic reinforcing fibers in composites for semi-structural and structural applications [3]. Bio-composites are the composites in which natural fibers are reinforced with either biodegradable or non-biodegradable matrices [4].

Plant based natural fibers are most commonly used lignocellulosic fibers in composite applications [5]. These fibers are derived from various parts of plants, such as stems, leaves, and seeds. The fibers derived from stem (bast fibers) such as jute, flax, hemp and kenaf etc. are more commonly used for reinforcement in composites due to their high tensile strength and high cellulose content [6]. Lignocellulosic fibers mainly consist of cellulose microfibrils in an amorphous matrix of lignin and hemicellulose. The percentage composition of each component varies for different fibers. However, cellulose is the major framework component in these fibers having 60 - 80% weightage and is responsible for providing strength, stiffness and structural stability to the fiber [7]. Among lignocellulosic fibers, jute is an abundant natural fiber used as a reinforcement in bio-composites [8] and occupies the second place in terms of world production levels of cellulosic fibers [9] after cotton.

The properties and aspect ratio of fibers and interfacial interaction between fibers and matrix govern the properties of composites. Good interfacial adhesion between fiber and polymer plays an important role in the transfer of stress from matrix to fiber and thus contributes to better performance of composite. Despite parallel advantages of lignocellulosic fibers, there is some drawback regarding their behaviour in polymer matrix apart from their performance and processing limitations. These fibers have poor compatibility with several polymer matrices. Weak fiber/matrix interface reduces the reinforcing efficiency of fibers due to less stress transfer from the matrix to the fiber resulting in a poor performance of composite [10]. To enhance the compability between fiber and matrix, different physical [11], chemical [6] and biological [12] treatments are used by researchers for fiber surface modification. However, the use of some novel and environment friendly methods such as laser, ozone and plasma, are less common. Moreover, stiff micro/nano cellulose fillers as reinforcing element in polymer matrices are also considered promising candidates in the improvement of interface interaction and hence the performance of composites.

2 Purpose and aim of the thesis

The overall objectives of this research are to investigate the effect of addition of stiff cellulose micro fibrils, nanocellulose extracted from jute waste and its coating over woven jute reinforcement and some novel environment friendly fiber treatment methods on the bulk properties such as mechanical, creep and dynamic mechanical properties of composites. Jute has been selected as the reinforcing fiber due to its good mechanical properties, along with other advantages, such as very low cost, easy availability and renewability. Jute waste obtained from a jute processing mill is used as a low cost source of producing cellulose fibrils/fillers and green epoxy has been chosen as a matrix because of its high biobased contents and low petroleum derived contents. The specific objectives are as follows;

- To investigate the incorporation of pulverized micro jute fibrils prepared from jute waste on the mechanical and dynamic mechanical properties of alkali treated woven jute/green epoxy composites.
- To characterize the mechanical and dynamic mechanical properties of green epoxy composites reinforced with nanocellulose coated jute fabric.
- To investigate the influence of some novel treatment methods such as CO₂ pulsed infrared laser, ozone, enzyme and plasma on the creep and dynamic mechanical properties of woven jute/green epoxy composites.
- To model the short term creep data of composites using four parameters (Burger's) model and to predict the long term creep performance based on experimental data using Burger's model, Findley's power law model and a simple two-parameter power law model.

3 Overview of the current state of problem

Natural fibers utilization as reinforcing component in polymer composites is an effective way to produce light weight, low cost, ecofriendly, hygienic, naturally degradable and CO₂ neutral materials without adversely affecting the rigidity of the composites [13]. Many researchers have focused to modify the surface properties of natural fibers in the last two decades using different physical and chemical treatments and tried to overcome the compatibility issue of natural fibers and polymer matrices. Different modification techniques such as alkali [14-16], acetylation [17], graft co-polymerisation [18], silane [19] enzyme [20, 21], plasma [22, 23], ultrasound [24] and ultraviolet [25] treatments have been reported in literature to overcome the incompatible surface properties of natural fiber and polymer matrix. Beside that, cellulose micro/nano fillers in polymers have attracted considerable interest by improving the strength and stiffness of resulting composites [26-28]. Various types of cellulosic resources are used as precursors to extract and purify cellulose fibrils from lignocellulosic fibers. In the previous literature, cellulose micro/nano fibrils obtained from different precursors such as hemp fibers [29], pineapple [30], isora fibers [28] and jute fibers [31] are used as reinforcing filler in polymer matrices and resulted in the improvement of composite properties. Polymer composites used in engineering applications are often subjected to stress for a long time and at high temperatures. Creep behavior is a very important end-use property for bio-composites, because both the natural fiber reinforcement and polymer matrix exhibit time and temperature dependent properties. Thus a time and temperature dependent degradation in modulus (creep) and strength (creep rupture) may occur over time, as a

consequence of the viscoelasticity of the polymer matrix. Considerable studies can be found in literature on the creep behavior of bio-composites [32-34] to study the effect of interfacial adhesion and reinforcing fillers in polymer matrices. Different mathematical modelling techniques have also been applied to analyze creep behavior of composite materials [35, 36].

In this active area of research, the use of some novel methods especially CO₂ pulsed infrared laser and ozone in such modification processes of natural fibers and to evaluate the creep behavior of these surface modified fiber reinforced composite are less common. No study is available on the use of pulverized micro fillers (prepared from jute waste) in composites to evaluate their mechanical, creep and dynamic behavior. Nanocellulose coating over reinforcement instead of using it as filler in matrix is also a novel idea which is not explored yet.

4 Methods used, studied materials

4.1 Materials

Jute yarn having linear density 386 tex and 124 twists/m, produced from tossa jute (*C. olitorius*) fibers was used to produce a woven fabric having areal density of 600 gm⁻² with 5-end satin weave design on a shuttle loom. Warp and weft densities of the fabric were 6.3 threads per cm and 7.9 threads per cm respectively. Jute fabric was washed with 2 wt% non-ionic detergent solution at 70 °C for 30 min. to remove any dirt and impurities and dried at room temperature for 48 h. Waste jute fibers, sourced from a jute mill, were used for pulverization and purification and extraction of cellulose. Green epoxy resin CHS-Epoxy G520 and hardener TELALIT 0600 were supplied by Spolchemie, Czech Republic. Sulphuric acid (H₂SO₄) and Sodium hydroxide (NaOH) were supplied by Lach-Ner, Czech Republic. Sodium sulfate (Na₂SO₄) and sodium hypochlorite (NaOCl) were supplied by Sigma-Aldrich, Czech Republic.

4.2 Methods

4.2.1 Chemical pre-treatment of jute fabric and waste jute fibers

Figure 1 presents the flow chart of chemical pre-treatment of jute fabric and waste jute fibers. The jute fabric and waste jute fibers were immersed separately in 2 % NaOH solution for 1 h at 80 °C maintaining a liquor ratio of 15:1. Alkali treated waste jute fibers were further treated with 7 g/l NaOCl solution at room temperature for 2 h under pH 10 - 11 and subsequently antichlored with 0.1 % Na₂SO₄ at 50 °C for 20 min. Both fabric and waste fibers, after chemical pretreatment, were washed with fresh water several times until the final pH was maintained at 7.0 and then allowed to dry at room temperature for 48 h and at 100 °C in an oven for 2 h.

4.2.2 Pulverization of waste jute fibers

Pulverization of chemically treated waste jute fibers was carried out using a high-energy planetary ball mill of Fritsch pulverisette 7. Pulverization process relies on the principle of energy release at the point of impact between balls as well as on the high grinding action created by friction of balls on the wall [37]. The sintered corundum container of 80 ml capacity and zirconium balls of 10 mm diameter were chosen for 1 hour of pulverization. The ball to material ratio (BMR) was kept at 10:1 and the speed was kept at 850 rpm.

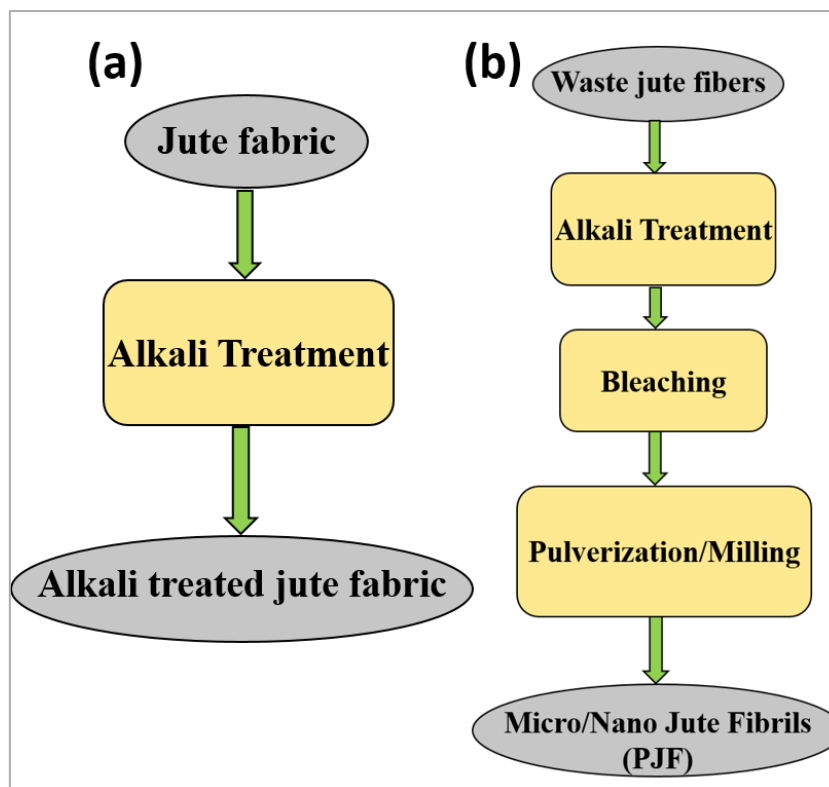


Figure 1. Process flow chart of chemical pre-treatment of (a) jute fabric and (b) waste jute fibers

4.2.3 Purification and extraction of nanocellulose from waste jute fibers and nanocellulose coating

The main steps followed to purify and extract nanocellulose from waste jute fibers are depicted in figure 2. Waste jute fibers were chopped to approximate length of 5 - 10 mm and immersed in 2 % sodium hydroxide (NaOH) solution for 2 h at 80 °C temperature maintaining a liquor ratio of 50:1. The process was repeated three times. The fibers were then washed with tap water several times to remove any traces of NaOH sticking to the fibers surface. The jute fibers were then bleached with 7 g/l sodium hypochlorite (NaOCl) solution at room temperature for 2 h under pH 10 - 11 and subsequently antichlored with 0.1 % sodium sulphate (Na₂SO₄) at 50 °C for 20 min. Finally, the fibers were washed with tap water several times until the final pH was maintained at 7.0 and then allowed to dry at room temperature for 48 h and at 100 °C in an oven for 2 h. Alkali and bleaching treatments were used to purify cellulose and to remove maximum amount of hemicellulose and lignin from the fibers. The bleached jute fibers were milled using a high-energy planetary ball mill of Fritsch pulverisette 7. Milling process relies on the principle of energy release at the point of impact between balls as well as on the high grinding action created by friction of balls on the wall [37]. The sintered corundum container of 80 ml capacity and zirconium balls of 10 mm diameter were chosen for 20 min of milling. The ball to material ratio (BMR) was kept at 10:1 and the speed was kept at 850 rpm. Acid hydrolysis of milled jute fibers was conducted for 1 hour at 45 °C under mechanical stirring using 65 % (w/w) H₂SO₄. The fiber content during acid hydrolysis was 5 % (w/w). The suspension was diluted with cold water (4 °C) to stop the reaction, neutralized with NaOH solution and discolored by NaOCl solution. The supernatant was removed from the sediment and replaced by new distilled water several times. Finally, 3 %, 5 % and 10 % (w/w) nanocellulose suspensions were prepared by increasing cellulose concentration and decreasing water concentration through filtration using Buchner funnel. The prepared nanocellulose suspensions (3, 5, and 10 wt %) were ultrasonicated for 5 min

with Bandelin ultrasonic probe and then applied on the surface of jute fabric by roller padding at room temperature. Finally, the coated fabrics were dried at 70 °C for 60 min.

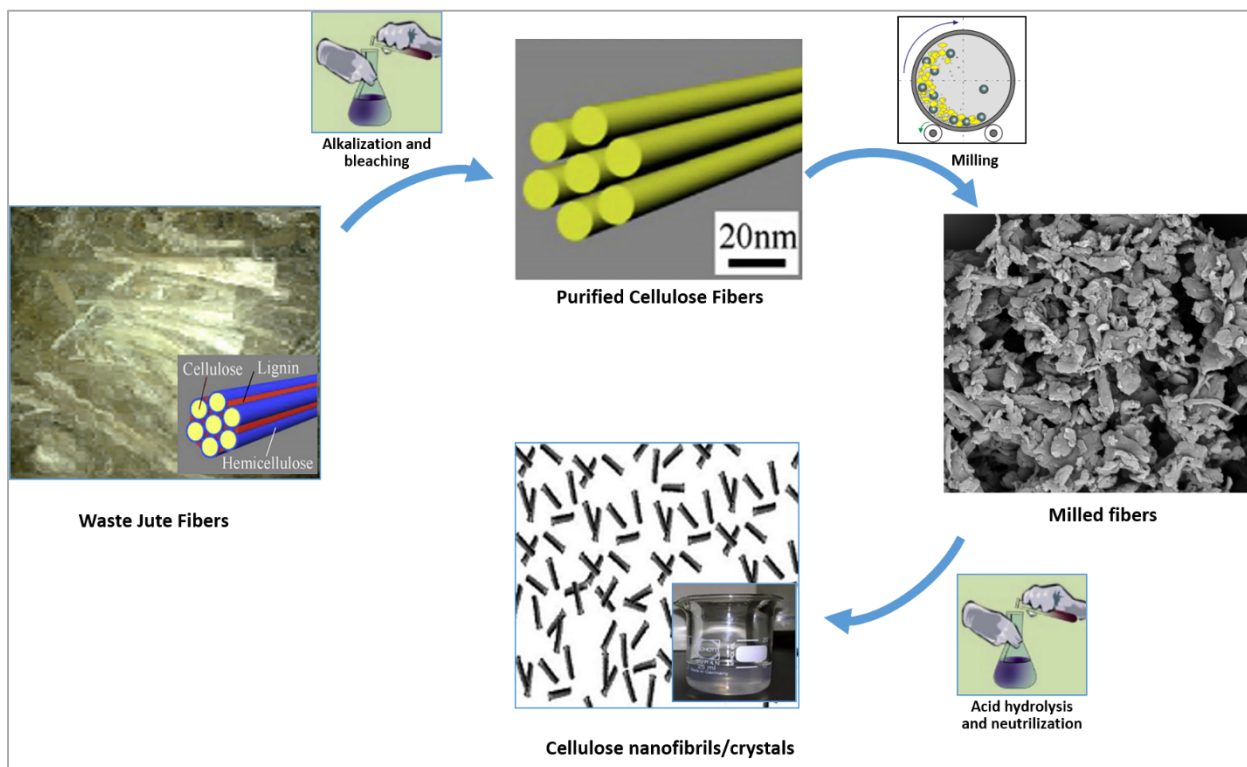


Figure 2. Steps adopted in the purification and extraction of cellulose nanofibrils from waste jute fibers

4.2.4 Treatment methods

Enzyme treatment

Untreated jute fabric was subjected to enzyme treatment. A solution, having 1 % owf Texazym DLG new, 3 % owf Texzym BFE and 0.2 g/l of Texawet DAF anti-foaming agent (all supplied by INOTEX, Czech Republic) in distilled water, was prepared. Texazym DLG new, catalyzes the decomposition of hemicellulose and partially lignin and can affect cellulose in fiber. Texzym BFE, helps the removal and decomposition of interfiber binding substances. Jute fabric was dipped in the solution at 50 °C for 2 h maintaining a liquor ratio of 10:1. After the treatment, the fabric was rinsed with fresh water several times and dried at room temperature for 48 h.

Ozone treatment

Ozone treatment was done by putting the jute fabric for 1.0 h in a closed container filled with ozone gas. The container was connected to ozone generator “TRIOTECH GO 5LAB-K” (TRIOTECH s.r.o. Czech Republic) which was continuously generating ozone gas at the rate of 5.0 g/h. Oxygen for the production of ozone gas was generated by “Kröber O2” (KröberMedizintechnik GmbH, Germany).

Laser treatment

Laser irradiation was performed on the surface of jute fabric with a commercial carbon dioxide pulse infrared (IR) laser “Marcatex 150 Flexi Easy-Laser” (Garment Finish Kay, S.L. Spain), generating laser beam with a wavelength of 10.6 μm. Parameters that determine marking

intensity of laser are marking speed [bits/ms], duty cycle [%] and frequency [kHz]. In this study, the marking speed was set to 200 bits/ms, the duty cycle (DC) to 50 % and frequency to 5 kHz. The used laser power was 100 W. Laser beams interact with fibers by local evaporation of material, thermal decomposition or changing the surface roughness [38].

Plasma treatment

Jute fabric was treated for 60 s with dielectric barrier discharge (DBD) plasma with discharge power of 190 W at atmospheric pressure using a laboratory device (Universal Plasma Reactor, model FB-460, Czech Republic).

4.2.5 Preparation of composites

The composite laminates were prepared by hand layup method. The resin and hardener were mixed in a ratio of 100:32 (by weight) according to manufacturer recommendations, before hand-layup. Three different categories of composite laminates were prepared using same green epoxy matrix. The first type of composite was consisted of 1, 5 and 10 wt % of pulverized micro jute fibers (PJF) used as fillers, along with alkali treated jute fabric. The second type was enclosed with nanocellulose coated jute fabric with different cellulose concentrations (3, 5 and 10 wt %) and third type was comprised of surface treated jute fabrics. The composite layup along with Teflon sheets were sandwiched between a pair of steel plates and cured at 120 °C for 1.0 h in mechanical convection oven with predetermined weight on it to maintain uniform pressure of about 50 kPa [39]. The fiber volume fraction (V_f) of all composites was in the range of 0.25 - 0.27 having 3 layers of fabric with orientation of each layer in the same direction. In first category, composites were designated as *U* (untreated), *A* - 0 % (alkali treated jute fabric with 0 wt % of PJF), 1 %, 5 % and 10 % (alkali treated jute fabric with 1, 5 and 10 wt % of PJF) respectively. In the second category, composite samples were designated as CF0 (uncoated), CF3 (3 wt % nanocellulose coated), CF5 (5 wt % nanocellulose coated) and CF10 (10 wt % nanocellulose coated) whereas, in third category, composites were designated as untreated (untreated jute fabric), enzyme (enzyme treated jute fabric), laser (laser treated jute fabric), ozone (ozone treated jute fabric) and plasma (plasma treated jute fabric).

4.2.6 Characterization and testing

Scanning electron microscopy (SEM)

The surface topologies of chemically treated and pulverized jute fibers, nanocellulose coated jute fabrics and surface treated jute fabrics, were observed with Vega-Tescan TS5130 scanning electron microscope. The surface of fibers was gold coated prior to SEM inspection to improve the conductivity of samples. The pictures were taken at a slow scanning speed to obtain higher quality image.

Fourier transform infrared spectroscopy (FTIR) and particle size distribution

FTIR spectroscopy was done to confirm the removal of non-cellulosic contents (e.g. hemicellulose and lignin) from alkali treated jute fabric and bleached jute fibers. A Thermo Fisher FTIR spectrometer, model Nicolet iN10, was used in this study. The spectrometer was used in the absorption mode with a resolution of 4 cm^{-1} . Moreover, in order to measure the size (width) distribution of pulverized jute fibers and nanocellulose using SEM images, the topology of PJF and cellulose nanofibrils was also observed on Zeiss Ultra Plus field emission scanning electron microscope (FE-SEM) at low accelerating voltage (1.0 kV) and low probe current (≈ 10

pA) to eliminate charging effect and sample damage due to interaction with primary electrons. The software used for image analysis was NIS Elements BR 3.22.

X-ray diffraction (XRD)

X-ray diffraction patterns were recorded on a PANalytical X' Pert PRO MPD diffraction system for untreated jute, bleached jute and jute cellulose nanofibrils in order to examine the change in crystallinity of the material after bleaching and acid hydrolysis.

Mechanical testing

Tensile and flexural tests

Tensile properties of first category of composites (incorporated with PJF) were measured on a universal testing machine whereas for second category of composites (reinforced with nanocellulose coated jute fabrics), were characterized on an MTS series 370 servo-hydraulic load frame equipped with 647 hydraulic wedge grip of 100 kN load capacity at a cross head speed of 2 mm/min and gauge length of 100 mm in accordance with ASTM D3039-00 [40] using rectangular specimens of dimension $200 \times 20 \times h$ mm³, where “*h*” is the actual thickness of specimen. Flexural test was performed for all categories of composites in three point bending mode on a universal mechanical testing machine, Shimadzu AGS-J with 5kN load cell, following ASTM D790-03 [41] standard at a cross head speed of 2 mm/min. The specimens of dimension $160 \times 12.7 \times h$ mm³ were used maintaining a span to thickness ratio of 32:1 according to standard recommendations (“*h*” is the actual thickness of specimen). Five specimens were tested for each condition and for each test to get an average value.

Fatigue test

The tension-tension fatigue performance of second category composites was experimentally evaluated at two different stress levels (80 % and 70 % of the ultimate tensile stress σ_u) assuming the same geometry of specimens as the one adopted in quasi-static tensile tests. Tests were performed at gage length of 100 mm under constant stress amplitude, stress ratio (R) of 0.1 (ratio of maximum to minimum stress during a loading cycle) and frequency of 5 Hz. Three specimens were tested for each stress level up to final failure of specimens. Tests were realized on the same MTS series 370 servo-hydraulic loading machine equipped with 647 hydraulic wedge grip of 100 kN load capacity.

Fracture toughness

Fracture toughness, K_{Ic} , of second category composites was determined by three point bending method using the single edge notch bend (SENB) specimens in accordance with the standard test method ASTM D5045-99 [42]. A sharp crack of length “*a*” between 0.45 W and 0.55 W was introduced by using a notch maker CEAST NOTCHVIS and a fresh razor blade at the notch tip (‘W’ is the width of specimen). The specifications of fixture and specimens are shown in figure 3.

The tests were performed using universal mechanical testing machine, Shimadzu AGS-J with 5 kN load cell, at a cross head speed of 10 mm/min. Five specimens were tested for each condition to get an average value. Statistical analysis of tensile, flexural and fracture toughness properties was done by one-way analysis of variance (ANOVA) and probability value $p \leq 0.05$ was considered as an indicative of statistical significance compared to the control samples.

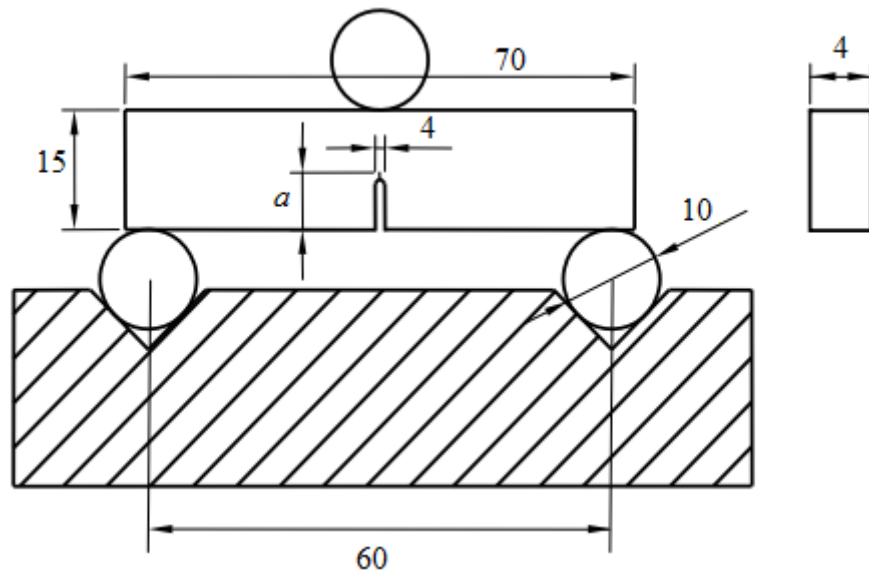


Figure 3. SENB (single edge notch bending) specimen and fixture dimensions for flexural test (dimensions in mm).

Creep tests

Short-term creep tests were performed for only first and third category of composites in three point bending mode at temperatures 40 °C, 70 °C and 100 °C using Q800 dynamic mechanical analysis (DMA) instrument of TA instruments (New Castle DL, USA) for 30 minutes. The static stress of 2.0 MPa was applied at the center point of long side of the sample through the sample thickness for 30 min after equilibrating at the desired temperature and creep strain was measured as a function of time. The static stress was selected after performing a strain sweep test, where the linear viscoelastic region was defined for each of the composites ensuring that the creep tests were conducted in the linear viscoelastic region. The time-temperature superposition principle (TTSP) was selected for short-term creep tests performed at various temperatures for first category composites (jute/green epoxy composites incorporated with various contents of PJF). The temperature range was 40 – 100 °C, in 5 °C steps, and the isothermal tests were run on the same specimen in the specified temperature range. The 2.0 MPa stress was applied for 10 min at each temperature. In every measurement, the specimen was equilibrated for 5 min at each temperature, in order to evenly adjust for the correct temperature of the specimen.

Dynamic mechanical analysis

The dynamic mechanical properties of all composite categories were measured in 3-point bending mode using the same instrument for creep testing. The testing conditions were controlled in the temperature range of 30 – 190 °C, with a heating rate of 3 °C/min, fixed frequency of 1 Hz, preload of 0.1 N, amplitude of 20 μm, and force track of 125 %. The samples having a thickness of 4 – 4.5 mm, width of 12 mm and span length of 50 mm were used for both creep and DMA testing. Two replicate samples were tested for each test condition and average values were reported.

Creep modelling

Four parameters (or the Burger's) model is one of the mostly used physical models to give the relationship between the morphology of polymer composites and their creep behavior [43, 44]. It is based on a series combination of a Maxwell element with a Kelvin–Voigt element. The total

creep strain is divided into three separate parts: ε_M the instantaneous elastic deformation (Maxwell spring), ε_K viscoelastic deformation (Kelvin unit) and ε_∞ viscous deformation (Maxwell dash-pot). Thus, total strain as a function of time can be represented by the following equations:

$$\varepsilon(t) = \varepsilon_M + \varepsilon_K + \varepsilon_\infty \quad [1]$$

$$\varepsilon(t) = \frac{\sigma_0}{E_M} + \frac{\sigma_0}{E_K} (1 - e^{-E_K t / \eta_K}) + \frac{\sigma_0}{\eta_M} t \quad [2]$$

where $\varepsilon(t)$ is the creep strain, σ_0 is the stress, t is the time, E_M and E_K are the elastic moduli of Maxwell and Kelvin springs, and η_M and η_K are the viscosities of Maxwell and Kelvin dashpots. η_K/E_K is usually denoted as τ , the retardation time required to generate 63.2 % deformation in the Kelvin unit [36]. ε_M is a constant value and does not change with time. ε_K represents the earliest stage of creep and attains a saturation value in short time and ε_∞ represents the trend in the creep strain at sufficiently long time, and appears similar to the deformation of a viscous liquid obeying Newton's law of viscosity. The values of four parameters E_M , E_K , η_M , η_K can be obtained by fitting the eq. 2 to the experimental data and can be used to describe the creep behavior of composites. The creep rate of viscoelastic materials can be obtained by taking the derivative of eq. 2.

$$\frac{d\varepsilon(t)}{dt} = \frac{\sigma_0}{E_K} (e^{-E_K t / \eta_K}) + \frac{\sigma_0}{\eta_M} \quad [3]$$

The Findley's power law model is an empirical mathematical model used to simulate the creep behavior of polymer composites. The model can be represented by the following eq. 4 [44];

$$\varepsilon(t) = at^b + \varepsilon_0 \quad [4]$$

where, a and b are the material constants and ε_0 is the instantaneous strain. The ability of Findley's power law model to simulate the creep data has been found to be satisfactory in several studies [33, 36, 45]. However, this model is not able to explain the creep mechanism of material. A two parameter empirical power law model has also been used in some studies [34, 46] to simulate the creep data. It has the form;

$$\varepsilon(t) = at^b \quad [5]$$

Where, a and b are the material constants.

The long term creep is an important parameter to evaluate the end-use performance of natural fiber polymer composites but it is often impractical to perform a creep test for an extremely long period of time. Time-temperature superposition (TTS) is one of the common estimation techniques to predict the long term creep behavior by shifting the curves from tests at different temperatures horizontally along the logarithmic time axis to generate a single curve known as master curve [43]. The shifting distance is called shift factor.

The Burger's model was used to simulate the short term creep data of first and third category of composites as well as long term creep prediction of only first category of composites whereas, the Findley's power law model and two parameters empirical power law model were used for long term creep prediction of first category of composites. The non-linear curve fit function of the OriginPro 9.0 software was used for modeling the creep curves and fitting the models to the experimental data. The minimum sum of squared deviation of experimental data from the creep models and coefficient of determination (R^2) were selected as criterion [47]. The R^2 is defined as model sum of squares divided by total sum of squares. A better goodness-to-fit is obtained when R^2 is closer to 1.

5 Summary of results achieved

5.1 Effect of pulverized micro jute fillers loading on the mechanical, creep and dynamic mechanical properties of jute/green epoxy composites

5.1.1 Characterization of jute fibers

FTIR analysis was carried out to confirm some removal of non-cellulosic contents (e.g. hemicelluloses and lignin) from the surface of jute fibers after pretreatments. The FTIR spectra of untreated and treated jute are shown in figure 4. The major difference observed between the spectra is the disappearance/reduction of peaks at $\sim 1730\text{ cm}^{-1}$ and $\sim 1240\text{ cm}^{-1}$. The peak at $\sim 1730\text{ cm}^{-1}$ is due to stretch vibration of C=O bonds in carboxylic acid and ester components of cellulose and hemicellulose [48] and also carbonyl group of lignin [49, 50]. The peak at $\sim 1240\text{ cm}^{-1}$ is due to C–O–C asymmetric stretching of the acetyl group of lignin [51]. The reduction/disappearance of these peaks confirm the partial removal of hemicellulose and opening up of the lignin structure in the jute fibers after pretreatments.

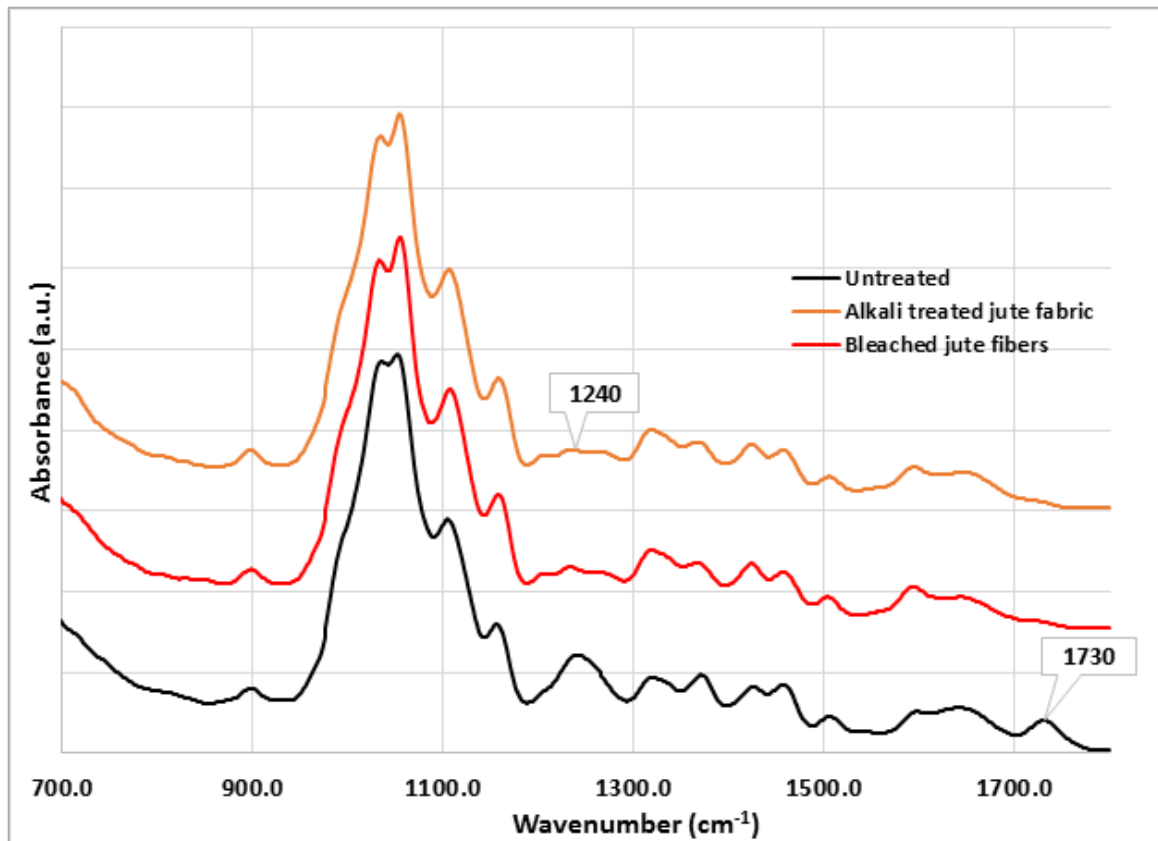


Figure 4. FTIR spectra of jute fibers.

The SEM image is precisely analyzed to measure the size (diameter) of pulverized jute fibers (PJF), after one hour of milling, as shown in figure 5a. The histogram of size distribution of 100 measurements is shown in figure 5b. The calculated average diameter (width) of PJF was found to be $1.856 \pm 0.899\ \mu\text{m}$.

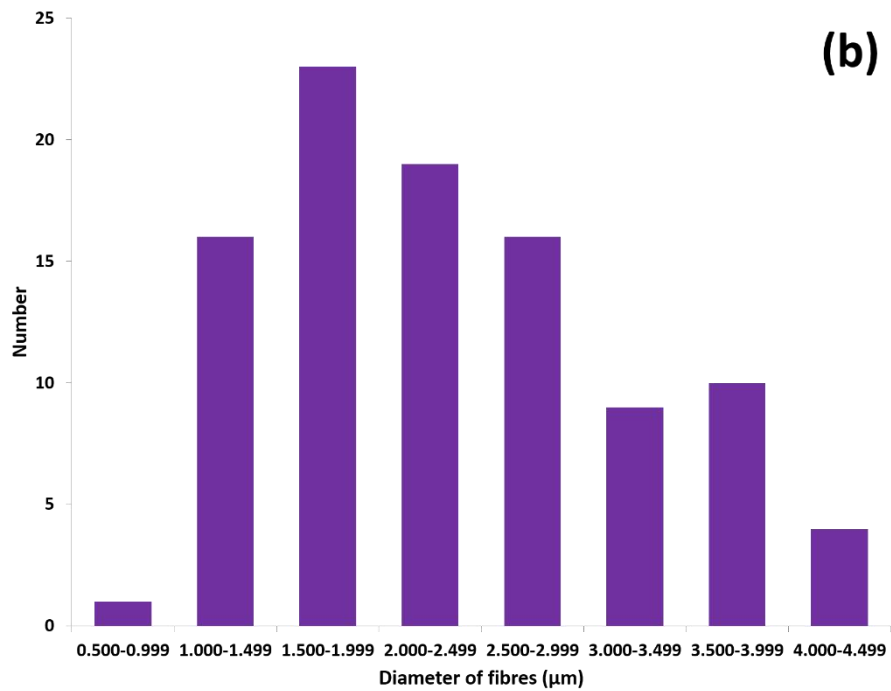
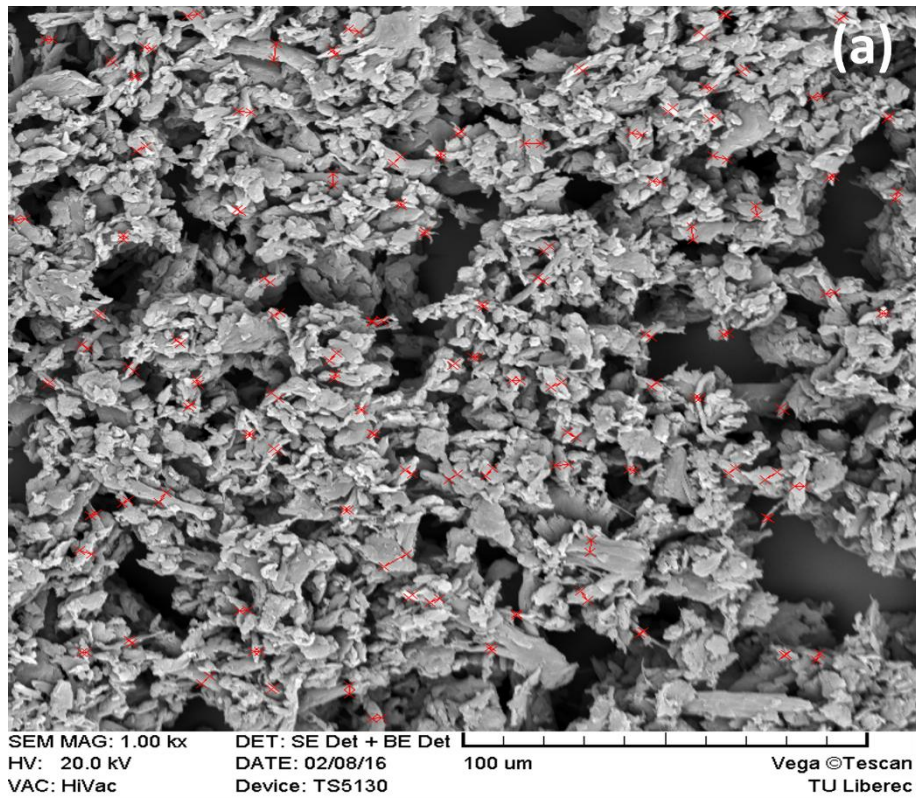


Figure 5. (a) SEM image of jute fibers after 1.0 h of pulverization and (b) histogram of particle width distribution.

5.1.2 Tensile properties

Figure 6 shows the average values and standard deviation of ultimate tensile strength and tensile modulus of alkali treated jute composites with different loadings of PJF. It is interesting to note that alkali treatment of jute fabric has resulted in a lowering of the tensile strength but increase in tensile strength and tensile modulus is observed with the incorporation of PJF. The tensile strength decreases from 42.48 MPa for untreated composite to 40.65 MPa for alkali treated composite thus presenting 4.3 % decrease on average. However, tensile strength improves by

factors of 4.9 %, 14 % and 8 % with 1, 5 and 10 % loading of PJF respectively as compared to untreated composite. Similarly, tensile modulus increases from 2.97 GPa for untreated composite to 3.05 GPa, 3.16 GPa, 3.20 GPa and 3.05 GPa for A-0 %, 1 %, 5 % and 10 % composites respectively, thus permitting 2.7 %, 6.3 %, 7.7 % and 2.7 % increase on average as shown in figure 6. We must keep in mind that the mechanics of textile composites is different from those of short fiber composites. The major contribution to strength in textile composites is the alignment of yarns in warp and weft direction. Alkali treatment results in the partial unwinding of yarns (as hemicellulose dissolves), and hence the alignment gets antagonized. This results in a lowering of the strength of composites [52]. The incorporation of PJF as filler in matrix provides a better reinforcing effect thus improving fiber/matrix interfacial interactions in composites and hence tensile properties. The ANOVA for the tensile strength ($p = 0.010$) shows the statistically significant difference but for tensile modulus ($p = 0.075$) does not show significant difference between the means at the 95.0% confidence level.

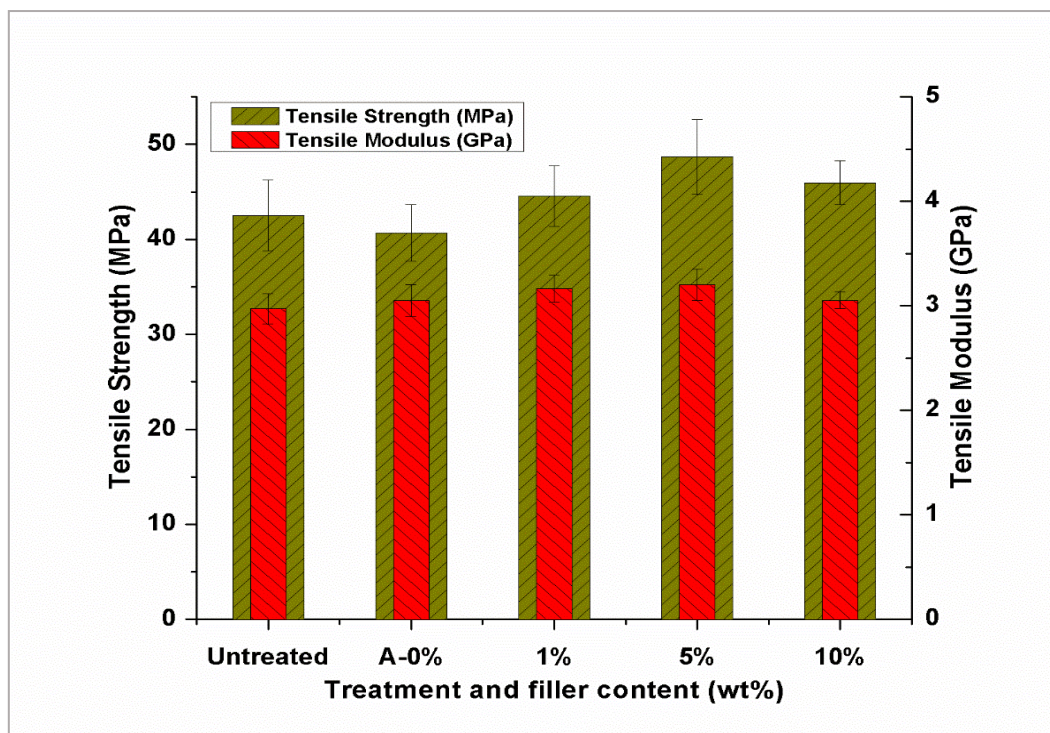


Figure 6. Tensile strength and modulus of composites incorporated with different loadings of PJF

5.1.3 Flexural properties

The flexural strength and modulus increase with the increase in contents of PJF in alkali treated jute composites as shown in figure 7. The flexural strength and modulus increase from 32.78 MPa and 3.83 GPa for untreated composite to maximum of 41.66 MPa and 4.35 GPa for composite loaded with 5 wt% of PJF respectively, thus allowing 27 % and 13.6 % increase on average as shown in figure 7. These findings also suggest better reinforcing effect provided by PJF thus contributing to strong interfacial interaction of fiber and matrix. However, the reason for a little reduction in the tensile and flexural properties of composite for 10 wt% loading of PJF (compared to 5 % composite) may be due to the aggregation of PJF, which generates defects in the material. Stress concentration is likely to occur within the resin or agglomerated particles, which could generate slippage within the material because of the external force, resulting in reduction tensile properties [53]. The ANOVA for the flexural strength ($p = 0.000$) and flexural

modulus ($p = 0.038$) showed the statistically significant difference between the means at the 95.0% confidence level.

5.1.4 Short term creep

Figure 8 shows the creep strains for jute composites as a function of time with 0, 1, 5 and 10 wt% of PJF content at three different temperature conditions. It is visibly apparent that the composites have low instantaneous deformation ϵ_M and creep strain at 40 °C due to higher stiffness of composites but this deformation increases at higher temperatures due to decrease in composites stiffness. The creep strain of all composites also increased at higher temperatures but the untreated jute composites was affected more than the others. The creep strain of alkali treated with 0% PJF composite is less than untreated one. This may be explained due to increase in surface roughness of jute fabric after alkali treatment and decrease in frictional slippage of matrix polymer chains at the fiber/matrix interface resulting in less creep deformation than untreated composite. The least creep strain is shown by composite incorporated with 10 % PJF at all temperatures followed by 5 % and 1 % PJF incorporated composites. At 100 °C, 5 % and 10 % PJF composites have almost same instantaneous elastic deformation but 10 % composite has less viscous deformation over time. This may be attributed to greater inhibition of slippage and reorientation of polymer chain with increasing contents of PJF. The Burger’s model curves show a satisfactory agreement with the experimental data (figure 8).

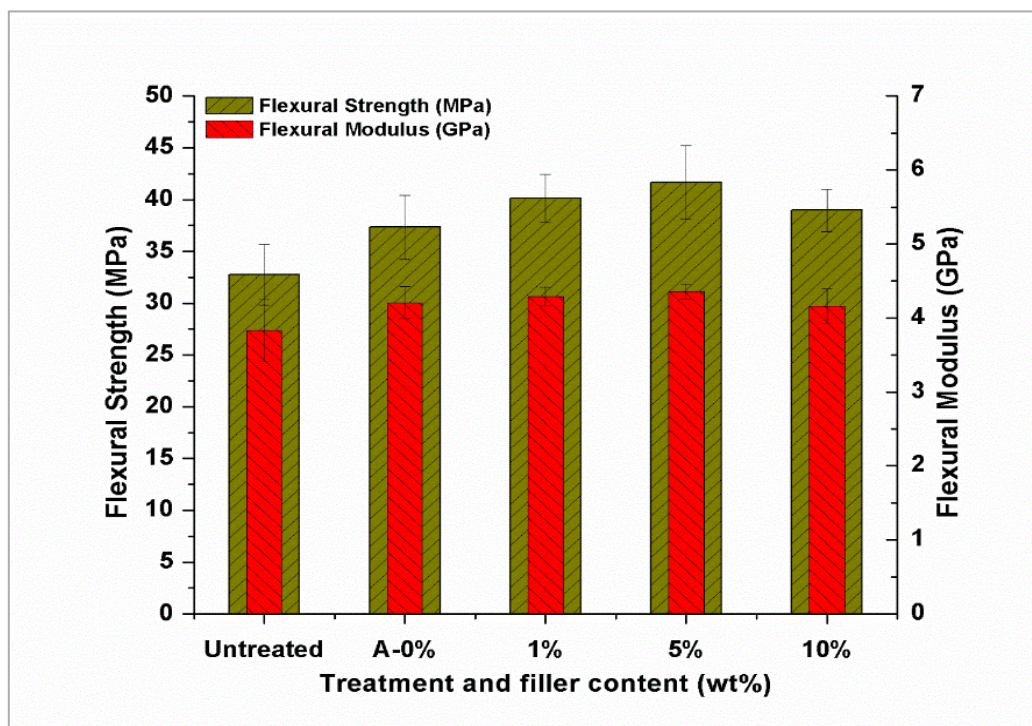


Figure 7. Flexural strength and modulus of composites incorporated with different loadings of PJF

The four parameters E_M , E_K , η_M , η_K of Burger’s model, used to fit the eq. 2 to the experimental data, are summarized in table 1. The first value is parameter estimator and value in parenthesis is corresponding standard deviation. All four parameters were found to decrease for all composites as temperature increased (table 1). E_M corresponds to the elasticity of the crystallized zones in a semicrystallized polymer. Compared to the amorphous regions, the crystallized zones are subjected to immediate stress due to their higher stiffness. The instantaneous elastic modulus is recovered immediately once the stress is removed. E_K is also coupled with the stiffness of

material. The decrease in parameters E_M , E_K resulted from the increase in the instantaneous and the viscoelastic deformations as temperature increased. The viscosity η_M corresponds to damage in the crystallized zones and irreversible deformation in the amorphous regions and the viscosity η_K is also associated with the viscosity of the amorphous regions in the semicrystallized polymer [54]. The decrease in viscosity parameters η_M , η_K propose an improvement in the mobility of molecular chains at higher temperature. The parameters for untreated and alkali treated with 0 % PJF composites have undergone a largest decrease, resulting in higher creep strain. The composites incorporated with PJF, especially 5 and 10 %, have comparatively better values of parameters particularly η_M which is related to the long term creep strain and validates less temperature dependence of these composites (figure 8). The viscosity η_M increases with the increase in PJF % and permanent deformation decreases. Figure 9a, b compares the creep strain and strain rate of untreated and 10 % PJF composites at various temperatures. Comparatively, temperature had more influence on the creep deformation of untreated jute composite than that of 10 % PJF composite.

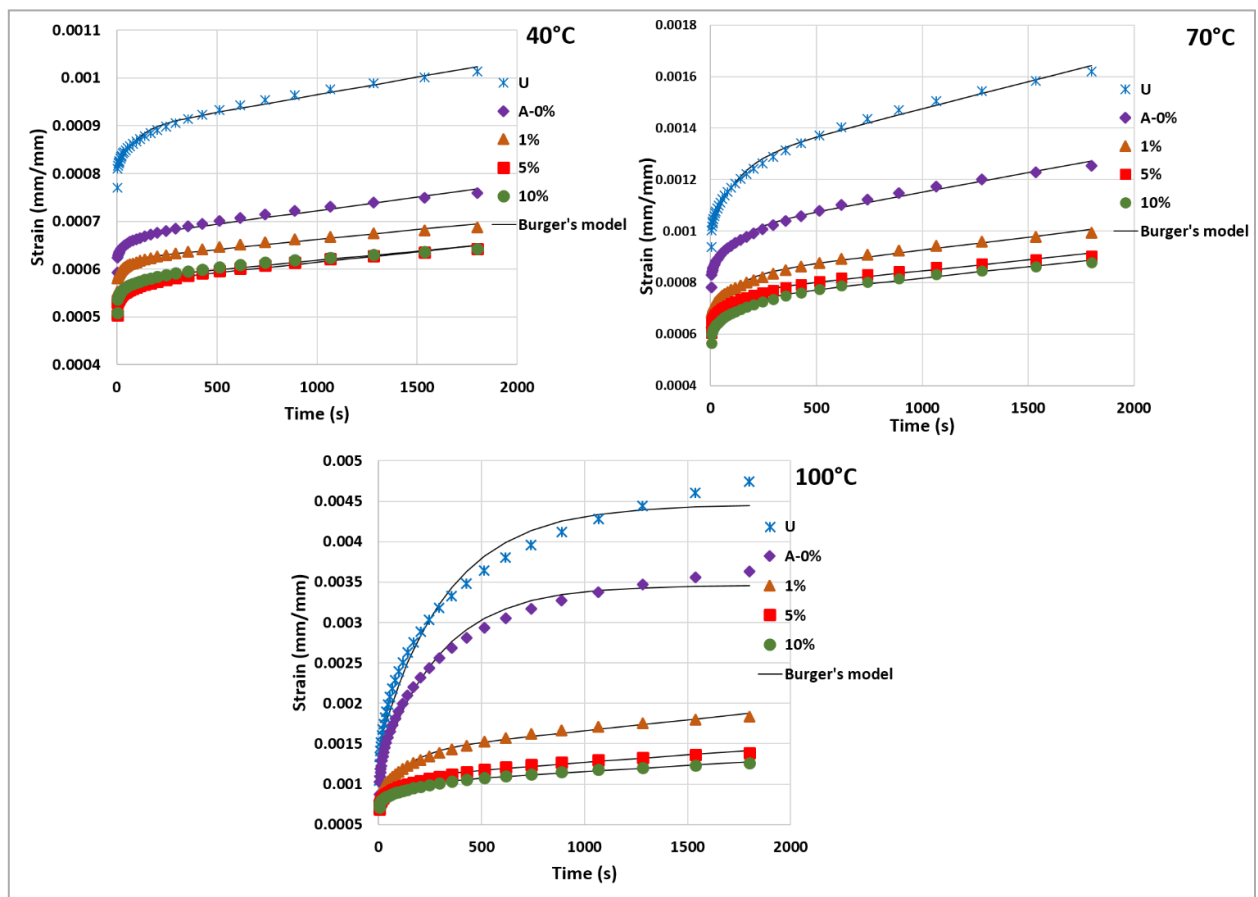


Figure 8. Creep curves of composites incorporated with different loadings of PJF at different temperatures.

5.1.5 Time-temperature superposition (TTS)

The creep curves corresponding to different temperature levels were shifted along the logarithmic time axis according to time-temperature superposition principle using TA Instruments Thermal Advantage™ software to generate a master curve at a reference temperature of 40 °C. The shifting procedure of this curve obeys the Williams–Landel–Ferry (WLF) equation. The WLF equation is given by eq. 6;

$$\log \alpha_T = \frac{-C_1(T-T_0)}{C_2+(T-T_0)} \quad [6]$$

Where α_T is the horizontal (or time) shift factor, C_1 and C_2 are constants, T_0 is the reference temperature [K] and T is the test temperature [K].

Table 1. Simulated four parameters in Burger's model for short term creep of the composites.

Temperature	Parameters	Composite types				
		Untreated	Alkali - 0 %	1 %	5 %	10 %
40 °C	E_m [MPa]	2477.24 (78.3)	3259.41(138.0)	3492.53 (133.8)	3810.53 (133.6)	3774.75 (149.1)
	E_k [MPa]	23876.27 (10854.5)	38244.62 (19726.9)	42496.38 (21110.6)	44220.12 (21281.1)	40549.80 (19016.6)
	η_m [Pa.s]	2.72E7 (1.33E7)	3.54E7 (1.22E7)	4.77E7 (2.04E7)	4.54E7 (1.97E7)	5.11E7 (2.47E7)
	η_k [Pa.s]	2.11E6 (2.38E6)	1.37E6 (2.09E6)	1.73E6 (2.5E6)	2.53E6 (3.49E6)	1.90E6 (2.62E6)
	SS^*	2.65033E-9	1.29037E-9	1.04302E-9	9.92292E-10	1.08146E-9
	$Adj. R^2$	0.97524	0.97061	0.96424	0.96929	0.96304
70 °C	E_m [MPa]	1985.89 (91.9)	2403.61 (102.7)	2921.19 (118.5)	3116.67 (118.6)	3323.10 (131.9)
	E_k [MPa]	7790.84 (2752.5)	11972.90 (4497.3)	14228.47 (5360.3)	16946.57 (6037.4)	15615.45 (5726.5)
	η_m [Pa.s]	9.48E6 (3.81E6)	1.32E7 (5.14E6)	1.98E7 (9.71E6)	2.33E7 (1.08E7)	2.27E7 (1.13E7)
	η_k [Pa.s]	956179.43 (6.90E5)	1.32E6 (1.09E6)	1.71E6 (1.34E6)	1.81E6 (1.45E6)	1.94E6 (1.44E6)
	SS^*	1.08937E-8	5.93037E-9	3.81543E-9	2.74811E-9	2.87718E-9
	$Adj. R^2$	0.98881	0.98689	0.9851	0.9847	0.98596
100 °C	E_m [MPa]	1380.05 (294.3)	1743.43 (306.1)	2417.83 (218.3)	2653.56 (183.6)	2616.45 (123.7)
	E_k [MPa]	665.35 (117.7)	865.63 (121.6)	3543.54 (958.0)	6087.72 (1783.7)	8457.41 (2683.5)
	η_m [Pa.s]	-4.13E20 (0.0)	-6.00E32 (0.0)	7.44E6 (3.92E6)	1.08E7 (5.26E6)	1.31E7 (5.97E6)
	η_k [Pa.s]	219089.75 (1.03E5)	255733.51 (9.91E4)	457813.67 (2.43E5)	705184.01(4.39E5)	1.11E6 (6.84E5)
	SS^*	8.30033E-7	3.37586E-7	2.87859E-8	1.31777E-8	6.79893E-9
	$Adj. R^2$	0.97565	0.98358	0.99023	0.98826	0.98971

SS^* : Sum of squared deviations

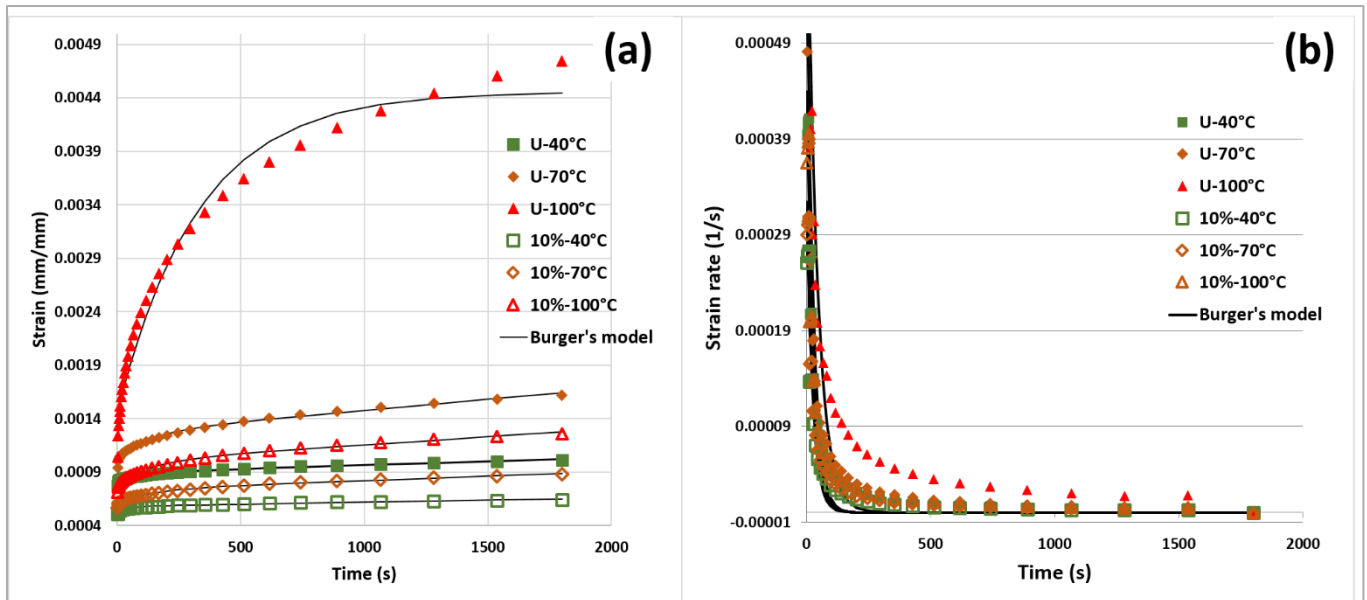


Figure 9. Creep strain (a) and strain rate (b) of untreated and 10 % PJF composites at different temperatures.

The master curves, which give an indication of long-term creep performance of composites, are plotted in log-log scale and presented in figure 10. The master curves show better creep resistance of composites with increasing content of PJF. It is obvious that the best long term performance is shown by composites incorporated with 5 and 10 % PJF indicating their good reinforcing effectiveness. It is also interesting to note that above log-time 4.0 seconds, the creep deformation of untreated, 0 and 1 % composites show a faster tendency of increase compared to 5 and 10% PJF composites. These findings show that under the small stress, the materials entered into a viscoelastic state over an extremely long period of time, and in viscoelastic state the role of 1 % incorporation of PJF in the reinforcement effectiveness is less than that of 5 and 10 % PJF.

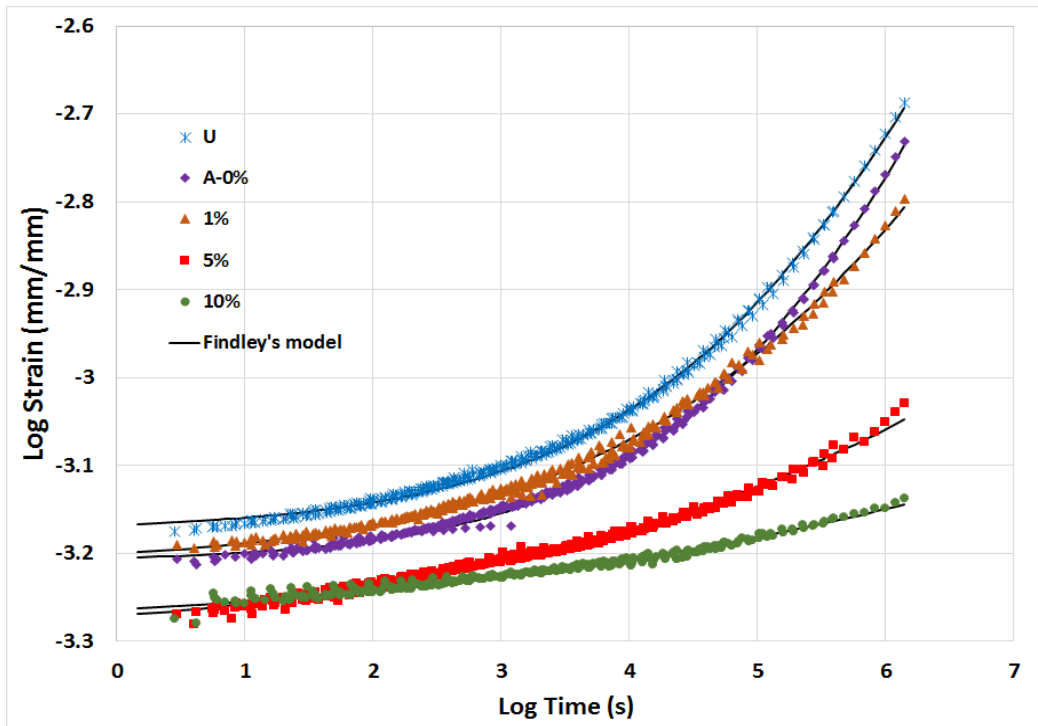


Figure 10. TTS master curves for creep of the composites incorporated with different loadings of PJF at a reference temperature of 40 °C.

The simulated parameters of Burger, Findley and two parameters power law models are summarized in table 2. The first value is parameter estimator and value in parenthesis is corresponding standard deviation. Based on the sum of squared deviations (SS) and R^2 values, it can be clearly seen that Findley's model is good to predict the long-term creep performance as compared to Burger's and two parameter power law model. It is also shown in figure 10 that the prediction ability of the Findley's model is good for the long-term creep behavior of composites. However, this model provides the adequate prediction ability within the steady state creep and given time interval as revealed by some researchers [55, 56] while for longer time duration, the calculated data may show considerable deviation from the experimental data. The sum of squared deviations and R^2 values, given in table 2, also suggest that the Burger's model shows some deviation and that of two parameter power law model shows a little large deviation from the experimental data. Similar findings were reported by other researchers [33, 57].

The parameters of Burger's model, resulted from fitting master creep curves, are very different from those of the short term creep tests. It can be seen from table 2 that all the Burger's model parameters increase with the increase in loading of PJF %. The η_M , which determines long-term creep, is lowest for untreated composite and highest for 10 % PJF composite. Therefore, the untreated composite shows the highest and 10 % PJF composite shows the lowest creep deformation. It is also obvious for Findley's model that the parameter a (reflecting short-term creep) increased and parameters ε_0 (reflecting the instantaneous initial creep strain) and b (reflecting log-term creep) decreased with the increasing content of PJF which indicates an enhanced long-term creep performance with PJF loading. Similarly, for two parameter power law model, parameter a (reflecting short-term creep) increased and parameter b (reflecting log-term creep) decreased with the increasing content of PJF.

Table 2. Simulated parameters of Burger's model, Findley's power law model and two parameters power law model for long term creep prediction of the composites at 40 °C.

Temperature	Parameters	Composite types				
		Untreated	Alkali - 0%	1 %	5 %	10 %
Burger's model	E_m [MPa]	2713.76 (193.6)	3002.45 (184.0)	2904.39 (179.0)	3478.01 (191.0)	3517.07 (125.5)
	E_k [MPa]	4781.98 (2005.8)	5470.29 (2194.5)	6271.53 (2337.0)	15949.06 (7113.4)	31490.67 (16174.2)
	η_m [Pa.s]	2.64E9 (1.29E9)	2.94E9 (1.29E9)	4.01E9 (2.19E9)	9.44E9 (6.93E9)	2.10E10 (2.04E10)
	η_k [Pa.s]	1.0227E8 (8.73E7)	1.35E8 (1.05E8)	9.24E7 (7.83E7)	6.76E7 (9.00E7)	9.49E7 (1.53E8)
	SS^*	4.86566E-7	3.00571E-7	2.96188E-7	1.2249E-7	4.56987E-8
	$Adj. R^2$	0.9696	0.97551	0.9658	0.92279	0.88442
Findley's model	a	1.05E-5 (4.83E-06)	6.49E-6 (3.69E-06)	1.79E-5 (1.14E-05)	3.49E-5 (3.45E-05)	3.35E-5 (5.92E-04)
	b	0.34341 (3.39E-02)	0.3699 (4.22E-02)	0.2803 (4.63E-02)	0.17143 (6.61E-02)	0.1284 (2.27E00)
	ε_0	6.70E-4 (2.68E-05)	6.17E-4 (2.58E-05)	6.13E-4 (3.82E-05)	5.00E-4 (5.74E-05)	5.11E-4 (9.03E-03)
	SS^*	3.83097E-8	4.27255E-8	4.37949E-8	1.91548E-8	1.30874E-8
	$Adj. R^2$	0.99761	0.99653	0.99496	0.98797	0.96701
Two parameter power law	a	4.63E-4 (1.41E-04)	4.24E-4 (1.39E-04)	4.82E-4 (1.00E-04)	4.85E-4 (3.61E-05)	5.22E-4 (2.08E-05)
	b	0.08443 (3.37E-02)	0.08145 (3.64E-02)	0.06828 (2.37E-02)	0.03723 (9.03E-03)	0.01951 (5.01E-03)

model						
	SS^*	2.4937E-6	2.31209E-6	1.0253E-6	9.22041E-8	2.50976E-8
	$Adj. R^2$	0.8452	0.8128	0.88238	0.94226	0.93694

SS^* : Sum of squared deviations

5.1.6 Dynamic mechanical properties

Dynamic mechanical analysis can characterize the viscoelastic properties of the materials and determine the information of storage modulus, loss modulus (the energy dissipation associated with the motion of polymer chains) and loss factor ($\tan \delta$) of polymer composites within the measured temperature range [58]. The variation of storage modulus (E') of composites incorporated with different content of PJF as a function of temperature at frequency of 1 Hz is shown in figure 11. It can be seen from figure 11a that there is a gradual fall in the storage moduli with temperature, which should be related with an energy dissipation phenomenon involving cooperative motions of the polymer chains with temperature [59]. The increase in storage modulus over the whole temperature range was observed for composites incorporated with different loadings of PJF, for example, addition of 1, 5 and 10% PJF causes a significant increase of ~18 %, 22 % and 43 % in the storage modulus respectively at 35 °C. Moreover, the storage modulus curves of composites have been shifted to higher temperatures after addition of the PJF, particularly 5 and 10 % loading. This significant improvement in storage modulus is due to better reinforcing effect of PJF leading to increased stiffness and the mobility restriction of polymer chains [33].

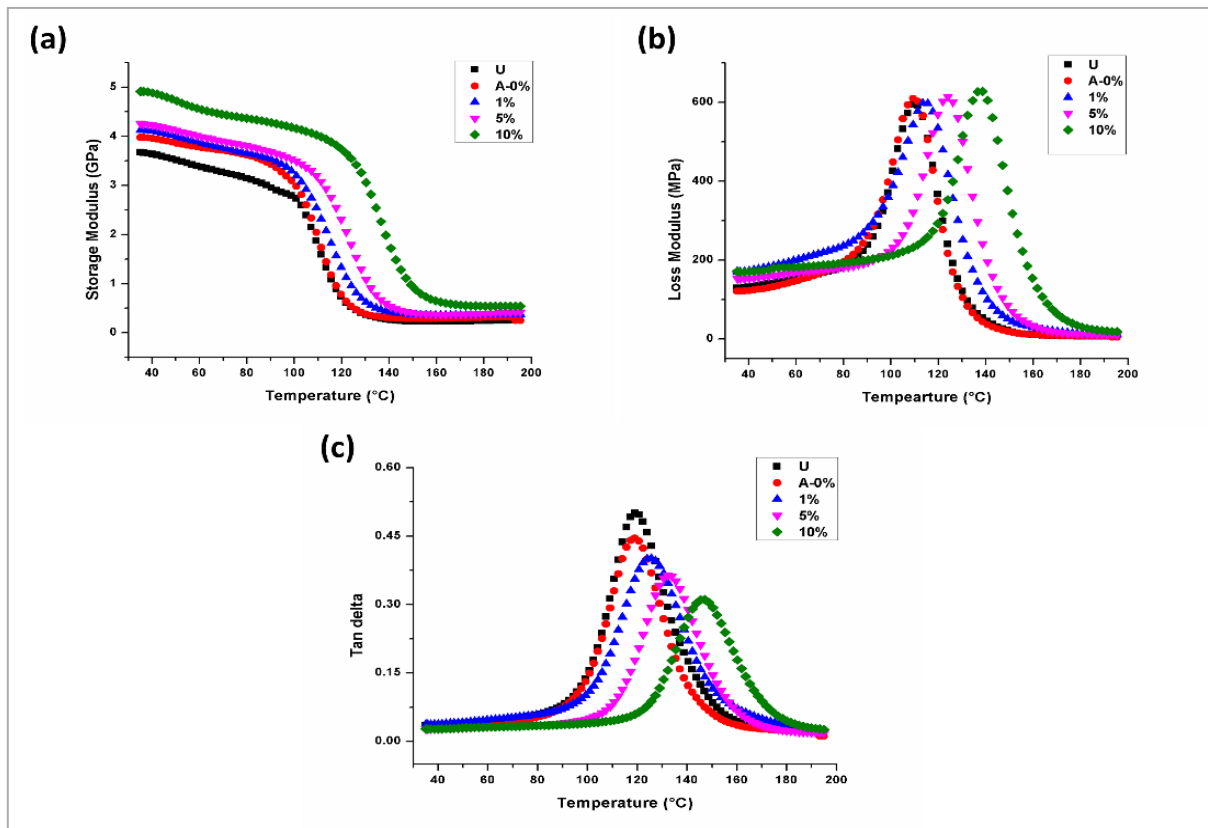


Figure 11. Dynamic mechanical properties of composites incorporated with different loadings of PJF; (a) storage modulus, (b) loss modulus, (c) tan delta.

The change in loss factor ($\tan \delta$, the ratio of loss modulus to corresponding storage modulus) of composites with different loading of PJF as a function of temperature is shown in figure 11c.

Untreated composite displayed a higher $\tan\delta$ peak value than others. This may be attributed to more energy dissipation due to frictional damping at the weaker fiber/matrix interface. The temperature at which $\tan\delta$ attains a maximum value can be referred to as the glass transition temperature (T_g) [60]. A positive shift in T_g can be observed for all composites incorporated with PJF compared to untreated composite. The lower $\tan\delta$ peak height is shown by composite incorporated with 10 % PJF followed by 5 % and 1 % PJF composites, exhibiting a strong fiber/matrix interfacial interactions which can restrict the segmental movement of the polymer chains leading to the increased T_g .

Table 3. T_g values obtained from E'' curves.

Composites	T_g from E''_{\max} curve [°C]
Untreated	110.10
Alkali-0%	110.60
1%	114
5%	123
10%	137

It has been reported that T_g values obtained from loss modulus (E'') curve peak are more realistic as compared to those obtained from loss factor ($\tan\delta$) [61]. A positive shift in T_g to higher temperature for all composites incorporated with PJF is observed, i.e. T_g increased from 110.1 °C for untreated to ~110.6, 114, 123 and 137 °C for composites incorporated with 0, 1, 5 and 10 % PJF respectively as presented in table 3 and figure 11b. This may be due to reduced mobility of matrix polymer chains and better reinforcement effect of PJF. It has been reported that systems containing more restrictions and a higher degree of reinforcement tend to exhibit higher T_g [62].

5.2 Extraction of nanocellulose from waste jute fibers and characterization of mechanical and dynamic mechanical behavior of nanocellulose coated jute/green epoxy composites

5.2.1 SEM study of chemically treated jute fibers and jute cellulose nanofibrils

Surface topologies of jute fibers after alkali treatment, bleaching and milling are examined by SEM and presented in figure 12. Figure 12a shows the jute fibers bound together in the form of fiber bundles by cementing materials e.g. hemicellulose and lignin but after repeated alkali treatment, splitting of fibers is observed due to destruction of mesh structure with a little rough and clean surface, may be due to majority of the removal of hemicellulose, lignin and other non-cellulosic materials [63, 64] as shown in figure 12b.

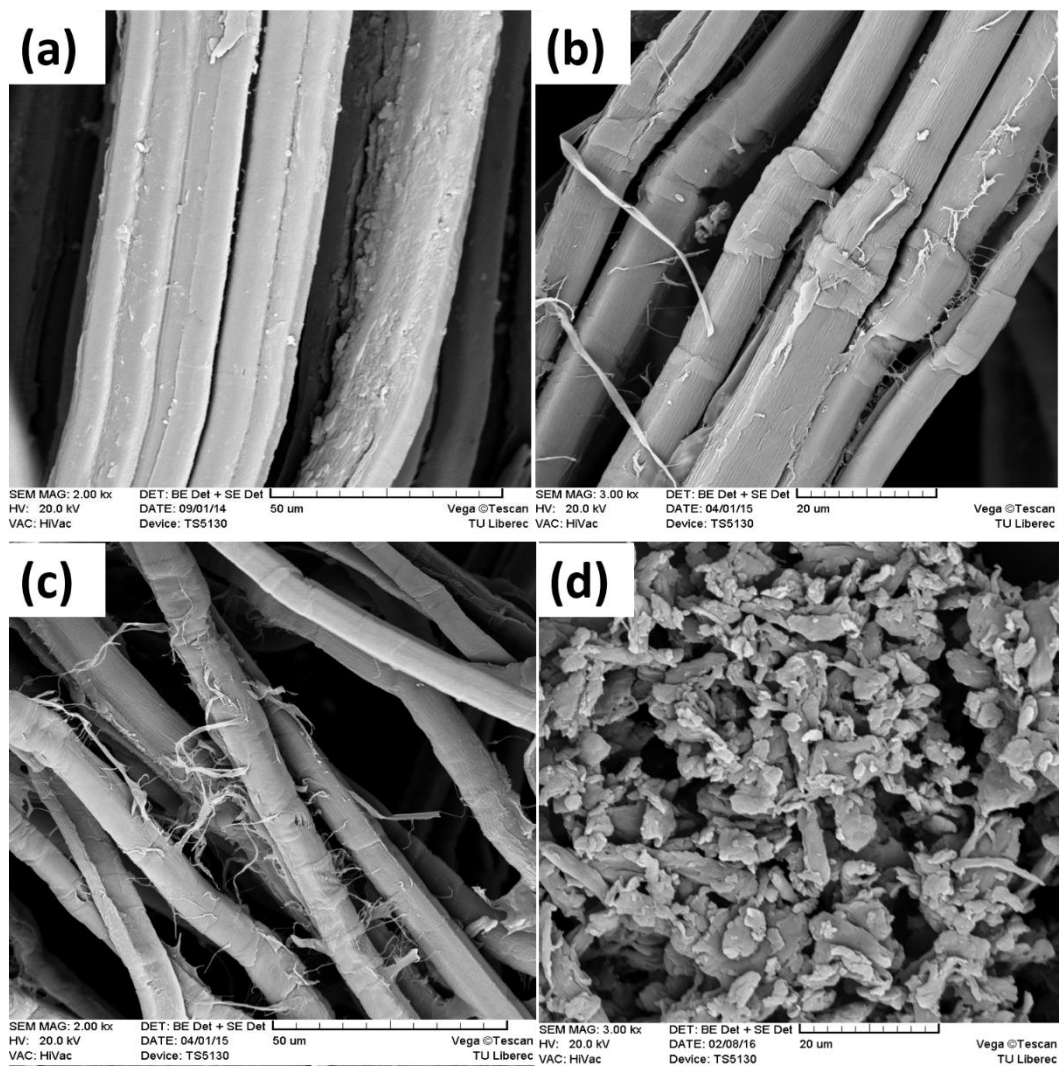


Figure 12. SEM images of jute fibers (a) untreated, (b) alkali treated, (c) bleached and (d) pulverized (milled).

The alkali treated fibers are further separated to individual fibers with more clean surface and fibrillation on the surface, may be due to more delignification after bleaching treatment [65], as shown in figure 12c. Figure 12d displays the milled jute fibers with size distribution of fibers in the micron range.

A high resolution FE-SEM image at nanoscale level is precisely analyzed to measure the size (width) of jute cellulose nanofibrils (CNF), after acid hydrolysis, as shown in figure 13a. The histogram of size distribution of 50 measurements is shown in figure 13b. The calculated average diameter (width) of CNF was found to be 57.40 ± 20.61 nm.

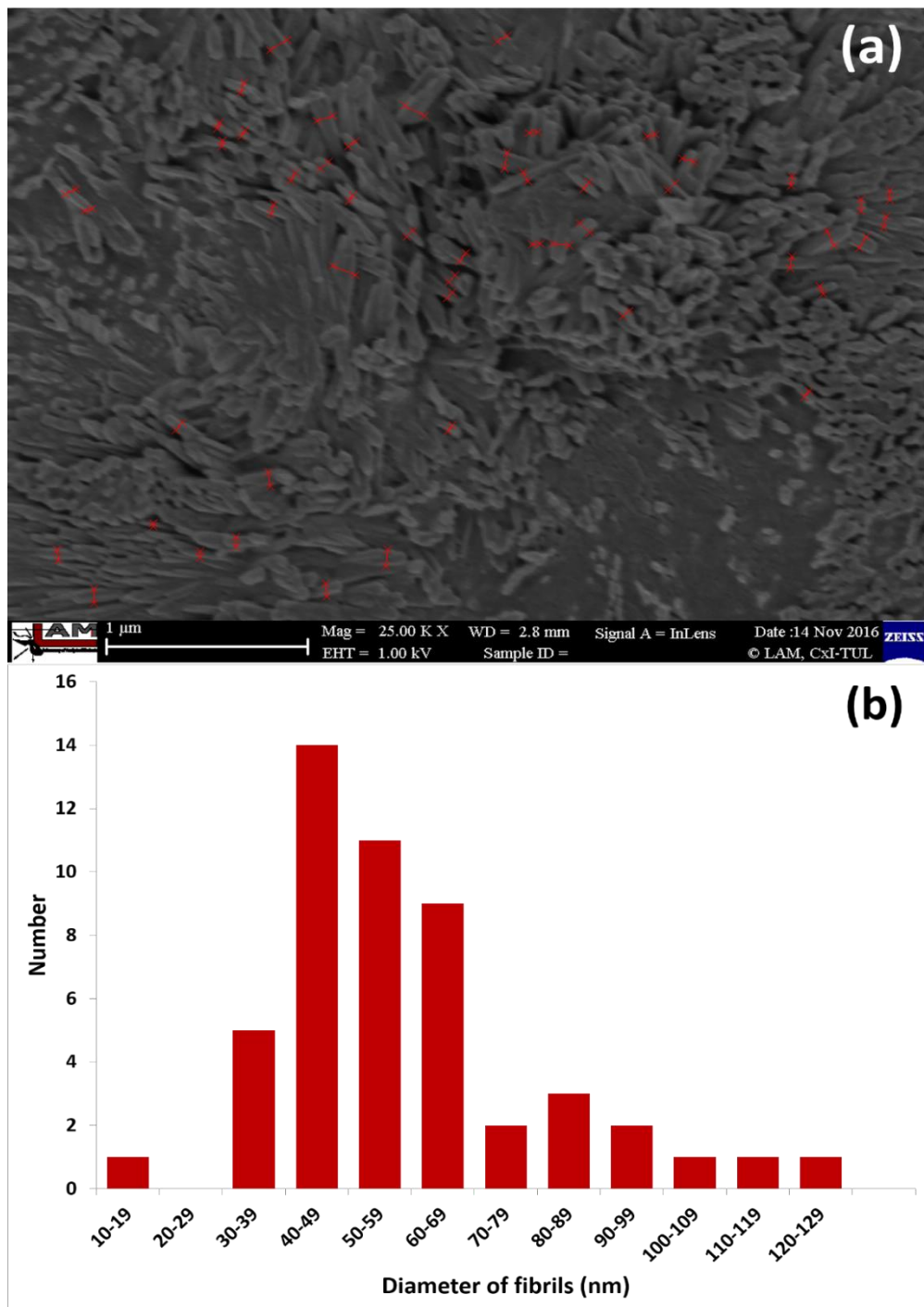


Figure 13. (a) FE-SEM image of jute cellulose nanofibrils. (b) Histogram of width distribution of cellulose nanofibrils.

5.2.2 Surface topology of nanocellulose coated jute fabric

The topological changes that occur on the surface of jute fabric after nanocellulose coating are shown in figure 14. It is apparent that there is depositing of nanocellulose on the fabric surface forming a layer. The layer thickness increases gradually with the increase in nanocellulose concentration as clear in figure 14b-d and the fabric surface coated with 10 wt% nanocellulose suspension is covered almost completely with cellulose as shown in figure 14d.

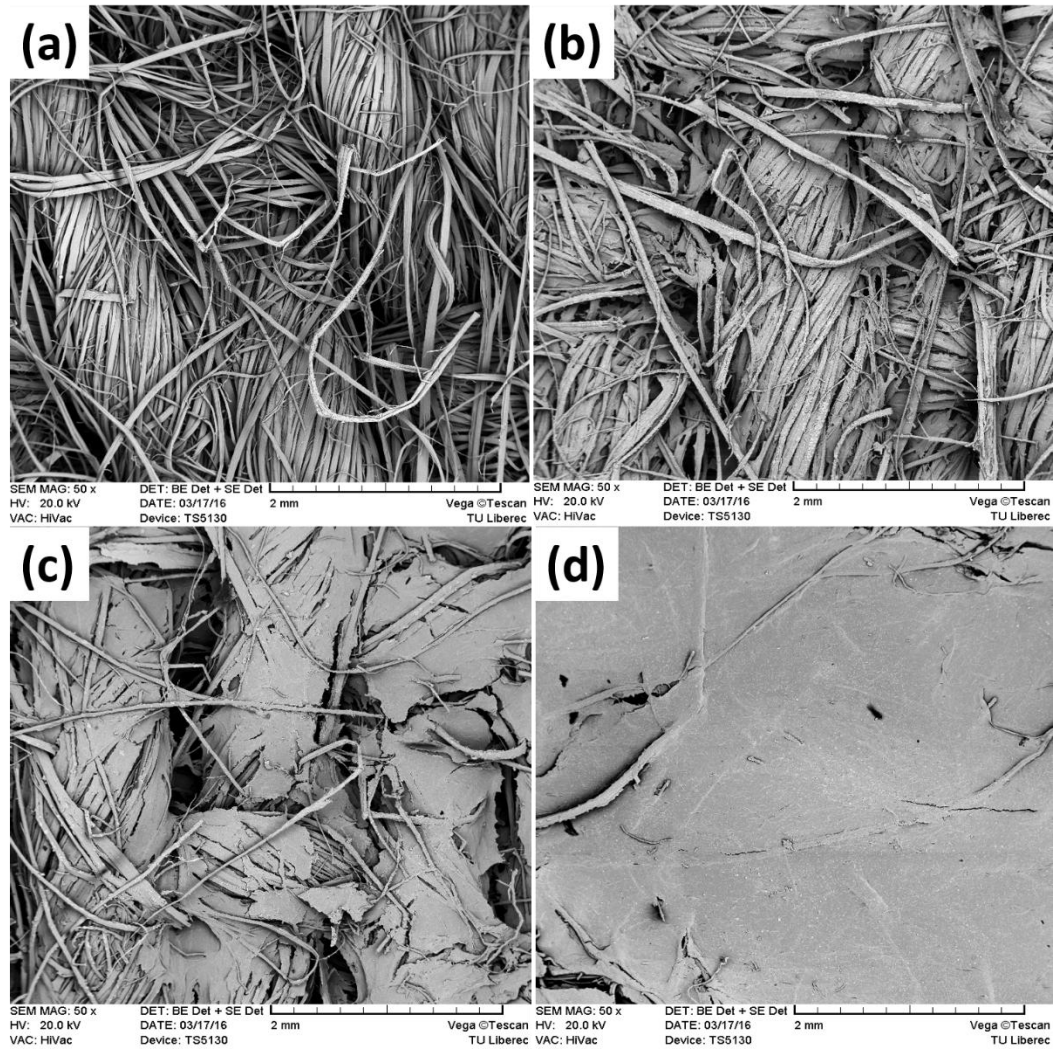


Figure 14. Surface topology of jute fabric coated with; (a) 0 wt%, (b) 3 wt%, (c) 5 wt%, (d) 10 wt% of nanocellulose suspensions.

5.2.3 XRD analysis of jute fibers

The X-ray diffraction patterns of untreated, bleached jute fibers and jute CNF are shown in figure 15. These diffraction patterns are typical of semicrystalline materials with an amorphous broad small hump and a large crystalline peak. Two well defined peaks around $2\theta \approx 16^\circ$ and 23° are typical of cellulose-I. The crystallinity index for all samples was determined by using the following formula [66]:

$$\text{Crystallinity \%} = 100 \times \frac{I_{200} - I_{non-cr}}{I_{200}} \quad [7]$$

Where I_{200} represents maximum intensity of the peak corresponding to the plane 2 0 0 at 2θ angle between 22 – 24 degrees and I_{non-cr} is the intensity for diffraction of non-crystalline material which is taken at 2θ angle of about 18 degree. The crystallinity index was calculated to be about 69.3 %, 76.5 % and 78.6 % for untreated fibers, bleached fibers and cellulose nanofibrils, respectively. The increase in crystallinity of bleached jute fibers as compared to untreated jute can be explained by the removal of amorphous non-cellulosic compounds induced by the alkali and bleaching treatments performed to purify cellulose and that of jute CNF, by removal of amorphous cellulosic domains due to acid hydrolysis.

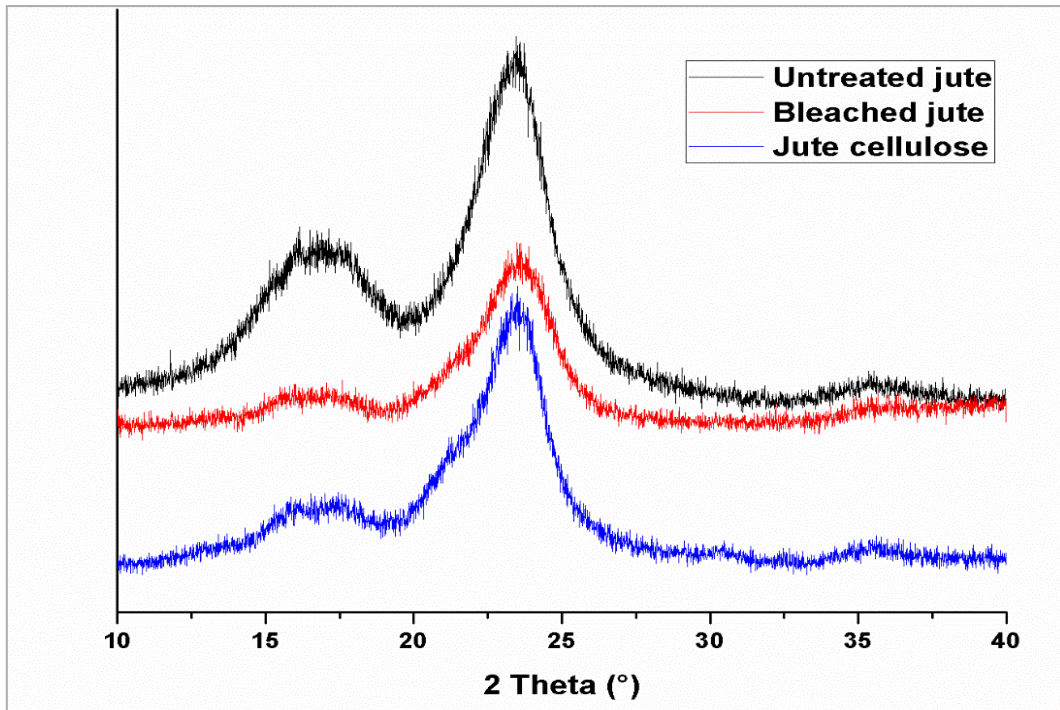


Figure 15. X-ray diffraction patterns of untreated, bleached jute fibers and jute cellulose nanofibrils.

5.2.4 Tensile properties

Figure 16a shows the typical stress-strain curves of uncoated and coated jute composites with different nanocellulose content. The stress-strain curve for uncoated (CF0) composite shows almost linear behavior until failure whereas the curves for composites coated with different nanocellulose content show linear behavior followed by change in slope showing nonlinear behavior, thus presenting plastic deformation and gradual debonding of fibers from the matrix just before failure. The tensile failure behavior also reveals more brittle nature of CF0 composite as compared to nanocellulose coated composites (figure 16a).

Figure 16b presents the average values and standard deviation of ultimate tensile strength and tensile modulus of composites. The tensile properties indicate the decrease in strength and increase in modulus (stiffness) of composites with the increase in nanocellulose concentration. For CF10 composite, the tensile modulus increases from 4.6 GPa to 5.58 GPa showing 21 % increase, thus presenting better fiber/matrix interfacial interaction and bonding which would be effective at the early stages of loading. However, the decrease in tensile strength of composites with the increase in nanocellulose concentration may be explained by the differences in failure strains of nanocellulose coated jute fabric reinforcement and the matrix. In other words, the reinforcement does not come into effect when the failure strain of matrix is much greater than that of reinforcement. So the composite shows a failure before the stress is transferred from matrix to reinforcement [26]. The ANOVA for the tensile strength ($p = 0.000$) and tensile modulus ($p = 0.008$) showed the statistically significant difference between the means at the 95.0% confidence level.

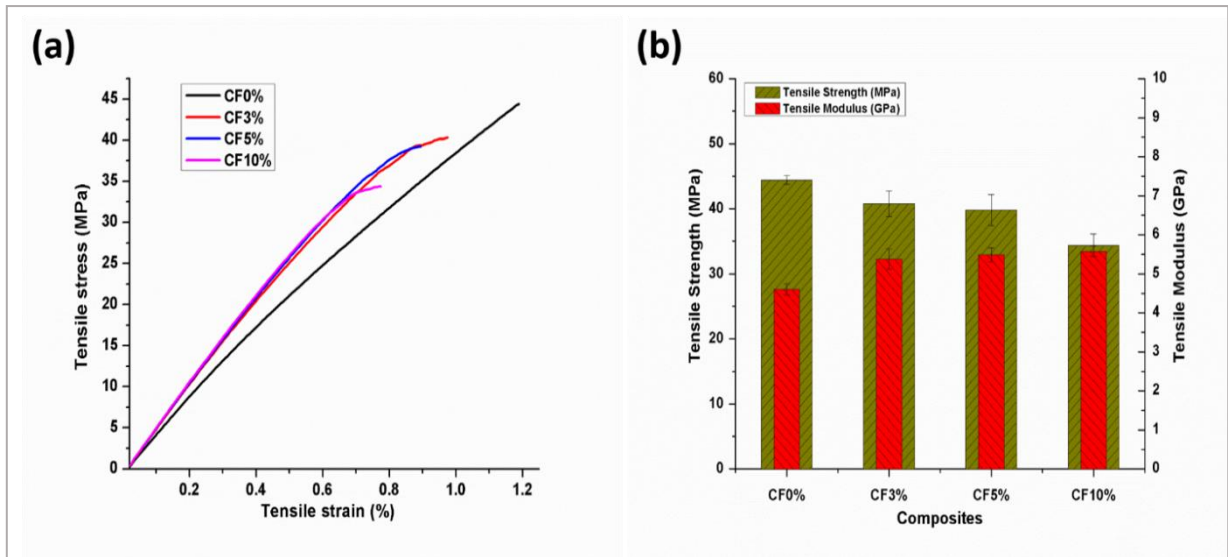


Figure 16. (a) Tensile stress-strain curves and (b) tensile strength and modulus of uncoated and nanocellulose coated jute composites.

5.2.5 Flexural properties

The flexural strength and modulus increase with the increase in nanocellulose concentration in composites. The flexural strength increases from 32.94 MPa for CF0 composite to 32.94 MPa, 43.53 MPa and 48.66 MPa for CF3, CF5 and CF10 composites, respectively thus allowing 26 %, 32 % and 47 % increase on average as shown in figure 17. Similarly, flexural modulus increases from 3.83 GPa for CF0 composite to 4.81 GPa, 4.73 GPa and 5.67 GPa for CF3, CF5 and CF10 composites, respectively thus permitting 25 %, 23.5 % and 48 % increase on average (figure 17). These findings may suggest the strong interaction between matrix and reinforcement after nanocellulose coating which increases with the increase in nanocellulose content. The other possibility of the enhancement of flexural properties may be the increase in bending stiffness/rigidity of jute reinforcement after coating with nanocellulose which also increases with the increase nanocellulose concentration [67, 68]. The ANOVA for the flexural strength ($p = 0.000$) and flexural modulus ($p = 0.000$) also showed the statistically significant difference between the means at the 95.0% confidence level.

5.2.6 Fatigue life

The S-N (fatigue life) curves of all composites in the considered stress range are shown in figure 18. The experimental fatigue data was fitted by semi-logarithmic function, $\sigma_{\max} = k \log N_f + a$ [69] (where k and a are the parameters to be defined by the least square method as given in table 4) to have a reliable predicting of the fatigue life corresponding to other stress levels in the considered stress range, which are not directly determined by testing. The quality of the fitting is related to the coefficient of determination R^2 [47]. Values of R^2 close to 1 confirm the better goodness-to-fit of experimental and predicted data. The curves in figure 18 have R^2 values in the range 0.92–0.98 (table 4).

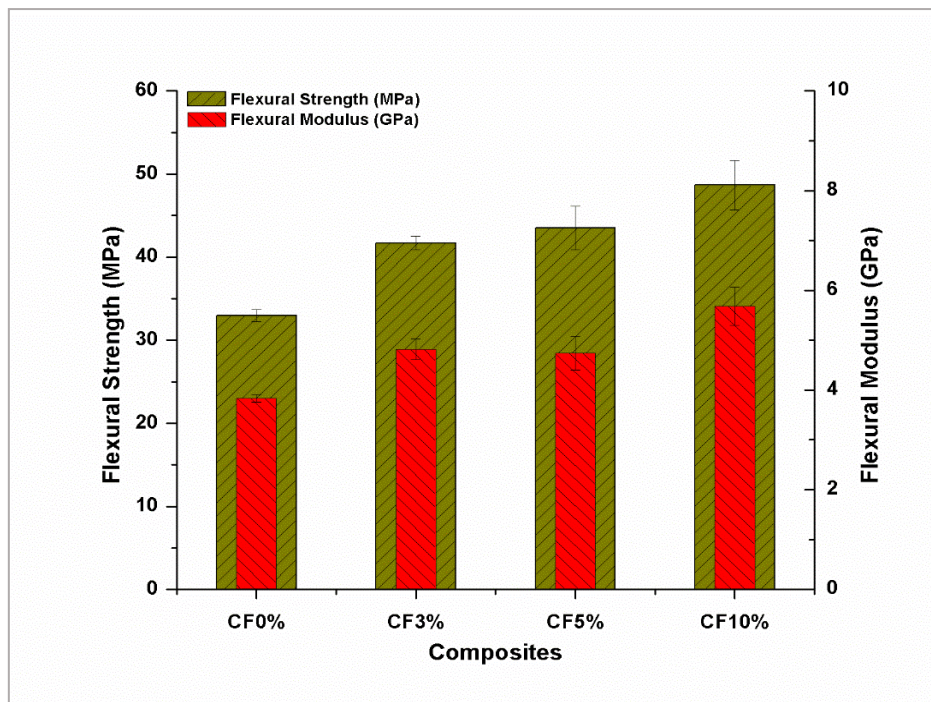


Figure 17. Flexural strength and modulus of uncoated and nanocellulose coated jute/green epoxy composites.

The negative slope k values of the linear fitting curves, listed in table 4, show a decreasing trend with the increase in nanocellulose content of the composites. This predicts an increase in fatigue life for composites containing higher contents of nanocellulose coated over woven jute reinforcement than that of uncoated jute composite. This is clearer in figure 19 when comparing the average number of cycles to failure for the two applied stress levels. CF3 composite has higher fatigue life at 80 % stress level (low cycles regime) whereas decreasing the stress level to 70 % (high cycles regime) causes a significant increase in the fatigue life of CF5 and CF10 composites.

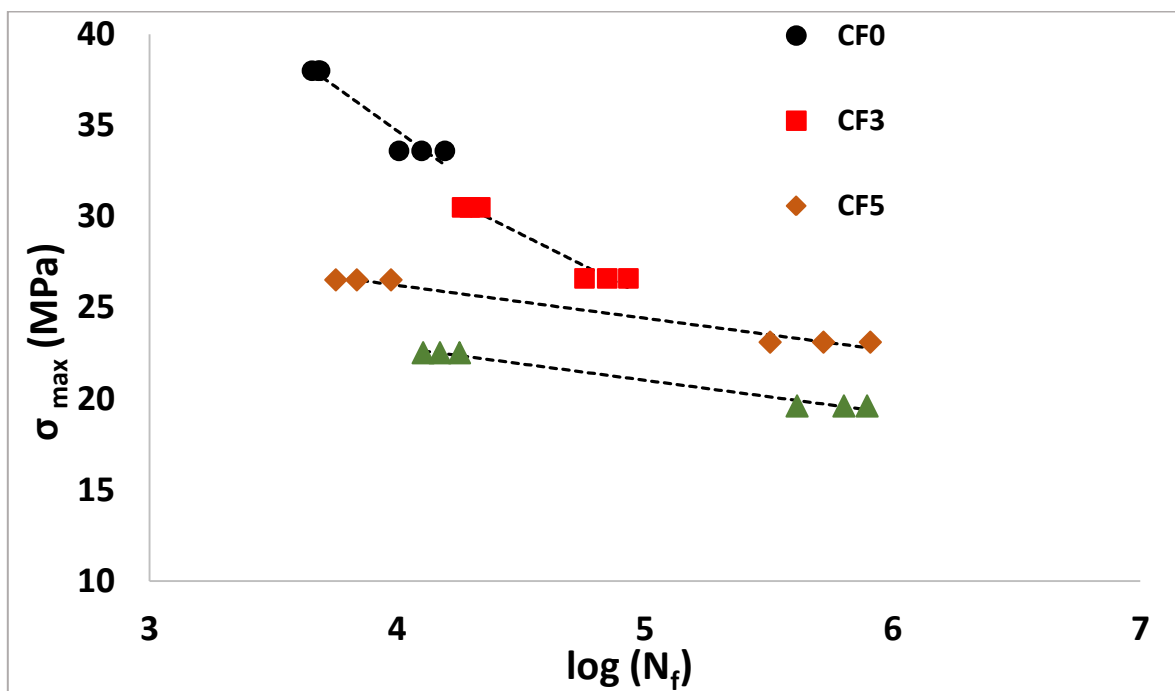


Figure 18. Maximum stress (σ_{max}) vs. logarithm of number of cycles to failure $\log(N_f)$ and semi-logarithm fitting for each composite.

Table 4. Parameters of the linear fitting of S-N curves.

Composites	k	a	$Adj. R^2$
CF0	-9.73 (3.06)	73.63 (11.90)	0.92287
CF3	-6.82 (1.69)	59.74 (7.73)	0.95104
CF5	-1.80 (0.32)	33.43 (1.55)	0.97462
CF10	-1.805(0.26)	30.03 (1.30)	0.98312

Note: Standard deviation in parentheses

The reliability of the above results on the fatigue life can be assessed by the confidence level index, based on the Student's t-distribution [47]. The confidence levels in table 5 show that, in strict statistics terms: the hypothesis “the nanocellulose coated jute composites have a longer fatigue life than the uncoated jute composite (CF0)” is valid with confidence level higher than 99 % for both stress levels except for CF5 composite which has confidence level > 88 % at 80 % stress level. The better fatigue life of nanocellulose coated jute composites can be interpreted as a better damage tolerance of these materials mainly due to increase in intermolecular and physical interactions thus forming a rigid and stiff network due to nanocellulose coating over woven jute reinforcement.

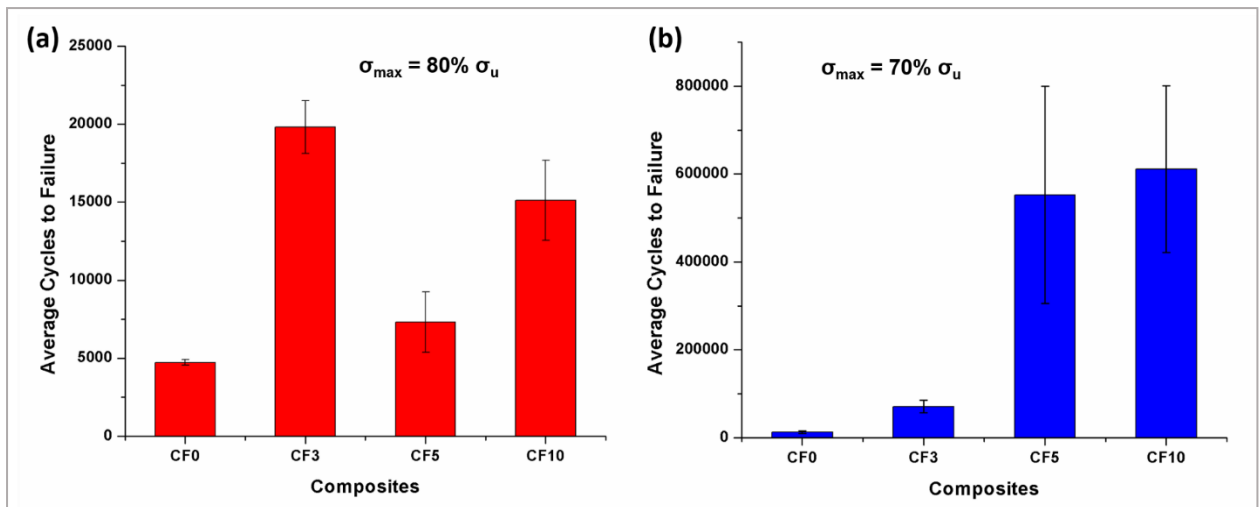


Figure 19. Comparison of average fatigue life of composites: (a) 80% and (b) 70% of σ_u .

Table 5. Confidence levels for three hypotheses (> means longer fatigue life)

Stress level [%]	Confidence level for hypotheses		
	CF3>CF0 [%]	CF5>CF0 [%]	CF10>CF0 [%]
70	99.8	99.4	99.9
80	99.9	88.8	99.3

5.2.7 Fracture toughness

Figure 20a shows the typical K_Q vs. displacement curves presenting the crack growth behavior of composites and figure 20b presents the fracture toughness (K_{Ic}) with respect to nanocellulose content in composites. The fracture mode was brittle for CF0 composite showing slip-stick behavior but as the nanocellulose content over jute reinforcement increased, the fracture mode changed from brittle to a little ductile and K_{Ic} values increased from 2.64 MPa.m^{1/2} for CF0 composite to 3.20 MPa.m^{1/2}, 3.21 MPa.m^{1/2} and 3.49 MPa.m^{1/2} for CF3, CF5 and CF10 composites, respectively resulting in 21 %, 21.5 % and 32 % increase on average (figure 20b). Thus, fracture toughness increases linearly with the increase in concentration of nanocellulose coating over reinforcement. The ANOVA for the fracture toughness, K_{Ic} ($p = 0.024$) showed the statistically significant difference between the means at the 95.0% confidence level.

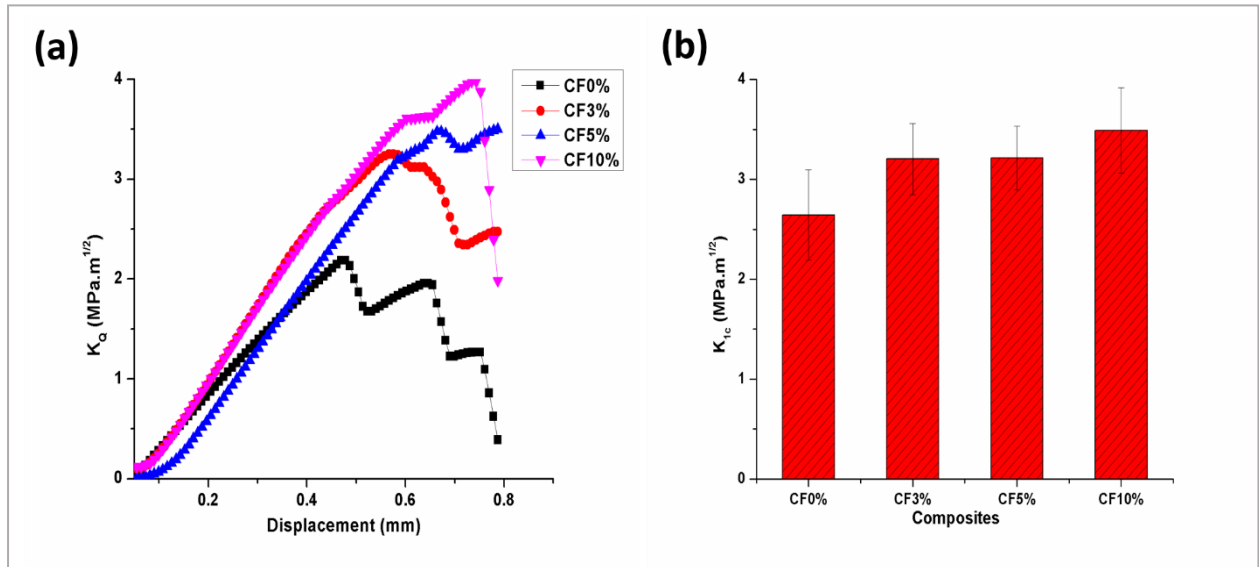


Figure 20. (a) Typical K_Q vs. displacement curves and (b) fracture toughness (K_{Ic}) of uncoated and cellulose coated jute/green epoxy composites.

Crack deflection, plastic deformation, voids, crack pinning/bridging, fiber pullout and debonding are the known toughening mechanisms in epoxy matrices, found in literature [70]. Figure 21a-d exhibits SEM images for all nanocellulose contents which clearly shows fiber fracture, fiber pullout and some voids for all composites. However, fiber pullout is a little more prominent mechanism for nanocellulose coated composites, may be due to increased fiber debonding during fracture resulting in increased crack propagation length during deformation and hence fracture toughness.

Figure 22 shows the fracture surface topologies in the matrix region. It can be seen from figure 22a that the fracture surface of green epoxy matrix of CF0 composite is very smooth and featureless, which indicates typical brittle fracture behavior with lack of significant toughness mechanism [71]. However, figure 22b-d show rougher fracture surfaces and river patterns in the matrix regions of nanocellulose coated jute composites. An increase in fracture surface roughness can be used as an indicator to the presence of plastic deformation and crack deflection mechanisms, which increase fracture toughness by increasing crack propagation length during deformation [72].

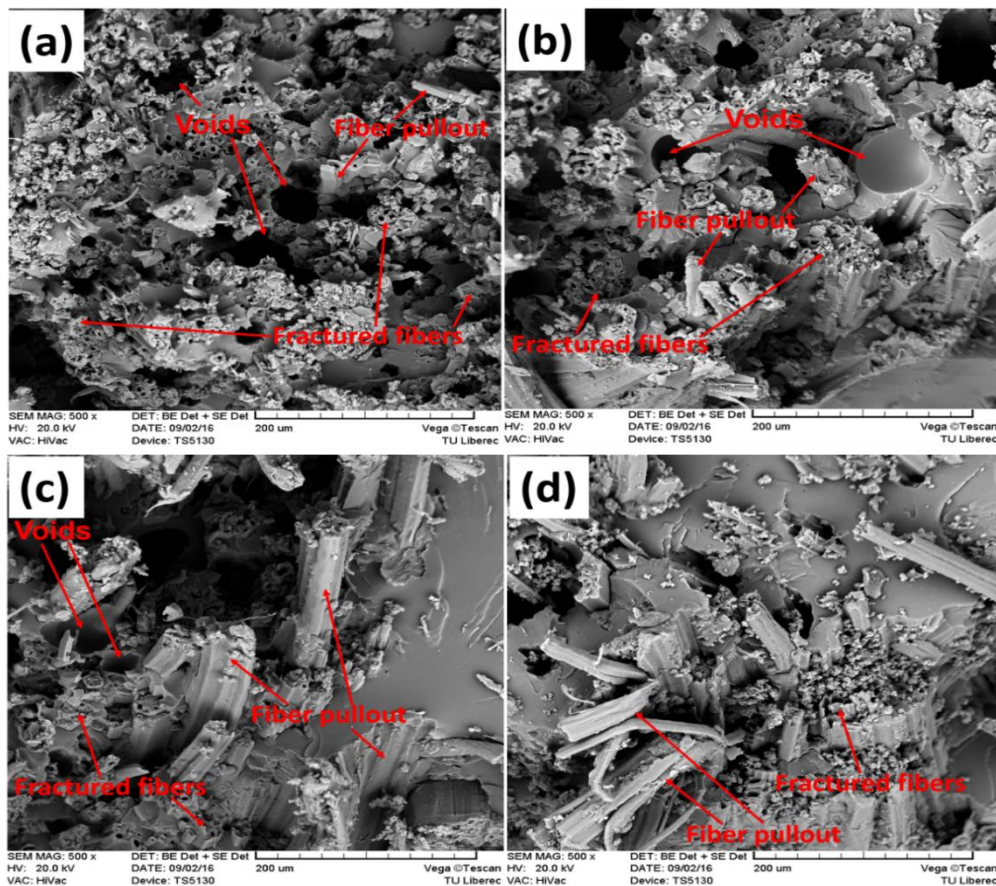


Figure 21. Fracture surface topology of nanocellulose coated jute/green epoxy composites; (a) CF0, (b) CF3, (c) CF5 and (d) CF10.

5.2.8 Dynamic mechanical analysis

The change in storage modulus as a function of temperature of different nanocellulose coated and uncoated jute composites is shown in figure 23a. It can be seen that the shape of storage modulus curves is almost same for all the samples and E' decreases with increase in temperature because of the transition from glassy to rubbery state. However, the storage modulus increases with increasing concentration of nanocellulose in composites both in glassy and rubbery regions showing superior reinforcing effects of nanocellulose coated jute fabrics throughout the specified temperature range. In the glassy region, components are highly immobile, close and tightly packed and intermolecular forces are strong [73] resulting in high storage modulus but as temperature increases intermolecular forces become weak, the components become more mobile and lose their close packing arrangement, resulting in loss of stiffness and hence storage modulus.

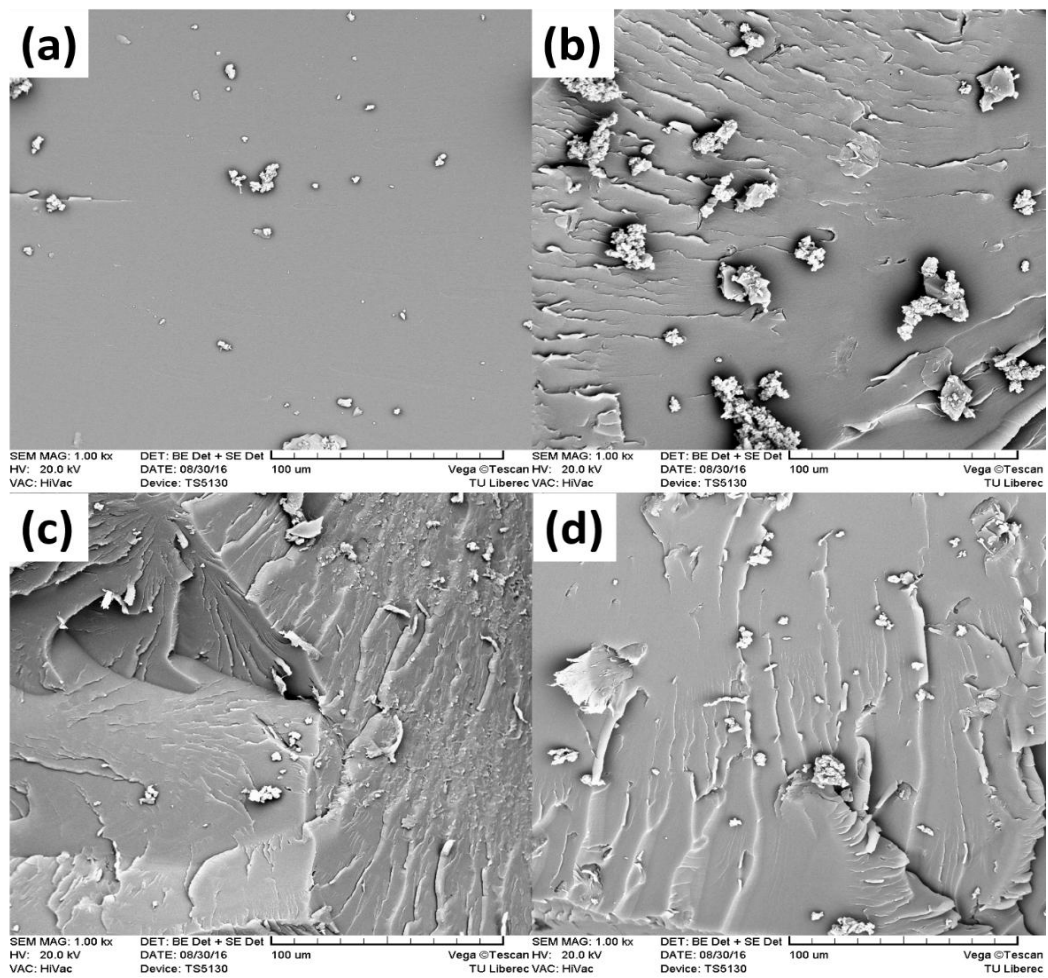


Figure 22. Fracture surfaces in the matrix region of jute/green composites; (a) CF0, (b) CF3, (c) CF5 and (d) CF10.

Figure 23a reveals that uncoated jute composite (CF0) has the lowest storage modulus throughout the specified temperature range. CF0 has 4.05 GPa of E' (measured at 30 °C), however, CF3, CF5, CF10 composites show maximum values of 4.72, 5.27 and 6.35 GPa, respectively resulting in an increase of 16 %, 30 % and 56 % in E' . Moreover, E' (measured at 150 °C) increased from 0.28 GPa for CF0 composite to 0.48, 0.71 and 0.94 GPa for CF3, CF5, CF10 composites, respectively representing 71 %, 153 % and 235 % increase. This shows that when nanocellulose concentration over the jute fabric is increased, the stiffness effect of reinforcement is progressively increased not only in the glassy region but also in the rubbery region. The above findings may be attributed to the fact that, as cellulose nanofibrils coated on jute fabric possess large surface area, it promotes the interfacial interactions between the reinforcement and matrix thus reducing the mobility of polymer chains [74] and better stress transfer at the interface [75]. The other fact is the increase in the stiffness of reinforcement with increasing nanocellulose concentration. Furthermore, the formation of rigid and stiff network interconnected by hydrogen bonds is the accepted theory to explain the excellent mechanical properties of composites incorporated with nanocellulose [53, 76-78].

Figure 23b presents the loss modulus (E'') versus temperature of different nanocellulose coated and uncoated jute composites. It is observed that the value of loss modulus increased and then decreased with the increase in temperature for all composites. The rapid rise in loss modulus in a system indicates an increase in the polymer chains free movements at higher temperatures due to

a relaxation process that allows greater amounts of motion along the chains that is not possible below the glass transition temperature [79]. Figure 23b also revealed that the value of loss modulus is increased with the increase in concentration of nanocellulose coating as compared to uncoated composite (CF0) representing a higher amount of energy dissipation associated with an increase in internal friction. It is interesting to note that T_g is decreased from 95 °C for CF0 composite to 88 °C and 91 °C for CF3 and CF5 composites, respectively but T_g of CF0 and CF10 composites are almost same. Simultaneously, a positive shift in T_g values to higher temperatures is noted with the increase in nanocellulose concentration in the system (figure 23b). A possible reason may be the change in crosslinking density of the network [80].

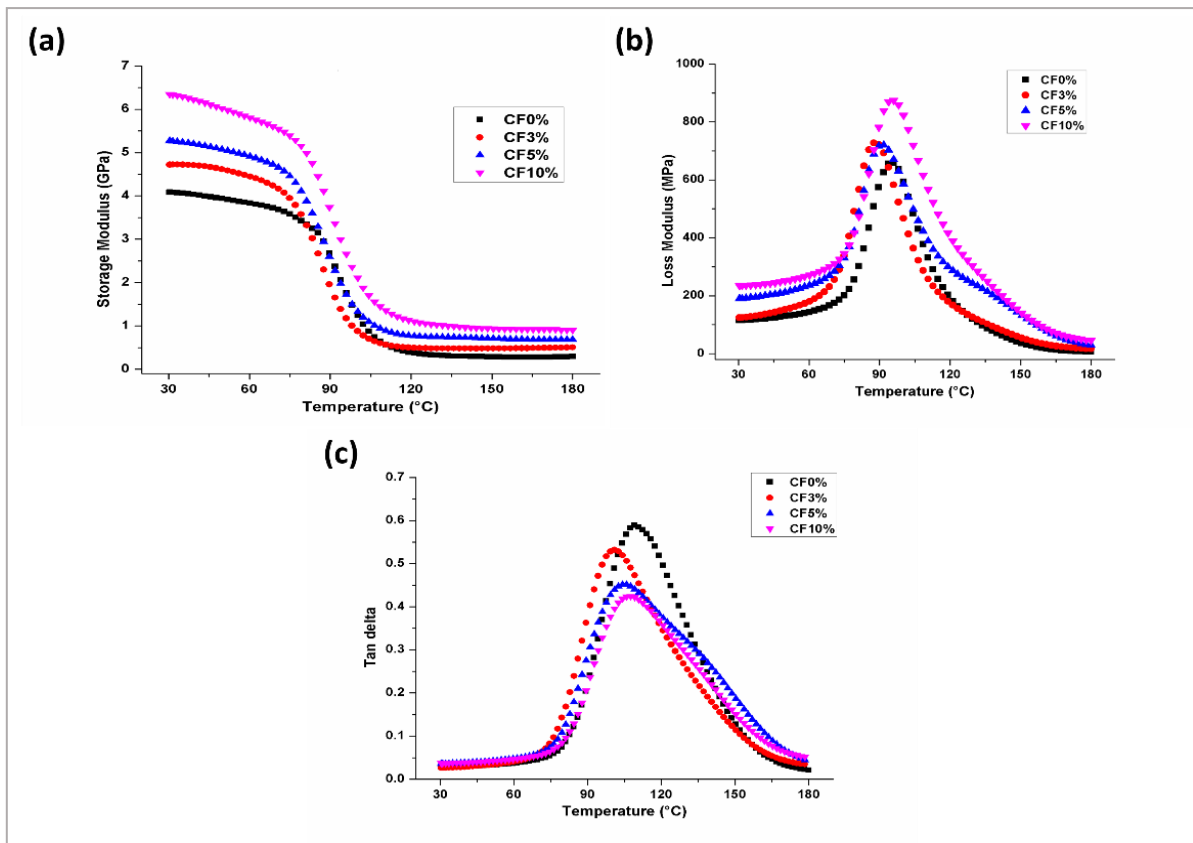


Figure 23. Dynamic mechanical properties of nanocellulose coated and uncoated jute composites; (a) storage modulus, (b) loss modulus and (c) tan delta.

The damping factor ($\tan\delta$) as a function of temperature of composites reinforced with different concentration of nanocellulose coated jute fabric is shown in figure 23c. The highest value of $\tan\delta$ peak is observed for CF0 composite resulting in more energy dissipation whereas a reduction in $\tan\delta$ peak height is observed in composites with the increase in concentration of nanocellulose coating. The peak height of 0.59 for CF0 composite is reduced maximum to 0.42 for CF10 composite representing a 40 % decrease (figure 23c) thus indicating that there are both strong intermolecular and physical interactions contributing to greater molecular restrictions at the interface and less energy dissipation and that the storage modulus is influenced more by the increase in nanocellulose concentration than loss modulus in the composites. The width of $\tan\delta$ peak becomes broader for nanocellulose coated jute composites especially for CF5 and CF10. The damping in materials generally depends on the molecular motions at the interfacial region [81]. Therefore, the increase in width of $\tan\delta$ peak of nanocellulose coated composites is suggestive of increased volume of interface [73] and an increase in the inhibition of relaxation

processes in composites thus decreasing the mobility of polymer chains within the system and a higher number of chain segments upon increase in concentration of nanocellulose in composites [82].

5.3 Flexural, creep and dynamic mechanical evaluation of novel surface treated woven jute/green epoxy composites

5.3.1 SEM observation of jute fibers after surface treatments

Significant changes in surface topology of fibers are observed after treatments. Figure 24a shows the multicellular nature of untreated jute fiber with a rather smooth surface whereas a rough and fragmented surface topology can be observed for enzyme treated fibers (figure 24b). This may be due to partial removal of cementing materials from the fiber surface after this treatment.

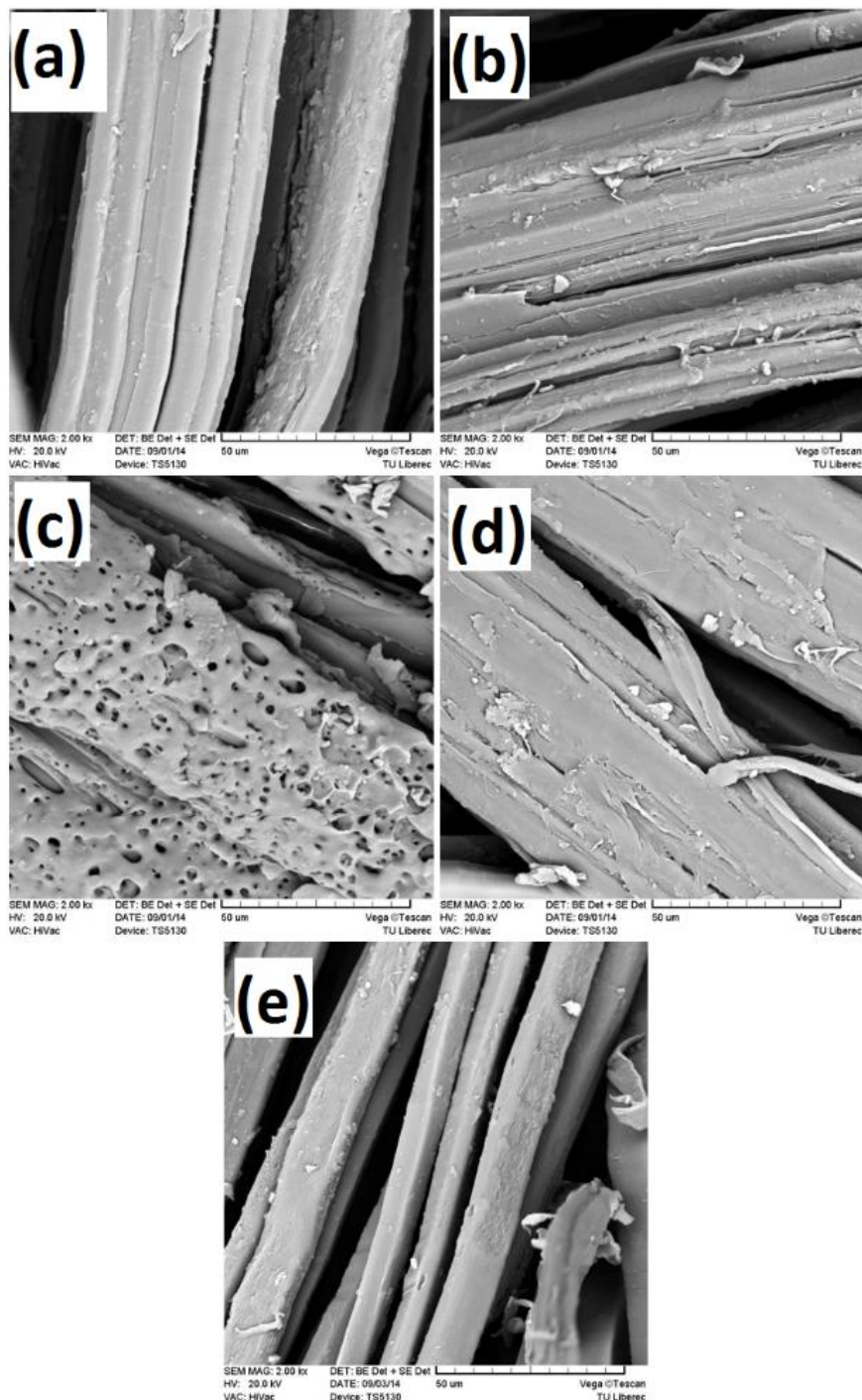


Figure 24. Surface topology of jute fibers: (a) untreated, (b) enzyme, (c) laser, (d) ozone, (e) plasma

Figure 24c displays the thermal degradation of surface fibers after laser treatment giving a porous and rough surface of fabric. The increase in roughness and cracks are noticeable on the surface of ozone treated jute fiber (figure 24d). Plasma treatment causes a minor increase in fiber surface roughness. Overall; SEM micrographs give an indication that all treatments have changed the surface topology of jute fibers.

5.3.2 FTIR analysis

The FTIR spectra of untreated and treated jute fibers are shown in figure 25. The peak at 1736 cm^{-1} is due to stretch vibration of C=O bonds in carboxylic acid and ester components of cellulose and hemicellulose and also non-conjugated carbonyls in lignin. This peak is slightly reduced for enzyme treated fibers which show the partial removal of hemicellulose and lignin components upon treatment. However, the intensity and peak height at 1736 cm^{-1} is increased by ozone and plasma treatments. The peak at 1599 cm^{-1} and 1508 cm^{-1} correspond to the aromatic ring vibrations in lignin. The increase in the intensity of peak at 1736 cm^{-1} and disappearance of peak after ozone treatment at 1508 cm^{-1} is possibly due to the oxidation of lignin [83].

The reduction in the shoulder height at 1105 cm^{-1} and peak height at 1055 cm^{-1} for IR laser gives a strong evidence that this treatment can alter the structure on the fiber surface. In addition, the increased peak intensity $\sim 3200\text{--}3600\text{ cm}^{-1}$ for ozone and plasma treated fibers gives an indication of a reaction of hydroxyl bonds with the carboxyl group and reduction of peak at the same wavenumber range may be ascribed to a decrease of hydroxyl and carboxyl groups on the surface of laser treated jute fiber due to thermal degradation. As a result; there is strong evidence that the used treatments have altered the surface chemistry of jute fibers.

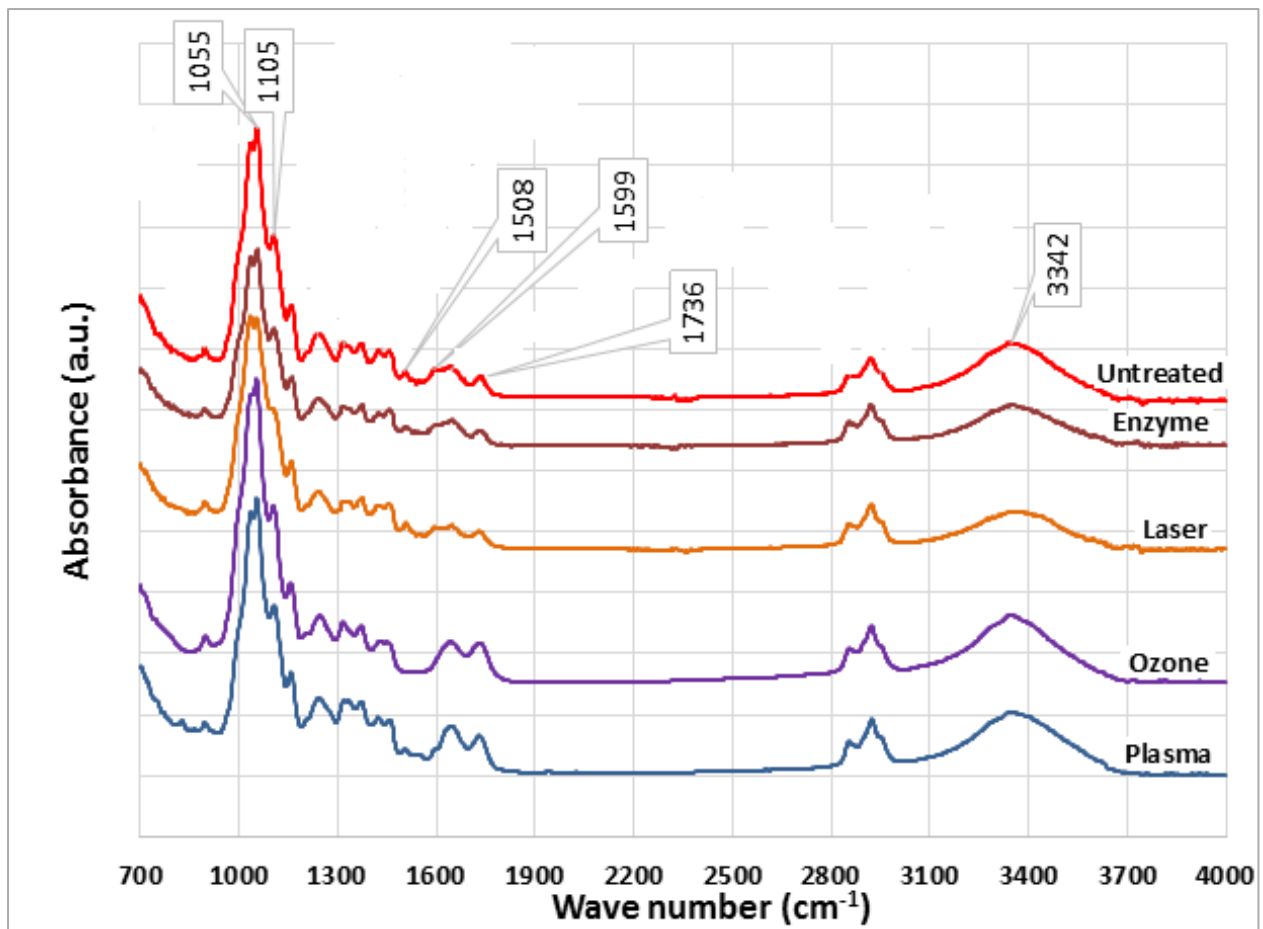


Figure 25. FTIR of untreated and treated jute.

5.3.3 Flexural properties

Flexural properties of untreated and treated composites are shown in figure 26. It is interesting to note that all treated jute composites exhibit higher flexural strength and flexural modulus than untreated composite. Of the various treatments used, ozone treatment provides better flexural strength and flexural modulus, which are 13.48 % and 16.16 % higher than the untreated one, followed by laser treatment. The flexural strength of laser treated composites is increased by 12.85 % and flexural modulus is increased by 13.28 % compared to untreated one. It has been reported that weak fiber /matrix interfacial adhesion contribute to poor flexural properties [84]. Therefore, the possible reason for the increase in flexural properties of composites may be attributed to the increase in fiber /matrix interfacial adhesion due to treatments. The ANOVA for the flexural strength (p -value = 0.013) and flexural modulus (p -value = 0.006) showed the statistically significant difference between the means at 95.0% confidence level.

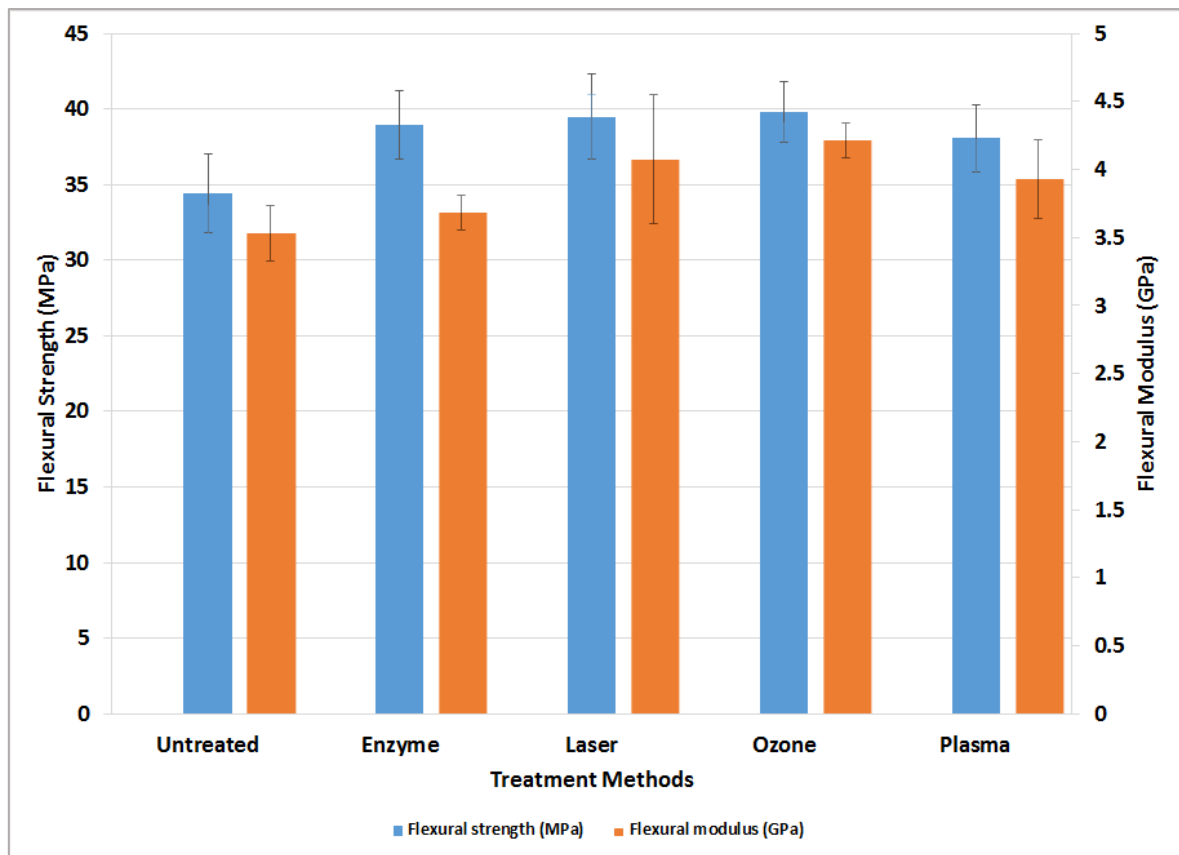


Figure 26. Flexural properties of untreated and treated jute/green epoxy composites.

5.3.4 Creep behavior

The creep behavior of jute composites with and without different fiber treatments at different temperatures (40 °C, 70 °C and 100 °C) is shown in figure 27. The Burger's model curves show a satisfactory agreement with the experimental data. It can be observed that the composites have low instantaneous deformation ϵ_M and creep strain at 40 °C due to higher stiffness of composites but this deformation increases at higher temperatures due to decrease in composites stiffness. The creep strain of all composites also increased at higher temperatures but the untreated jute composite was affected more than the treated composites. When the stress is applied to the composite material, the fiber/matrix interactions are of frictional type and shear load at the interface is responsible for the matrix/interface material flow in shear [85] and untreated composite is more prone to creep due to weak fiber/matrix interface. It is also clear from figure 27 that creep strain is low for treated jute composites at all temperatures compared to untreated one. The less creep strain is shown by laser and ozone treated composites at all temperatures followed by plasma and enzyme treated ones. The laser treated composite has greater instantaneous elastic deformation at higher temperatures (70 °C and 100 °C) but less viscous deformation over time as compared to other treated composites resulting in less creep deformation. The better fiber/matrix adhesion contributes to elastic rather than viscous behavior of composite materials. The better performance of laser treated composite may be attributed to possibility of increase in mechanical interlocking between the fiber and matrix due to formation of micro-pores on fiber surface (figure 24c) resulting in an increase in the shear interfacial strength and lower creep deformation of the composite.

The four parameters E_M , E_K , η_M , η_K of Burger's model, used to fit the eq. 2 to the experimental data, are summarized in table 6. The first value is parameter estimator and value in parenthesis is

corresponding standard deviation. All four parameters were found to decrease for all composites as temperature increased. The parameters for untreated composites have undergone a largest decrease, resulting in higher creep strain. The laser and ozone treated composites have comparatively better values of parameters especially η_M which is related to the long term creep strain and validates less temperature dependence of these composites.

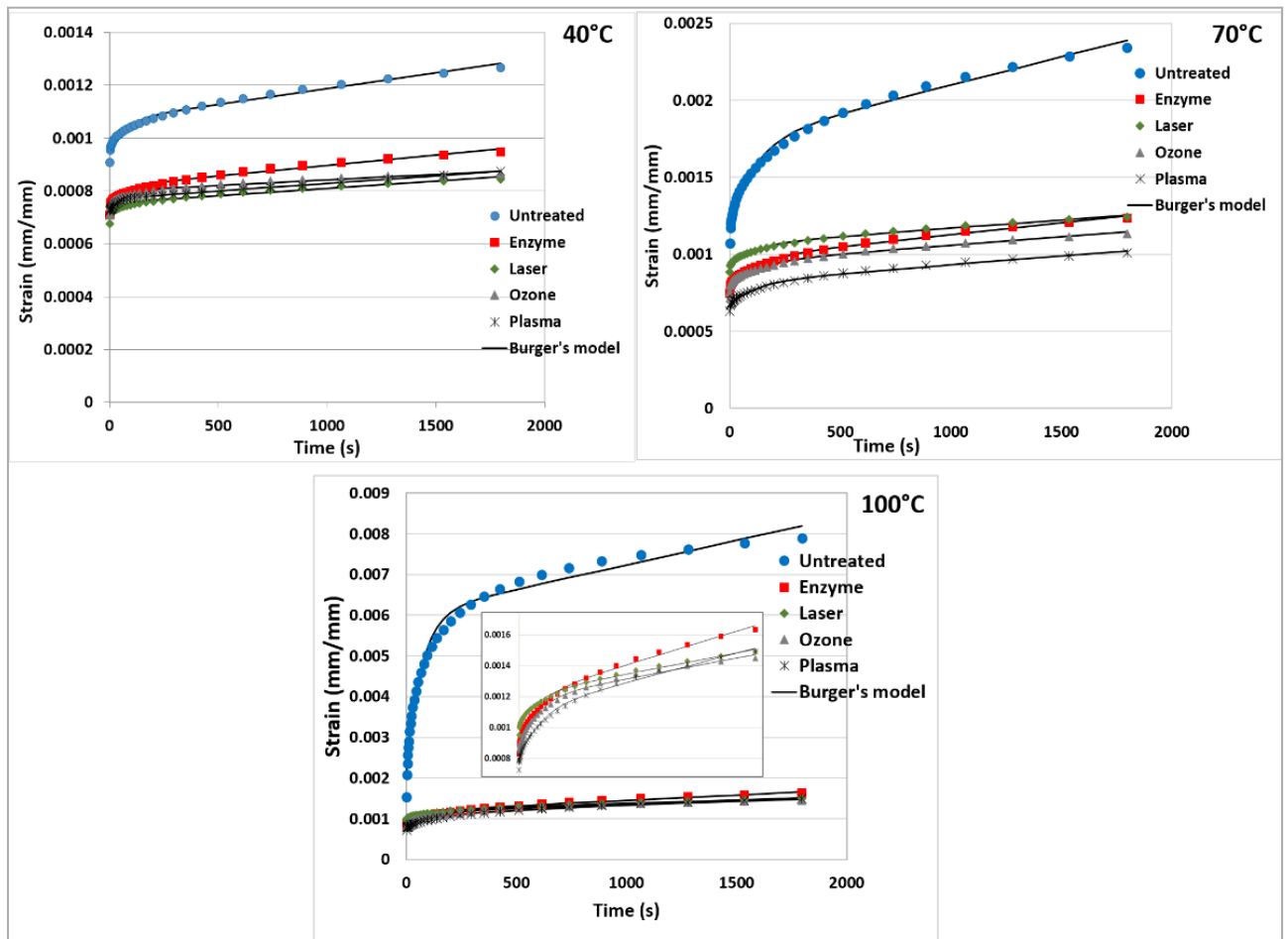


Figure 27. Creep curves of composites at different temperatures.

Table 6. Summary of four parameters in Burger's model for short term creep of the composites.

Temperature	Parameters	Treatments				
		Untreated	Enzyme	Laser	Ozone	Plasma
40 °C	E_m [MPa]	2095.9 (69.4)	2685.9 (81.1)	2846.8 (88.5)	2697.7 (76.9)	2761.4 (86.4)
	E_k [MPa]	17761.7 (7160.8)	27557.5 (13056.1)	38654.8 (19501.0)	34269.9 (16812.2)	43244.2 (23485.5)
	η_m [Pa.s]	1.67E13 (5.94E6)	2.53E13 (1.04E7)	3.57E13 (1.45E7)	4.79E13 (3.05E7)	3.44E13 (1.18E7)
	η_k [Pa.s]	1.32E6 (1.37E6)	2.28E12 (2.66E6)	1.88E12 (2.71E6)	2.28E12 (2.98E6)	1.59E12 (2.52E6)
	SS^*	4.22E-9	2.28E-9	1.53E-9	1.76E-9	1.35E-9

	Adj. R^2	0.9822	0.97795	0.96798	0.95771	0.9692
70 °C	E_m [MPa]	1673.7 (115.7)	2505.8 (90.9)	2153.9 (62.9)	2488.5 (79.2)	2976.5 (109.8)
	E_k [MPa]	3719.6 (1129.2)	11303.05 (4056.9)	15196.9 (5887.2)	13682.5 (5398.7)	13819.5 (4914.4)
	η_m [Pa.s]	5.47E12 (2.28E6)	1.31E13 (5.04E6)	1.83E13 (8.05E6)	1.85E13 (9.07E6)	1.74E13 (7.28E6)
	η_k [Pa.s]	4.36E11 (2.69E5)	1.48E12 (9.97E5)	1.68E12 (1.37E6)	1.85E12 (1.34E6)	1.71E12 (1.19E6)
	SS^*	3.71E-8	4.82E-9	3.88E-9	3.81E-9	3.43E-9
	Adj. R^2	0.98969	0.9903	0.98508	0.98696	0.98868
100 °C	E_m [MPa]	935.6 (262.6)	2225.8 (103.3)	1989.6 (63.3)	2325.5 (113.6)	2537.9 (124.0)
	E_k [MPa]	513.9 (108.7)	6710.2 (2246.4)	9710.1 (3494.3)	6157.4 (1826.2)	6202.9 (1995.9)
	η_m [Pa.s]	1.66E12 (1.05E6)	7.76E12 (2.73E6)	1.21E13 (4.96E6)	1.24E13 (6.79E6)	8.89E12 (3.64E6)
	η_k [Pa.s]	3.51E10 (1.96E4)	9.62E11 (5.62E5)	1.35E12 (8.69E5)	8.46E11 (4.53E5)	9.93E11 (5.05E5)
	SS^*	1.44E-6	1.04E-8	6.04E-9	1.04E-8	9.33E-9
	Adj. R^2	0.98555	0.99268	0.9904	0.98994	0.99314

SS^* : Sum of squared deviations

5.3.5 Dynamic mechanical analysis

The variation of storage modulus (E') of untreated and treated jute fiber composites as a function of temperature at frequency of 1 Hz is shown in figure 28a. It can be seen that there is a gradual fall in the storage modulus of all treated jute composites when the temperature is increased compared to untreated jute composite which had a very steep fall in E' . The DMA curves of the treated and untreated composites present two distinct region, a glassy region and a rubbery region [86]. The glassy region is below the glass transition temperature (T_g) while the rubbery region is above T_g . In the glassy region, components are highly immobile, close and tightly packed resulting in high storage modulus [87] but as temperature increases the components become more mobile and lose their close packing arrangement resulting in loss of stiffness and storage modulus. There is not a big difference in the storage modulus values of composites in the glassy region but all treated composites have higher values of storage modulus in the rubbery region. This might be due to better fiber/matrix interaction at the interface, decreased molecular mobility of polymer chains and better reinforcing effect of treated fibers which increases the thermal and mechanical stability of the material at higher temperatures [88] as shown prominently by laser treated jute composite (figure 28a).

It has been reported that T_g values obtained from loss modulus (E'') are more realistic as compared to those obtained from damping factor ($\tan\delta$) [61]. A positive shift in T_g to higher temperature for all treated jute composites is observed as given in table 7 due to reduced mobility of matrix polymer chains and better reinforcement effect. It can be reasoned that the interfaces were markedly changed by the fiber treatments. According to Almeida *et al.* [62] systems containing more restrictions and a higher degree of reinforcement tend to exhibit higher T_g . The T_g increased from 105 °C for untreated to 126 - 146 °C for treated composites, especially the laser treated one with a value of 146 °C.

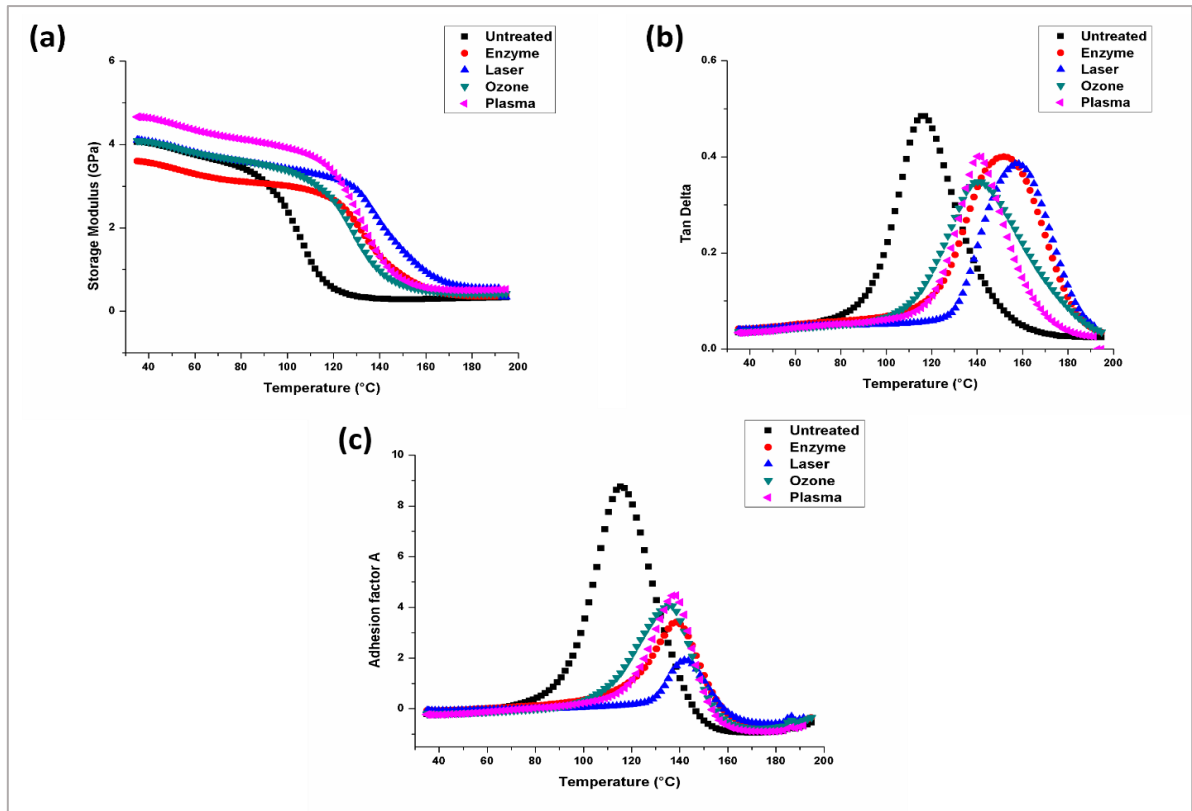


Figure 28. Temperature dependence of (a) storage modulus, (b) $\tan \delta$ and (c) adhesion factor for untreated and treated jute composites.

The change in damping factor ($\tan \delta$) of untreated and treated jute composites with respect to temperature is shown in figure 28b. Untreated composite displayed a higher $\tan \delta$ peak value compared to treated composites. This may be attributed to more energy dissipation due to frictional damping at the weaker untreated fiber/matrix interface. When a composite material, consisting of fibers (essentially elastic), polymer matrix (viscoelastic) and fiber/matrix interfaces, is subjected to deformation, the deformation energy is dissipated mainly in the matrix and at the interface. If matrix, fiber volume fraction and fiber orientation are identical, as it is the situation in current study, then $\tan \delta$ can be used to evaluate the interfacial properties between fiber and matrix. The composites with poor fiber/matrix interface have a tendency to dissipate more energy than the composites with good interface bonding i.e. poor interfacial adhesion leads to greater damping [73, 89]. The lower $\tan \delta$ peak height is shown by ozone treated composite followed by laser treated one, among the treated composites, exhibiting a better adhesion between jute fibers and green epoxy matrix. The reduction in $\tan \delta$ peak also represents the good load bearing capacity of a particular composite [90]. The broadening of $\tan \delta$ peak is also observed for enzyme, ozone and laser treated samples when compared with $\tan \delta$ peak of untreated composite (figure 28b). This indicates the occurrence of molecular relaxations at the interfacial region of composite material.

Table 7. T_g values obtained from E'' curve.

Composites	T_g from E''_{\max} curve [°C]
Untreated	105.60
Enzymes	137.43

Laser	146.13
Ozone	126.78
Plasma	134.57

The effect of treatments on the interfacial adhesion between jute fibers and green epoxy resin was verified by adhesion factor (A) for fiber/matrix interface using the following formula [19];

$$A = \frac{\tan\delta_c(T)}{(1-V_f)(\tan\delta_m(T))} - 1 \quad [8]$$

Where V_f is the fiber volume fraction in the composite, $\tan\delta_c(T)$ and $\tan\delta_m(T)$ are the values of $\tan\delta$ at temperature T of the composite and neat matrix respectively. Low A values suggest greater interaction between the fiber and matrix. Figure 28c expresses low adhesion factor curves of treated fiber composites compared to untreated composite which reveals the improvement in fiber matrix adhesion with fiber treatments. Laser treated composite has the lowest adhesion factor.

6 Evaluation of results and new findings

In this research work, woven jute/green epoxy composites were prepared using three different categories of reinforcement viz. novel surface treated jute fabrics, pulverized micro/nano jute fillers and cellulose coated jute fabrics. Mechanical, dynamic mechanical and creep properties were evaluated. The modeling of creep data was satisfactorily conducted by using Burger's model. The long term creep performance of micro/nano filled jute composites was successfully predicted by using Burger's model, Findley's power law model and a simpler two-parameter power law model. The following findings were drawn from the results;

- ◆ The tensile and flexural properties were found to improve with the incorporation of PJF in alkali treated jute/green epoxy composites except the decrease in tensile strength of composite reinforced with only alkali treated jute fabric.
- ◆ Tensile modulus, flexural strength, flexural modulus, fatigue life and fracture toughness of composites were found to improve with the increase in concentration of nanocellulose coating over jute reinforcement except the decrease in tensile strength.
- ◆ Flexural properties of composites were enhanced after fiber treatments especially for laser and ozone treated ones.
- ◆ The creep resistance of PJF filled jute composites was found to improve significantly with the increase of filler content in matrix. This may be attributed to the inhibited mobility of polymer matrix molecular chains initiated by large interfacial contact area of PJF as well as their interfacial interaction with the polymer matrix.
- ◆ The surface treated jute composites showed less creep deformation than untreated one at all temperatures. The least creep deformation is shown by laser treated composite which dominantly exhibited elastic behavior rather than viscous behavior, especially at higher temperatures.
- ◆ The Burger's model fitted well the short term creep data. The creep strain was found to increase with temperature.
- ◆ The master curves, generated by time-temperature superposition principle (TTSP), indicated the prediction of the long-term performance of composites.

- ◆ The Findley's power law model was satisfactory for fitting and predicting the long-term creep performance of composites compared to Burger and two parameter model.
- ◆ Dynamic mechanical analysis revealed the increase in storage modulus and reduction in tangent delta peak height of composites with the increase in filler content, increase in concentration of nanocellulose coating over jute reinforcement and of surface treated jute composites.

6.1 Proposed applications and limitations

The possible applications of these composites can be in automotive interiors especially, boot liners, door panels, spare tire cover and interior vehicle linings. Despite the advantages of sustainability of these composites and cheaper availability of jute fibers, the main drawback is a little high cost of green epoxy resin compared to synthetic ones. The utilization of jute waste as precursor to extract and purify cellulose is a positive aspect of this work. The methods used in this study for fiber treatment especially, the ozone and laser are environment friendly and easy to perform but the laser treatment can be applied effectively on a little thick fabric substrate.

7 References

- [1] M. Kabir, *et al.*, "Chemical treatments on plant-based natural fibre reinforced polymer composites: An overview," *Composites Part B: Engineering*, vol. 43, pp. 2883-2892, 2012.
- [2] H. Ku, *et al.*, "A review on the tensile properties of natural fiber reinforced polymer composites," *Composites Part B: Engineering*, vol. 42, pp. 856-873, 2011.
- [3] L. Dányádi, *et al.*, "Effect of various surface modifications of wood flour on the properties of PP/wood composites," *Composites Part A: Applied Science and Manufacturing*, vol. 41, pp. 199-206, 2010.
- [4] N. Lu and S. Oza, "Thermal stability and thermo-mechanical properties of hemp-high density polyethylene composites: Effect of two different chemical modifications," *Composites Part B: Engineering*, vol. 44, pp. 484-490, 2013.
- [5] M. P. Dicker, *et al.*, "Green composites: A review of material attributes and complementary applications," *Composites Part A: Applied Science and Manufacturing*, vol. 56, pp. 280-289, 2014.
- [6] X. Li, *et al.*, "Chemical treatments of natural fiber for use in natural fiber-reinforced composites: a review," *Journal of Polymers and the Environment*, vol. 15, pp. 25-33, 2007.
- [7] D. N. Saheb and J. Jog, "Natural fiber polymer composites: a review," *Advances in polymer technology*, vol. 18, pp. 351-363, 1999.
- [8] F. Corrales, *et al.*, "Chemical modification of jute fibers for the production of green-composites," *Journal of Hazardous Materials*, vol. 144, pp. 730-735, 2007.
- [9] Y. Cai, *et al.*, "Dyeing of jute and jute/cotton blend fabrics with 2: 1 pre-metallised dyes," *Dyes and Pigments*, vol. 45, pp. 161-168, 2000.
- [10] C. Hong, *et al.*, "Mechanical properties of silanized jute-polypropylene composites," *Journal of Industrial and Engineering Chemistry*, vol. 14, pp. 71-76, 2008.
- [11] S. Mukhopadhyay and R. Fanguero, "Physical modification of natural fibers and thermoplastic films for composites—a review," *Journal of Thermoplastic Composite Materials*, vol. 22, pp. 135-162, 2009.
- [12] Y. Li and K. L. Pickering, "Hemp fibre reinforced composites using chelator and enzyme treatments," *Composites science and technology*, vol. 68, pp. 3293-3298, 2008.

- [13] S. Mahdavi, *et al.*, "Comparison of mechanical properties of date palm fiber-polyethylene composite," *BioResources*, vol. 5, pp. 2391-2403, 2010.
- [14] A. Bledzki, *et al.*, "Unidirectional hemp and flax EP and PP composites: Influence of defined fiber treatments," *Journal of applied polymer science*, vol. 93, pp. 2150-2156, 2004.
- [15] S. H. Aziz and M. P. Ansell, "The effect of alkalization and fibre alignment on the mechanical and thermal properties of kenaf and hemp bast fibre composites: Part 1—polyester resin matrix," *Composites science and technology*, vol. 64, pp. 1219-1230, 2004.
- [16] M. Sayeed, *et al.*, "Mechanical properties of surface modified jute fiber/polypropylene nonwoven composites," *Polymer Composites*, vol. 35, pp. 1044-1050, 2014.
- [17] S. Mohanty, *et al.*, "Effect of MAPP as a coupling agent on the performance of jute–PP composites," *Journal of Reinforced Plastics and Composites*, vol. 23, pp. 625-637, 2004.
- [18] A. Karmaker and J. Youngquist, "Injection molding of polypropylene reinforced with short jute fibers," *Journal of applied polymer science*, vol. 62, pp. 1147-1151, 1996.
- [19] B. K. Goriparthi, *et al.*, "Effect of fiber surface treatments on mechanical and abrasive wear performance of polylactide/jute composites," *Composites Part A: Applied Science and Manufacturing*, vol. 43, pp. 1800-1808, 2012.
- [20] Y. Karaduman and L. Onal, "Dynamic mechanical and thermal properties of enzyme-treated jute/polyester composites," *Journal of Composite Materials*, vol. 47, pp. 2361-2370, 2013.
- [21] Y. Karaduman, *et al.*, "Effect of enzymatic pretreatment on the mechanical properties of jute fiber-reinforced polyester composites," *Journal of Composite Materials*, p. 0021998312446826, 2012.
- [22] E. Sinha, *et al.*, "Study of the structural and thermal properties of plasma treated jute fibre," *Applied Physics A*, vol. 92, pp. 283-290, 2008.
- [23] E. Bozaci, *et al.*, "Effects of the atmospheric plasma treatments on surface and mechanical properties of flax fiber and adhesion between fiber–matrix for composite materials," *Composites Part B: Engineering*, vol. 45, pp. 565-572, 2013.
- [24] J. Laine and D. Goring, "Influence of ultrasonic irradiation on the properties of cellulosic fibres," *Cellul Chem Technol*, 1977.
- [25] J. Gassan and V. S. Gutowski, "Effects of corona discharge and UV treatment on the properties of jute-fibre epoxy composites," *Composites science and technology*, vol. 60, pp. 2857-2863, 2000.
- [26] M.-J. Cho and B.-D. Park, "Tensile and thermal properties of nanocellulose-reinforced poly (vinyl alcohol) nanocomposites," *Journal of Industrial and Engineering Chemistry*, vol. 17, pp. 36-40, 2011.
- [27] S.-Y. Lee, *et al.*, "Nanocellulose reinforced PVA composite films: effects of acid treatment and filler loading," *Fibers and Polymers*, vol. 10, pp. 77-82, 2009.
- [28] C. J. Chirayil, *et al.*, "Nanofibril reinforced unsaturated polyester nanocomposites: morphology, mechanical and barrier properties, viscoelastic behavior and polymer chain confinement," *Industrial Crops and Products*, vol. 56, pp. 246-254, 2014.
- [29] D. Dai, *et al.*, "Fabrication of nanocelluloses from hemp fibers and their application for the reinforcement of hemp fibers," *Industrial Crops and Products*, vol. 44, pp. 192-199, 2013.
- [30] L. M. M. Costa, *et al.*, "Bionanocomposites from electrospun PVA/pineapple nanofibers/*Stryphnodendron adstringens* bark extract for medical applications," *Industrial Crops and Products*, vol. 41, pp. 198-202, 2013.

- [31] K. Das, *et al.*, "Physicomechanical and thermal properties of jute-nanofiber-reinforced biocopolyester composites," *Industrial & Engineering Chemistry Research*, vol. 49, pp. 2775-2782, 2010.
- [32] B. A. Acha, *et al.*, "Creep and dynamic mechanical behavior of PP–jute composites: Effect of the interfacial adhesion," *Composites Part A: Applied Science and Manufacturing*, vol. 38, pp. 1507-1516, 2007.
- [33] Y. Jia, *et al.*, "Creep and recovery of polypropylene/carbon nanotube composites," *International Journal of Plasticity*, vol. 27, pp. 1239-1251, 2011.
- [34] Y. Xu, *et al.*, "Creep behavior of bagasse fiber reinforced polymer composites," *Bioresource Technology*, vol. 101, pp. 3280-3286, 2010.
- [35] M. Faraz, *et al.*, "Characterization and modeling of creep behavior of a thermoset nanocomposite," *Polymer Composites*, vol. 36, pp. 322-329, 2015.
- [36] J.-L. Yang, *et al.*, "On the characterization of tensile creep resistance of polyamide 66 nanocomposites. Part II: Modeling and prediction of long-term performance," *Polymer*, vol. 47, pp. 6745-6758, 2006.
- [37] V. Baheti and J. Militky, "Reinforcement of wet milled jute nano/micro particles in polyvinyl alcohol films," *Fibers and Polymers*, vol. 14, pp. 133-137, 2013.
- [38] J. Dembický, "Impact of Laser Thermal Stress on Cotton Fabric," *Fibres & Textiles in Eastern Europe*, vol. 18, p. 80, 2010.
- [39] R. Mishra, *et al.*, "Novelties of 3-D woven composites and nanocomposites," *The Journal of The Textile Institute*, vol. 105, pp. 84-92, 2014.
- [40] "ASTM D3039 - 00," in *Standard test method for tensile properties of polymer matrix composite materials*, ed. West Conshohocken, PA: ASTM International, 2006.
- [41] "ASTM D790 - 03," in *Standard test method for flexural properties of unreinforced and reinforced plastics and electrical insulating materials*, ed. West Conshohocken, PA: ASTM International, 2003.
- [42] "ASTM D5045 - 99," in *Standard test Method for plane-strain fracture toughness and strain energy release rate of plastic materials*, ed. West Conshohocken, PA: ASTM International, 1999.
- [43] I. M. Ward and J. Sweeney, *Mechanical properties of solid polymers*: John Wiley & Sons, 2012.
- [44] W. N. Findley, *et al.*, *Creep and relaxation of nonlinear viscoelastic materials: With an introduction to linear viscoelasticity*. New York: Dover Publications, Inc., 1989.
- [45] A. Plaseied and A. Fatemi, "Tensile creep and deformation modeling of vinyl ester polymer and its nanocomposite," *Journal of Reinforced Plastics and Composites*, vol. 28, pp. 1775-1788, 2008.
- [46] M. Tajvidi, *et al.*, "Time–temperature superposition principle applied to a kenaf-fiber/high-density polyethylene composite," *Journal of applied polymer science*, vol. 97, pp. 1995-2004, 2005.
- [47] M. Meloun and J. Militky, *Statistical data analysis: A practical guide*: Woodhead Publishing, Limited, 2011.
- [48] M. Morshed, *et al.*, "Plasma treatment of natural jute fibre by RIE 80 plus plasma tool," *Plasma Science and Technology*, vol. 12, p. 325, 2010.

- [49] M. M. Haque, *et al.*, "Physico-mechanical properties of chemically treated palm and coir fiber reinforced polypropylene composites," *Bioresource Technology*, vol. 100, pp. 4903-4906, 2009.
- [50] V. Tserki, *et al.*, "A study of the effect of acetylation and propionylation surface treatments on natural fibres," *Composites Part A: Applied Science and Manufacturing*, vol. 36, pp. 1110-1118, 2005.
- [51] W. Liu, *et al.*, "Effects of alkali treatment on the structure, morphology and thermal properties of native grass fibers as reinforcements for polymer matrix composites," *Journal of Materials Science*, vol. 39, pp. 1051-1054, 2004.
- [52] M. Jacob, *et al.*, "Novel woven sisal fabric reinforced natural rubber composites: tensile and swelling characteristics," *Journal of Composite Materials*, vol. 40, pp. 1471-1485, 2006.
- [53] H. Kargarzadeh, *et al.*, "Cellulose nanocrystal: A promising toughening agent for unsaturated polyester nanocomposite," *Polymer*, vol. 56, pp. 346-357, 2015.
- [54] J. Militký and A. Jabbar, "Comparative evaluation of fiber treatments on the creep behavior of jute/green epoxy composites," *Composites Part B: Engineering*, vol. 80, pp. 361-368, 2015.
- [55] S. Siengchin and J. Karger-Kocsis, "Structure and creep response of toughened and nanoreinforced polyamides produced via the latex route: Effect of nanofiller type," *Composites Science and Technology*, vol. 69, pp. 677-683, 2009.
- [56] S. Siengchin, "Dynamic mechanic and creep behaviors of polyoxymethylene/boehmite alumina nanocomposites produced by water-mediated compounding Effect of particle size," *Journal of Thermoplastic Composite Materials*, vol. 26, pp. 863-877, 2013.
- [57] A. Hao, *et al.*, "Creep and recovery behavior of kenaf/polypropylene nonwoven composites," *Journal of Applied Polymer Science*, vol. 131, DOI: 10.1002/app.40726, 2014.
- [58] X. Wang, *et al.*, "Temperature dependence of creep and recovery behaviors of polymer composites filled with chemically reduced graphene oxide," *Composites Part A: Applied Science and Manufacturing*, vol. 69, pp. 288-298, 2015.
- [59] Q.-P. Feng, *et al.*, "Synthesis of epoxy composites with high carbon nanotube loading and effects of tubular and wavy morphology on composite strength and modulus," *Polymer*, vol. 52, pp. 6037-6045, 2011.
- [60] D. Shanmugam and M. Thiruchitrambalam, "Static and dynamic mechanical properties of alkali treated unidirectional continuous palmyra palm leaf stalk fiber/jute fiber reinforced hybrid polyester composites," *Materials & Design*, vol. 50, pp. 533-542, 2013.
- [61] M. Akay, "Aspects of dynamic mechanical analysis in polymeric composites," *Composites science and technology*, vol. 47, pp. 419-423, 1993.
- [62] J. H. S. Almeida Jr, *et al.*, "Study of hybrid intralaminar curaua/glass composites," *Materials & Design*, vol. 42, pp. 111-117, 2012.
- [63] A. Mukherjee, *et al.*, "Structural mechanics of jute: the effects of hemicellulose or lignin removal," *Journal of the Textile Institute*, vol. 84, pp. 348-353, 1993.
- [64] D. Ray, *et al.*, "Effect of alkali treated jute fibres on composite properties," *Bulletin of materials science*, vol. 24, pp. 129-135, 2001.
- [65] M. D. H. Beg and K. L. Pickering, "Accelerated weathering of unbleached and bleached Kraft wood fibre reinforced polypropylene composites," *Polymer Degradation and Stability*, vol. 93, pp. 1939-1946, 2008.

- [66] N. Terinte, *et al.*, "Overview on native cellulose and microcrystalline cellulose I structure studied by X-ray diffraction (WAXD): Comparison between measurement techniques," *Lenzinger Berichte*, vol. 89, pp. 118-131, 2011.
- [67] B. M. Kale, *et al.*, "Dyeing and stiffness characteristics of cellulose-coated cotton fabric," *Cellulose*, vol. 23, pp. 981-992, 2016.
- [68] B. M. Kale, *et al.*, "Coating of cellulose-TiO₂ nanoparticles on cotton fabric for durable photocatalytic self-cleaning and stiffness," *Carbohydrate Polymers*, vol. 150, pp. 107-113, 2016.
- [69] V. Carvelli, *et al.*, "Fatigue and Izod impact performance of carbon plain weave textile reinforced epoxy modified with cellulose microfibrils and rubber nanoparticles," *Composites Part A: Applied Science and Manufacturing*, vol. 84, pp. 26-35, 2016.
- [70] B. Wetzel, *et al.*, "Epoxy nanocomposites—fracture and toughening mechanisms," *Engineering fracture mechanics*, vol. 73, pp. 2375-2398, 2006.
- [71] H. Alamri and I. M. Low, "Characterization of epoxy hybrid composites filled with cellulose fibers and nano-SiC," *Journal of Applied Polymer Science*, vol. 126, DOI: 10.1002/app.36815, 2012.
- [72] S. Zhao, *et al.*, "Improvements and mechanisms of fracture and fatigue properties of well-dispersed alumina/epoxy nanocomposites," *Composites Science and Technology*, vol. 68, pp. 2976-2982, 2008.
- [73] L. A. Pothan, *et al.*, "Dynamic mechanical analysis of banana fiber reinforced polyester composites," *Composites Science and Technology*, vol. 63, pp. 283-293, 2003.
- [74] C. J. Chirayil, *et al.*, "Rheological behaviour of nanocellulose reinforced unsaturated polyester nanocomposites," *International Journal of Biological Macromolecules*, vol. 69, pp. 274-281, 2014.
- [75] D. Ray, *et al.*, "Dynamic mechanical and thermal analysis of vinylester-resin-matrix composites reinforced with untreated and alkali-treated jute fibres," *Composites science and technology*, vol. 62, pp. 911-917, 2002.
- [76] J. Lu, *et al.*, "Preparation and properties of microfibrillated cellulose polyvinyl alcohol composite materials," *Composites Part A: Applied Science and Manufacturing*, vol. 39, pp. 738-746, 2008.
- [77] M. A. S. A. Samir, *et al.*, "Cellulose nanocrystals reinforced poly (oxyethylene)," *Polymer*, vol. 45, pp. 4149-4157, 2004.
- [78] J.-M. Raquez, *et al.*, "Surface-modification of cellulose nanowhiskers and their use as nanoreinforcers into polylactide: a sustainably-integrated approach," *Composites Science and Technology*, vol. 72, pp. 544-549, 2012.
- [79] A. Martínez-Hernández, *et al.*, "Dynamical–mechanical and thermal analysis of polymeric composites reinforced with keratin biofibers from chicken feathers," *Composites Part B: Engineering*, vol. 38, pp. 405-410, 2007.
- [80] A. Brunner, *et al.*, "The influence of silicate-based nano-filler on the fracture toughness of epoxy resin," *Engineering fracture mechanics*, vol. 73, pp. 2336-2345, 2006.
- [81] S. Dong and R. Gauvin, "Application of dynamic mechanical analysis for the study of the interfacial region in carbon fiber/epoxy composite materials," *Polymer Composites*, vol. 14, pp. 414-420, 1993.
- [82] J. H. S. A. Júnior, *et al.*, "Study of hybrid intralaminar curaua/glass composites," *Materials & Design*, vol. 42, pp. 111-117, 2012.

- [83] J. B. Gadhe, *et al.*, "Surface modification of lignocellulosic fibers using high-frequency ultrasound," *Cellulose*, vol. 13, pp. 9-22, 2006.
- [84] H. A. Khalil, *et al.*, "Conventional agro-composites from chemically modified fibres," *Industrial Crops and Products*, vol. 26, pp. 315-323, 2007.
- [85] M. A. Hidalgo-Salazar, *et al.*, "The effect of interfacial adhesion on the creep behaviour of LDPE–Al–Fique composite materials," *Composites Part B: Engineering*, vol. 55, pp. 345-351, 2013.
- [86] V. Sreenivasan, *et al.*, "Dynamic mechanical and thermo-gravimetric analysis of Sansevieria cylindrica/polyester composite: Effect of fiber length, fiber loading and chemical treatment," *Composites Part B: Engineering*, vol. 69, pp. 76-86, 2015.
- [87] M. Jacob, *et al.*, "Dynamical mechanical analysis of sisal/oil palm hybrid fiber reinforced natural rubber composites," *Polymer Composites*, vol. 27, pp. 671-680, 2006.
- [88] M. J. John and R. D. Anandjiwala, "Chemical modification of flax reinforced polypropylene composites," *Composites Part A: Applied Science and Manufacturing*, vol. 40, pp. 442-448, 2009.
- [89] A. Afaghi-Khatibi and Y.-W. Mai, "Characterisation of fibre/matrix interfacial degradation under cyclic fatigue loading using dynamic mechanical analysis," *Composites Part A: Applied Science and Manufacturing*, vol. 33, pp. 1585-1592, 2002.
- [90] M. Jawaid, *et al.*, "Effect of jute fibre loading on tensile and dynamic mechanical properties of oil palm epoxy composites," *Composites Part B: Engineering*, vol. 45, pp. 619-624, 2013.

8 List of papers published by the author

8.1 Publications in journals (relevant to theme of PhD dissertation)

- **Jabbar A.**, Militky J., Wiener J., Kale BM, Rwawiire S, Ali U "Nanocellulose coated woven jute/green epoxy composites: characterization of mechanical and dynamic mechanical behavior" *Composites Structures*. 2017; 161:340-349.
(Impact factor = 3.853)
- **Jabbar A**, Militky J, Kale BM, Rwawiire S, Nawab Y, Baheti V. "Modeling and analysis of the creep behavior of jute/green epoxy composites incorporated with chemically treated pulverized nano/micro jute fibers". *Industrial Crops and Products*. 2016; 84:230-240.
(Impact factor = 3.449)
- Militky J, **Jabbar A.**" Comparative evaluation of fiber treatments on the creep behavior of jute/green epoxy composites". *Composites Part B: Engineering*. 2015; 80:361-368.
(Impact factor = 3.850)
- **Jabbar A**, Militky J, Wiener J, Karahan M. "Static and dynamic mechanical properties of novel treated jute/green epoxy composites". *Textile Research Journal*. 2016; 86 (9):960-74.
(Impact factor = 1.229)
- **Jabbar, A**, J. Militky, J. Wiener, M. Usman Javaid and S. Rwawiire "Tensile, Surface and Thermal Characterization of Jute Fibers after Novel Treatments". *Indian Journal of Fiber and Textile Research*. 2016; 41:249-254
(Impact factor = 0.420)

8.2 Contribution in conference proceedings (relevant to theme)

- **Jabbar**, J. Militký “Creep behavior of novel treated jute/green epoxy composites” Workshop Světlanka, ISBN 978-80-7494-229-7 September 2015, pp 52-57.
- **A. Jabbar**, J. Militký “Investigation of the mechanical, creep and dynamic mechanical properties of jute/green epoxy composites incorporated with chemically treated nano/micro jute fibers” Aachen-Dresden-Denkendorf International Textile Conference November 2016.
- **A. Jabbar**, J. Militký “Investigation of the creep and dynamic mechanical properties of jute/green epoxy composites incorporated with chemically treated pulverized nano/micro jute fibers”. Workshop Bila Voda, ISBN 978-80-7494-293-8 September 2016, pp 56-61.

8.3 Citations (as on 04.02.2017)

Article: **Jabbar A**, Militký J, Kale BM, Rwawiire S, Nawab Y, Baheti V. Modeling and analysis of the creep behavior of jute/green epoxy composites incorporated with chemically treated pulverized nano/micro jute fibers. *Industrial Crops and Products*. 2016; 84:230-240.

(Cited in)

1. Ali, *et al.*, "Hydrophobic treatment of natural fibers and their composites—A review," *Journal of Industrial Textiles*, DOI: 10.1177/1528083716654468, 2016.
2. Jabbar, *et al.*, "Nanocellulose coated woven jute/green epoxy composites: Characterization of mechanical and dynamic mechanical behavior," *Composite Structures*, vol. 161, pp. 340-349, 2017.
3. V. Baheti, *et al.*, "Reinforcement of ozone pre-treated and enzyme hydrolyzed longer jute micro crystals in poly lactic acid composite films," *Composites Part B: Engineering*, vol. 95, pp. 9-17, 2016.
4. X. P. Zhang, *et al.*, "Mechanical and thermal properties of Al_2O_3 -filled epoxy composites," in *Materials Science Forum*, 2016, pp. 111-117.
5. R. Hunter, *et al.*, "Experimental study of the effect of microspheres and milled glass in the adhesive on the mechanical adhesion of single lap joints," *The Journal of Adhesion*, pp. 1-17, 2016.
6. S. Rwawiire, *et al.*, "Short-term creep of barkcloth reinforced laminar epoxy composites," *Composites Part B: Engineering*, vol. 103, pp. 131-138, 2016.

Article: **Jabbar A.**, Militky J., Wiener J., Kale BM, Rwawiire S, Ali U “Nanocellulose coated woven jute/green epoxy composites: characterization of mechanical and dynamic mechanical behavior” *Composites Structures*. 2017; 161:340-349.

(Cited in)

1. N. Saba, *et al.*, "Mechanical, morphological and structural properties of cellulose nanofibers reinforced epoxy composites," *International Journal of Biological Macromolecules*, vol. 97, pp. 190–200, 2017.

Article: Militký J, **Jabbar A**. Comparative evaluation of fiber treatments on the creep behavior of jute/green epoxy composites. *Composites Part B: Engineering*. 2015; 80:361-368.

(Cited in)

1. Jabbar, *et al.*, "Modeling and analysis of the creep behavior of jute/green epoxy composites incorporated with chemically treated pulverized nano/micro jute fibers," *Industrial Crops and Products*, vol. 84, pp. 230-240, 2016.
2. A. Ali, *et al.*, "Hydrophobic treatment of natural fibers and their composites—A review," *Journal of Industrial Textiles*, DOI: 10.1177/1528083716654468, 2016.
3. M. Ridzuan, *et al.*, "Thermal behaviour and dynamic mechanical analysis of Pennisetum purpureum/glass-reinforced epoxy hybrid composites," *Composite Structures*, vol. 152, pp. 850-859, 2016.
4. A. Jabbar, *et al.*, "Nanocellulose coated woven jute/green epoxy composites: Characterization of mechanical and dynamic mechanical behavior," *Composite Structures*, vol. 161, pp. 340-349, 2017.
5. V. Baheti, *et al.*, "Reinforcement of ozone pre-treated and enzyme hydrolyzed longer jute micro crystals in poly lactic acid composite films," *Composites Part B: Engineering*, vol. 95, pp. 9-17, 2016.
6. C.-m. Liu, *et al.*, "Enhanced tensile creep stability of immiscible poly (l-lactide)/poly (ethylene vinyl acetate) blends achieved by adding carbon nanotubes," *Composites Part B: Engineering*, vol. 107, pp. 174-181, 2016.
7. S. Rwawiire, *et al.*, "Short-term creep of barkcloth reinforced laminar epoxy composites," *Composites Part B: Engineering*, vol. 103, pp. 131-138, 2016.
8. V. Fiore, *et al.*, "Aging resistance of bio-epoxy jute-basalt hybrid composites as novel multilayer structures for cladding," *Composite Structures*, vol. 160, pp. 1319-1328, 2017.
9. N. P. Lorandi, *et al.*, "Dynamic Mechanical Analysis (DMA) of Polymeric Composite Materials," *Scientia cum Industria*, vol. 4, pp. 48-60, 2016.

Article: Jabbar A, Militký J, Wiener J, Karahan M. Static and dynamic mechanical properties of novel treated jute/green epoxy composites. *Textile Research Journal*. 2016; 86 (9):960-974.

(Cited in)

1. M. Karahan, *et al.*, "Investigation of the properties of natural fibre woven fabrics as a reinforcement materials for green composites," *Fibres & Textiles in Eastern Europe*, vol. 4(118) pp. 98-104, 2016.
2. M. Koyuncu, *et al.*, "Static and dynamic mechanical properties of cotton/epoxy green composites," *Fibres & Textiles in Eastern Europe*, vol. 4 (118), pp. 105--111, 2016.
3. A. Jabbar, *et al.*, "Nanocellulose coated woven jute/green epoxy composites: Characterization of mechanical and dynamic mechanical behavior," *Composite Structures*, vol. 161, pp. 340-349, 2017.
4. J. P. Patel and P. H. Parsania, "Fabrication and comparative mechanical, electrical and water absorption characteristic properties of multifunctional epoxy resin of bisphenol-C and commercial epoxy-treated and-untreated jute fiber-reinforced composites," *Polymer Bulletin*, DOI: 10.1007/s00289-016-1725-0.

Curriculum Vitae

Educational Qualifications

- ❑ PhD Textile Technics and Material Engineering (in progress)
Technical University of Liberec, Czech Republic
- ❑ M.Sc. Textile Engineering (2010-2012)
National Textile University, Faisalabad-37610 Pakistan
- ❑ B.Sc. Textile Engineering (2002-2006)
National Textile University, Faisalabad-37610 Pakistan



Impact factor Journal Publications

- ❑ **Jabbar A.**, Militky J., Wiener J., Kale BM, Rwawiire S, Ali U “Nanocellulose coated woven jute/green epoxy composites: characterization of mechanical and dynamic mechanical behavior” **Composites Structures**. 2017; 161:340-349.
- ❑ **S Rwawiire, B Tomkova, J Wiener, J Militky, A Kasedde, B M Kale, A Jabbar.** “Short-term creep of barkcloth reinforced laminar epoxy composites” **Composites Part B: Engineering**. 2016; 103:131-138.
- ❑ U Hussain, S Irshad, W Anam, H Abbasi, F Ahmed, **A Jabbar.** “ Effect of Different Conditioning Methods on the Properties of Hosiery Yarn and Knitted Fabric” **Journal of Engineered Fibers and Fabrics**” Vol. 10(3), 2015, pp. 12-19.
- ❑ K. Shaker, **A. Jabbar**, M. Karahan, N. Karahan, Y. Nawab “Study of dynamic compressive behavior of aramid and UHMWPE composites using Split Hopkinson Pressure Bar”. DOI: 10.1177/0021998316635241 **Journal of Composite Materials**” 2017; 51(1):81-94.
- ❑ **Jabbar A**, Militký J, Kale BM, Rwawiire S, Nawab Y, Baheti V. “Modeling and analysis of the creep behavior of jute/green epoxy composites incorporated with chemically treated pulverized nano/micro jute fibers”. **Industrial Crops and Products**. 2016; 84:230-240.
- ❑ B.M. Kale, J. Wiener, J. Militky, S. Rwawiire, R. Mishra, **A. Jabbar** “Dyeing and stiffness characteristics of cellulose-coated cotton fabric” DOI 10.1007/s10570-015-0847-0. **Cellulose**” 2016; 23:981-992.
- ❑ J. Militký, **A. Jabbar** “Comparative evaluation of fiber treatments on the creep behavior of jute/green epoxy composites” Volume 80, pp 361-368, October 2015, **Composites Part B: Engineering**
- ❑ S. Rwawiire, B. Tomkova, J. Militky, **A. Jabbar**, B. M. Kale. “Development of a biocomposite based on green epoxy polymer and natural cellulose fabric (bark cloth) for automotive instrument panel applications” Volume 81, pp 149-157, November 2015, **Composites Part B: Engineering**
- ❑ **Jabbar A**, Militký J, Wiener J, Karahan M. “Static and dynamic mechanical properties of novel treated jute/green epoxy composites”. **Textile Research Journal**. 2016; 86 (9):960-74.
- ❑ **Jabbar, A**, J. Militký, J. Wiener, M. Usman Javaid and S. Rwawiire “Tensile, Surface and Thermal Characterization of Jute Fibres after Novel Treatments”. **Indian Journal of Fibre and Textile Research**. 2016; 41:249-254
- ❑ S. Rwawiire, B. Tomkova, E. Gliscinska, I. Krucinska, M. Michalak, J. Militky, **A. Jabbar** “INVESTIGATION OF SOUND ABSORPTION PROPERTIES OF BARK CLOTH NONWOVEN FABRIC AND COMPOSITES” 2015; 15:173-180, **AUTEX Research Journal**, DOI: 10.1515/aut-2015-0010.
- ❑ M. Karahan, **A. Jabbar**, N. Karahan “Ballistic impact behavior of the aramid and UHMWPE composites” Vol. 34(1), 2015, pp. 37-48 doi:10.1177/0731684414562223 **Journal of Reinforced Plastics and Composites**”.
- ❑ M. Awais, M. Tausif, **A. Jabbar**, F. Ahmad, S. Ahmad “Inclusion of recycled PPTA

fibres in the development of cut resistant gloves” DOI: 10.1080/00405000.2014.922246 “**Journal of the Textile Institute**” 2015; 106:354-358.

- ❑ N. Haleem, S. Ibrahim, Z. Ali, **A. Jabbar**, M. H. Malik “Determining the light transmission of woven fabric through different measurement methods and its correlation with air permeability” Volume 9, Issue 4, 2014, pp 76-82. “**Journal of Engineered Fibers and Fabrics**”.
- ❑ T. Hussain, M. Usman Ashraf, **A. Jabbar** “Effect of cotton fibre and yarn characteristics on colour variation in woven fabric dyed with vat dyes” DOI: 10.1080/00405000.2014.887239 “**Journal of the Textile Institute**” 2014; 105:1287-1292.
- ❑ T. Hussain, **A. Jabbar**, S. Ahmed “Comparison of regression and adaptive neuro-fuzzy models for prediction of compressed air consumption in air jet weaving”. “**Fibres and Polymers**” Vol. 15(2), 2014, pp. 390-395.
- ❑ **Jabbar**, S. Ahmed, T. Hussain, N. Haleem, F. Ahmed “Statistical Model for Predicting the Compressed Air Consumption on Air-Jet Looms”. “**Journal of Engineered Fibers and Fabrics**” Vol. 09(3) 2014, pp. 50-56.
- ❑ **Jabbar**, M. H. Malik, T. Hussain, A. Zulifqar and M. Tausif “Comparison of mechanical and ballistic performance of composite laminates produced from single-layer and double-layer interlocked woven structures”. “**Polymer Composites**” Vol. 35(8), August 2014, pp. 1583-1591.
- ❑ **Jabbar**, T. Hussain and A. Moqheet “Impact of Carding Parameters and Drawframe Doubling on the Properties of Ring Spun Yarn”. “**Journal of Engineered Fibers and Fabrics**” Vol. 8(2), June 2013, pp. 72-78.
- ❑ Moqheet, **A. Jabbar**, T. Hussain, Z. Ali and Z. Haq “Influence of Splicing Parameters on Retained Splice Strength, Elongation and Appearance of Spliced Cotton/Flax Blended Yarn”. “**Indian Journal of Fibre and Textile Research**” Vol. 38(1), March 2013, pp. 74-80.

Conference Publications

- ❑ **A. Jabbar**, M. H. Malik, T. Hussain, A. Zulifqar and M. Tausif “Experimental study of the low and high velocity impact performance of composites produced from single layer and double layer interlocked woven fabrics”. Proceedings of TexComp-11 held in KU Leuven, Belgium 19-20 September, 2013.
- ❑ A. Zulifqar, T. Hussain, , M. H. Malik, **A. Jabbar** and Y. Nawab “Development and characterization of novel woven structures for ballistic protective applications”. Proceedings of 14th Autex held in Bursa, Turkey 26-28 May, 2014.
- ❑ **A. Jabbar**, J. Militký “Creep behavior of novel treated jute/green epoxy composites” Workshop Světlanka, ISBN 978-80-7494-229-7, September 2015, pp 52-57.
- ❑ **A. Jabbar**, J. Militký “Investigation of the creep and dynamic mechanical properties of jute/green epoxy composites incorporated with chemically treated pulverized nano/micro jute fibers”. Workshop Bila Voda, ISBN 978-80-7494-293-8 September 2016, pp 56-61.
- ❑ **A. Jabbar**, J. Militký “Investigation of the Mechanical, Creep and Dynamic Mechanical Properties of Jute/Green Epoxy Composites Incorporated with Chemically Treated Nano/Micro Jute Fibers” Aachen-Dresden-Denkendorf International Textile Conference November 2016.

Book Chapters

- ❑ **A. Jabbar**, J. Militký “Comparative evaluation of novel fiber treatments on the mechanical, thermo mechanical and creep behavior of jute/green epoxy composites” Recent Developments in Fibrous Material Science, ISBN 978-80-87269-45-9.

	<input type="checkbox"/> Jabbar A , Militký J, Kale BM, Rwawiire S, Baheti V. “Study of creep and thermo-mechanical properties of jute/green epoxy composites incorporated with chemically treated pulverized nano/micro jute fibers”. Recent Developments in Fibrous Material Science, ISBN 978-80-87269-48-0.	
Projects Handled	<input type="checkbox"/> Student grant scheme project (SGS - 21085) was successfully handled as leader in 2015-16. <input type="checkbox"/> Student grant scheme project (SGS - 21158) was successfully handled as leader in 2016-17.	
Honors and Awards	<input type="checkbox"/> Get Travel grant from Higher Education Commission, Islamabad to participate in TexComp-11 conference, Leuven Belgium <input type="checkbox"/> 1st position holder in M.Sc. Textile Engineering, session 2010-2012. <input type="checkbox"/> Winner of 3rd prize at “Young Researcher Competition Award” organized by Textile Institute of Pakistan, Karachi-Pakistan. <input type="checkbox"/> Winner of “Innovation Award” at “Invention to Innovation Summit 2013” organized by Pakistan Science Foundation held at University of the Punjab, Lahore- Pakistan.	
Working Experience	<input type="checkbox"/> National Textile University (NTU), Faisalabad, Pakistan September 2009 to present (Lecturer) Teaching and research activities related to short staple yarn manufacturing and advanced courses like high performance fibers, nonwovens and technical textiles and composites. <input type="checkbox"/> Riaz Textile Mills Limited Sheikhpura, Pakistan January 2007 to August 2009 (Assistant Manager to Deputy Manager) Managed and supervised the yarn quality, machines maintenance and process control. This is a private staple spun cotton yarn manufacturing company.	
Competencies and skills	<input type="checkbox"/> OriginLab, MiniTAB, MATLAB, MS Office	
Personal Details	<input type="checkbox"/> Nationality: Pakistani <input type="checkbox"/> Date of Birth: 3 rd March, 1983 <input type="checkbox"/> Languages: English, Urdu, Punjabi	<input type="checkbox"/> Address: Department of Material Engineering Faculty of Textile Engineering, Technical University of Liberec Studentska 2 Liberec Czech Republic <input type="checkbox"/> Cell: +420 776144717 <input type="checkbox"/> Email: abdujabbarntu@gmail.com , abdujabbar@tul.cz

Brief description of the current expertise, research and scientific activities

Doctoral Studies	Full-time student at the Faculty of Textile Engineering, Department of Material Engineering Specialization: Textile Technics and Material Engineering
List of Exams Passed	[1]. Heat and Mass Transfer in Porous Media [2]. Structure and Properties of Textile Fibers [3]. Textile Metrology [4]. Mathematical Statistics and Data Analysis [5]. Experimental Technique of Textile
State Doctoral Examination	Passed
Research Projects	Two projects handled as leader SGS-21085 and SGS-21158 Contributed two book chapter for the Department's Material Science book.

9 Record of the state doctoral exam

ZÁPIS O VYKONÁNÍ STÁTNÍ DOKTORSKÉ ZKOUŠKY (SDZ)

Jméno a příjmení doktoranda: **Abdul Jabbar, M.Sc.**

Datum narození: **3. 3. 1983**

Doktorský studijní program: **Textilní inženýrství**

Studijní obor: **Textile Technics and Materials Engineering**

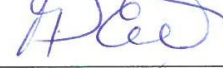
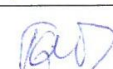
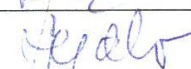
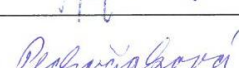
Termín konání SDZ: **7. 12. 2016**

prospěl

~~**neprospěl**~~

Komise pro SDZ:

Podpis

Předseda:	prof. Ing. Jakub Wiener, Ph.D.	
Místopředseda:	doc. Ing. Maroš Tunák, Ph.D.	
Členové:	prof. Dr. Ing. Miroslav Černík, CSc.	
	prof. Ing. Michal Šejnoha, Ph.D., DSc.	
	doc. Ing. Antonín Potěšil, CSc.	
	doc. Ing. Pavel Rydlo, Ph.D.	
	Ing. Miroslava Pechočiaková, Ph.D.	

V Liberci dne 7. 12. 2016

O průběhu SDZ je veden protokol.



Recommendation of the supervisor

Supervisor's recommendation on PhD thesis of Abdul Jabbar M.Sc.

Date: 07.02.2017

Thesis title: Characterization of mechanical and thermomechanical behavior of sustainable composite materials based on jute

The PhD thesis titled "Characterization of mechanical and thermomechanical behavior of sustainable composite materials based on jute" is quite comprehensive and fulfills the objectives outlined in his thesis. The thesis is written according to required format, I believe and the objectives of the thesis are clear. The candidate has done all his work quite systematically with specific objectives, organized and analyzed data scientifically and discussion of the results is logical with citations of previous work where necessary. The quality of figures and tables is good and understandable. The language level of the thesis is good and meets the PhD level.

His publication activities show that he is an outstanding researcher. During his research work in TUL on the PhD theme, he has published 5 papers in high ranked impact factor journals, 2 book chapters and 3 articles in conference proceedings. Apart that, from 2013 to present, he is the author/co-author of total 20 impact factor journal articles.

The extraction of cellulose fibrils from jute waste is economical and surface treatment methods explored in this thesis are environment friendly. The conclusions of the thesis are interesting, novel and ready to be used in practice. I therefore recommend the thesis for final defense.


Prof. Ing. Jiří Militký, CSc. EURING
Supervisor

Assessment of PhD Thesis

Aspirant:	Abdul Jabbar, M.Sc.
Thesis title:	Characterization of Mechanical and Thermomechanical Behavior of Sustainable Composite Materials Based on Jute
Specialization:	Textile Technics and Materials Engineering
Supervisor:	prof. Ing. Jiří Militký, CSc.
Reviewer:	doc. Ing. Antonín Potěšil, CSc.

Topicality of the thesis
<p>Comment:</p> <p>The topic of this dissertation thesis is up to date and respects current and future innovative trends towards the use of bio-waste arising from textile technologies. The processors' efforts are subsequently utilized in a number of industries, including the development and production of new biodegradable products that do not degrade irreplaceable natural resources.</p>
<p>excellent¹ <input checked="" type="checkbox"/> above standard <input type="checkbox"/> standard <input type="checkbox"/> substandard <input type="checkbox"/> weak <input type="checkbox"/></p>
¹ Mark selected with a cross

Meet the objectives of the thesis
<p>Comment:</p> <p>The presented work has a very well described part and describes the approaches to the preparation and testing of bio-composites made of jute fibers of different character, which form the filler in the polymer composite. Work is also good factual content, specifying of laboratory technologies that are designed to improve the adhesive properties fills with polymer matrix. Samples prepared by the graduate were then tested in a variety of experimental methods. After studying the dissertation thesis as a whole, it was stated that the stated goals of the thesis and the intentions of the doctoral candidate were fulfilled.</p>
<p>excellent <input type="checkbox"/> above standard <input type="checkbox"/> <input checked="" type="checkbox"/> standard <input type="checkbox"/> substandard <input type="checkbox"/> weak <input type="checkbox"/></p>

Methods and solutions
<p>Comment:</p> <p>In the characterization of the properties of the graduate-made bio-composite structures a number of standard test methods, procedures and measuring devices (SEM, FTIR, DMA, mechanical tests, etc.) were used. The thesis demonstrates the autonomy of the graduate's approach to these experimental activities.</p>
<p>excellent <input type="checkbox"/> above standard <input type="checkbox"/> <input checked="" type="checkbox"/> standard <input type="checkbox"/> substandard <input type="checkbox"/> weak <input type="checkbox"/></p>

Results of the Thesis - specific benefits of the student					
Comments:					
The main contribution of the dissertation is the identification and comparison of the mechanical properties of several types of bio-composites with a structure treated by different physical-chemical processes, even under different temperature and climatic conditions. The results of the experimental findings are processed by statistics and provide useful information for material engineers and product designers.					
excellent	above standard	<input checked="" type="checkbox"/>	standard	substandard	weak

Significance for practice and for the development of the scientific branch					
Comments:					
Work is a good starting point for further research and development activities in the field of bio-composite use in various industrial applications. I recommend that the follow-up work be deeper into the theoretical areas of physical properties of composite materials, both with regard to the follow-up processing technologies in the production of products and their industrial applications in a specific sense.					
excellent	<input checked="" type="checkbox"/>	above standard	standard	substandard	weak

Formal layout of the Thesis and its language level					
Comments:					
The work has a logical structure, the English text is comprehensible, the Czech text of the abstracts text has no editing errors.					
excellent	<input checked="" type="checkbox"/>	above standard	standard	substandard	weak

Comments and questions	
<ol style="list-style-type: none"> The properties of prepared bio-composites are measured only in room and in elevated temperatures. The application in automotive and aviation industry requires knowledge of properties in the range from -60 to 90°C including coefficient of linear thermal expansion (CLTE). Did you run the experiments in subzero temperatures? What method was used to set volume fraction of fibrous reinforcement and of matrix in prepared bio-composites? Explain the relation between mass and volume fraction of reinforcement and matrix in composite structure. For any predictive CAE simulations it is necessary to describe composites as anisotropic, respectively orthotropic material continuum. What relations are in such cases used to describe relationship between stress and strain? Give examples. 	

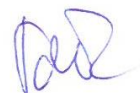
Final evaluation of the Thesis	
Based on the above review I recommend submitted thesis for defense in front of the scientific committee for the defense of doctoral thesis.	

I recommend after a successful defense of the dissertation grant Ph.D. ²	yes	<input checked="" type="checkbox"/>	no	<input type="checkbox"/>
---	-----	-------------------------------------	----	--------------------------

² Delete where applicable

Place and Date: In Liberec 18.05.2017

Signature: Antonín Potěšil





Posudek disertační práce

Uchazeč: Abdul Jabbar, MSc.

Název disertační práce: Characterization of mechanical and thermomechanical behavior of sustainable composite materials based on jute

Studijní obor _____

Školitel Prof. Ing. Jiří Militký, CSc.

Oponent: Prof. Ing. Michal Šejnoha, Ph.D., DSc.

e-mail: sejnom@fsv.cvut.cz

Aktuálnost tématu disertační práce

komentář: Scientific relevance of the submitted work

Green composites made of natural fiber reinforcements bonded to a biodegradable matrix have been recognized as a suitable material for the replacement of more traditional synthetic fiber based composites in many applications thus reducing both the production cost and the environmental impact. However, a high variability of basic material properties such as stiffness and strength predestined these material systems to mostly non-structural application. For these materials to enter the field of structural applications requires a thorough research in the area of mechanical properties to identify various drawbacks and suggest routes for the stabilization and potential improvements of the mechanical behavior of such composites. Although limited mostly to experimental investigation, the present thesis opens the way to achieve such goals. The scientific relevance of the chosen topic is, therefore, undoubtedly high.

vynikající nadprůměrný průměrný podprůměrný slabý

Splnění cílů disertační práce

komentář: Goals of the work and their achievements

The main research objectives were clearly stated in the first chapter of the thesis. From the experimental point of view, their achievement presented undoubtedly a rather challenging task. Although the final summary of the results given in the last chapter of this thesis is less comprehensive, it is evident from the content of the thesis that all of the goals set were addressed and in the main part also successfully met.

vynikající nadprůměrný průměrný podprůměrný slabý

Metody a postupy řešení

komentář: Treatment of the topic - methodical and conceptual approach

The scientific content of the work meets very high quality standards. In the first two chapters the state-of-the-art is broadly discussed including a large literature survey. Apparently, Mr. Jabbar had to devote a considerable amount of time to gain a sufficient scientific background, particularly in the field of experimental investigation of these material systems which in turn called for a sound knowledge of chemistry and mechanics of composite materials in general.

The principal findings of the present work are summarized in Chapters 3 to 6 addressing virtually all of the present issues concerning the improvement of the mechanical response broadly classified in Chapter 2. While Chapter 3 outlines individual types of experiments conducted in the course of this thesis, Chapters 4-6 provide summary of the achieved results for tested material systems. For the sake of clarity, these were

classified into three main groups. An extensive experimental program, though not fully consistent for all groups, was conducted to address the influence of matrix and reinforcement surface treatment on the mechanical behavior of the final product based on standard properties such as stiffness and strength but also from the long term behavior point of view by specifying the creep, fatigue and dynamic properties of the investigated systems.

The assumed list of experiments was correctly selected to allow for a clear distinction of various treatment techniques and their impact on the monitored properties and consequently to suggest the most promising technique, or their combination, for a particular application. However, a sufficiently broad discussion in this regard is missing. This invites a few questions whose answers, if included, would certainly improve the quality of the theses. In particular:

1. Chapter 4 is concerned mainly with the modification of the matrix properties while chapters 5 and 6 concentrate on the surface treatment of the jute textile reinforcement. A parametric study combining both techniques is missing. Could the author briefly comment on that during the thesis defense?
2. A detailed comparison of the two types of surface treatment discussed in Chapter 5 and 6 is also missing. A comment on that, at least from the common types of experiments conducted point of view, is also welcome. Choose, e.g. the strength and stiffness properties and make a quantitative comparison on a common graph.

Chapter 7 is therefore in my opinion too brief in comparison to the effort devoted to and the amount of results presented in the thesis.

vynikající nadprůměrný průměrný podprůměrný slabý

Výsledky disertace - konkrétní přínosy disertanta

komentář: Thesis results - author's specific contribution

The author examined most of the common treatment of green composites applied both to the matrix and reinforcements with particular application to jute. As mentioned above, the results provide bases for the selection of optimal technique and opens a way for numerical simulations, which should with no doubt support the experimental work. More complex creep models in case of theoretical approach and more elaborative dynamic analysis introducing a broad range of frequencies in case of experimental approach are just two specific examples of future research directions benefiting from the results achieved in the present thesis.

vynikající nadprůměrný průměrný podprůměrný slabý

význam pro praxi a pro rozvoj vědního oboru

komentář: Extent of new knowledge and contribution to the practice

I am not an expert in this field so I suggest the author to give, during the thesis defense, his own opinion on a potential applicability of the jute textile reinforced composites going beyond non-structural applications, which I suppose is the principal objective of the author's research effort.

vynikající nadprůměrný průměrný podprůměrný slabý

Formální úprava disertační práce a její jazyková úroveň

komentář: Organization of the work and overall comprehensiveness

The thesis are written in good English with only few grammatical errors limited mostly to the lack of articles. The thesis is well structured and easy to follow. A potential improvement of the clarity, which does not however reduce the thesis high standard, can be seen, e.g. in

1. Introduction of a list of abbreviations as a large number are used throughout the thesis and these are difficult to remember
2. Scales on some figures are in some cases difficult to see.
3. A comprehensive table summarizing the types of experiments selected for individual types of composites included for example in Chapter 3 would make easier to follow the subsequent chapters.

vynikající nadprůměrný průměrný podprůměrný slabý

Připomínky

Comments and questions:

Apart from already posted comments the following questions are welcome to answer:

1. What is the reason for choosing the particular creep models if these are not generally possible to use in simulations. Among them, only the Burger's model can be extended into a chain model and modified to adopt the temperature shift factor. Can you comment on that?
2. The discussion related to Fig. 5.7 is related to the fact that the applied load is selected based on the tensile strength pertinent to a given composite according to Fig. 5.5. It can be expected that for e.g. the CF0 composite the fatigue live would increase if loaded by stress difference associated with the lowest strength observed for CF10 composite. Can you comment on that?
3. I suppose the composites labeled as CF0 in Fig. 5.6 and untreated in Fig. 6.3 are the same. Can you please make a comment on why there is such a big difference in flexural modulus while the strength is comparable?
4. I do not really understand the explanation regarding the decreasing strength with improving the interfacial properties in Fig. 5.5? Can you provide some numbers related to the strength of the matrix and reinforcements? Have you made the same type of measurements also for the composites discussed in Chapter 6? If the reasoning for the stress reduction was correct that this trend would be the same for any composite regardless of the surface treatment. A comment on that is again welcome.

Závěrečné zhodnocení disertace

Final statement:

Based on the submitted review, consisting of an assessment of the scientific relevance, fulfillment of the goals of the work, the quality of treatment of the topic and the extent of new knowledge, it is concluded that this work meets very high quality standards.

As it complies with the requirements for a Ph.D. work, I recommend the thesis for further defense and if successful to appoint Mr. Abdul JABbar, MSc. the title

doctor (Ph.D.)

Doporučuji po úspěšné obhajobě disertační práce udělení titulu Ph.D. ano ne

Datum: 20.05.2017

Podpis oponenta: 